CHARACTERISTICS OF RED RIVER CLAYS PERTAINING TO VERTISOLIC CRITERIA AND MACROPORE FLOW

BY

CURTIS G. CAVERS

A Thesis
Submitted to the Faculty of Graduate Studies
in Partial Fulfillment of the Requirements
for the Degree of

Master of Science

Department of Soil Science
University of Manitoba
Winnipeg, Manitoba

February, 1996

ISBN 0-612-13015-0

THE UNIVERSITY OF MANITOBA

FACULTY OF GRADUATE STUDIES

*****

COPYRIGHT PERMISSION

CHARACTERISTICS OF RED RIVER CLAYS PERTAINING TO VERTISOLIC CRITERIA AND MACROPORE FLOW

BY

CURTIS G. CAVERS

A Thesis/Practicum submitted to the Faculty of Graduate Studies of The University

of Manitoba in partial fulfillment of the requirements for the degree

of

MASTER OF SCIENCE

ACKNOWLEDGMENTS

The author would like to express his sincere thanks for the contributions of the following people/organizations:

- NSERC, whose funding in the form of a post-graduate scholarship made this project possible;

- the advisory committee of Mr. R. G. Eilers, Dr. T. B. Goh, and Dr. R. Sri Ranjan, for all their suggestions, assistance and encouragement;

- Thayalan Karthigesu, Department of Agricultural Engineering, for his timely guidance in operation and maintenance of the liquid bubble flow meter;

- Edwin Yee and Randy Webber of the Manitoba Hazardous Waste Management Corporation, for their cooperation and assistance in our study of the Montcalm site;

- Dr. M. H. Entz, Plant Science Department, for the use of his crop rotations study at The Point;

- Dr. Dan Reynolds, for all his helpful suggestions in the operation of the Guelph Permeameter;

- Bob Betcher and Mary Ellen Patton, for their assistance in isotope analysis of groundwater;

- Ray Guertin and Dr. Cathy Fox, for sample preparation and interpretation of thin sections;

- Sergio Mejia, Department of Geological Sciences, for the use of petrographic microscope used for analysis of thin sections;

- Dr. L. Lamari, Department of Plant Science, for use of image analysis technology to calculate porosity of thin sections;

- Dr. Sue Trumbore, University of California, Berkeley, for ^{14}C analysis of plant roots;

- Dr. Walter Michalyna, Hugo Veldhuis, Michelle Fitzgerald, Don Swidinsky, Rehana Mirza and the rest of Soil Survey Staff for their technical assistance on numerous occasions;

- Drs. G. J. Racz, C. F. Shaykewich, and M. E. Cerrato, for their academic assistance;

- Helen Nemeth and Pearl Novotny, Department of Soil Science general office, for all the joy they bestowed on anyone in their midst and for all their administrative help;

- Gregg Morden, Val Huzel and the rest of the Department of Soil Science, for technical and academic assistance;

- Soil Science graduate students at the time (Brian Wiebe, Bill Dubbin, Ross Malegus, Les Fuller, Ramona Mohr, Lana Smith, Dale Tomasiewicz, Johnson Kamwaga, Ralph Wright, Sheri Grift, Jessica Audette, John Fitzmaurice, Michelle Fitzgerald, Colleen Flynn, David Hay, Mike Kagan, Kristina Anderson, Dave Blatta, Kristina Graham), for computer assistance and just for being there to identify and relate to the plight of a fellow graduate student;

- family and friends, for putting up with someone who spends the bulk of his time "playing in the dirt";

- last, but not least, thanks be to God for the strength and opportunity to complete this work - may the knowledge gained here be used in some small way to improve the way we care for His creation.

TABLE OF CONTENTS

LIST OF TABLES

LIST OF FIGURES

ABSTRACT

Cavers, Curtis G. M.Sc., The University of Manitoba, February, 1996. Characteristics of Red River Clays Pertaining to Vertisolic Criteria and Macropore Flow. Major Professors; R. G. Eilers, Tee Boon Goh.

Clay soils predominately composed of montmorillonite possess a high shrink-swell potential that has taxonomic and practical implications. The presence of slickensides and evidence of high shrink-swell in these soils may meet revised criteria which would place these soils under a Vertisolic Order, or as vertic intergrades of Chernozemic, Gleysolic, Luvisolic or Solonetzic Orders in the Canadian System of Soil Classification. The presence of large cracks and biological pathways in these soils may result in higher rates of water flow and potential for pollutant transport than previously expected.

Several analyses were conducted on three clay soils with contrasting hydrologic regimes. The purpose was to identify features and processes which may serve as diagnostic criteria for classification, and which may affect the permeability of the soil. Visual analysis of contiguous cores from two sites identified physical features such as texture, structure, carbonates, salts, mottles, slickensides, roots, cracks, and biopores and mapped their location according to depth. Micromorphological analysis of the soil fabric, tritium analysis of groundwater, and ^{14}C analysis of root material were conducted to aid in assessing the potential for downward movement of water and dissolved materials in these soils.

Saturated flux versus hydraulic gradient relationships were examined in the laboratory using a liquid bubble flow meter and pressure transducer on four contiguous core samples. At hydraulic gradients less than 1.2 m/m, there is a deviation from the straight-line relationship of Darcy's Law, with saturated fluxes at low hydraulic gradients about one order of magnitude lower than predicted by Darcy's Law. This non-Darcian flow occurs due to a portion of the water molecules in the pores immobilized by the attractive forces of the clay. Samples with pathways conducive to macropore flow follow Darcian behavior but saturated flux may be an order of magnitude higher than expected for samples of heavy clay texture.

Saturated hydraulic conductivity was measured at three depths on four different cropping/tillage practices over two years on a Black Lake series (Cumulic Regosol) using a Guelph Permeameter. Of the four cropping/tillage practices, soil under continuous alfalfa had the highest saturated hydraulic conductivity at all three depths.

Analysis of slickensides and shrink-swell properties confirmed that the other two soils investigated (Red River series, Dencross series) would meet criteria to be classified as a Humic Vertisol and a Vertic Rego Black respectively. Analysis of water movement through these soils revealed that under low-gradient flow these heavy clay soils is conducive to non-Darcian flow. However, the presence of physical features that produce preferential pathways may result in macropore flow that could have serious environmental implications.

INTRODUCTION

Soils in the Red River basin of Manitoba have a heavy clay texture and have developed from sediments of glacial Lake Agassiz (Fenton et. al. 1983). The montmorillonitic nature of these clays results in a high shrink-swell potential and extensive surface cracking. The presence of slickensides at depth in these soils indicates that soil shearing and displacement has taken place. These characteristics are typical of Vertisolic soils found in several locations throughout the world (Jenny, 1980).

Prior to 1982, these soils in Canada could not be classified as Vertisols under the American soil classification system (Soil Taxonomy) because of climatic limitations (Soil Survey Staff, 1975). The Canadian System of Soil Classification has no Vertisolic order to date, and as a result the clay soils of the Red River basin have been classified as subgroups of the Chernozemic, Luvisolic, Solonetzic and Gleysolic orders. Evidence of soil displacement has been recognized at the family level in the Canadian classification system, where very fine textured, montmorillonitic soils may be classified as having "grumic" properties (Expert Committee on Soil Survey, 1987). After 1982, however, the climatic restriction for Vertisols was lifted in Soil Taxonomy and now many of these Canadian soils either fully or partially meet the criteria for Vertisols. The updated criteria for Vertisols in Soil Taxonomy (Soil Survey Staff, 1987) is "other soils that:

1. Do not have a lithic or paralithic contact, petrocalcic horizon, or duripan within 50 cm of the surface; and

2. After the soil to a depth of 18 cm has been mixed, as by plowing, have 30 percent or more clay in all subhorizons to a depth of 50 cm or more; and

3. Have, at some time in most years unless irrigated or cultivated, open cracks at a depth of 50 cm that are at least 1 cm wide and extend upward to the surface or to the base of the plow layer or surface crust; and

4. Have one or more of the following:
   a. Gilgai;
   b. At some depth between 25 cm and 1 m, slickensides close enough to intersect;
   c. At some depth between 25 cm and 1 m, wedge-shaped natural structural aggregates that have their long axes tilted 10 to 60 degrees from the horizontal."

The Canadian System of Soil Classification recently created a Vertisolic Order together with intergrade subgroups for Chernozemic, Gleysolic, Luvisolic and Solonetzic orders. In the key to soil orders, the Vertisolic Order was recognized immediately following the Cryosolic and Organic orders. The Vertisolic Order was described as "other soils that have both a vertoturbic horizon and a slickenside horizon, the top of which occurs within 1 m of the surface." A slickenside horizon contains more than two slickensides which may be intersecting. A vertoturbic horizon is a horizon that has been strongly affected by shrinking and swelling so that the formation of other diagnostic horizons is prevented or severely disrupted. This horizon is characterized by the presence of:

1. Irregular shaped, randomly oriented, intrusions of displaced materials within the solum, and

2. Vertical cracks, often containing sloughed-in surface materials.

To be classified in the Vertisolic order, both a slickenside horizon and a vertoturbic horizon must be present in soils with at least 60% clay and 30% of the total soil made up of swelling clay (smectite). Vertic intergrades in the Chernozemic, Gleysolic, Luvisolic and Solonetzic orders show evidence of shrinking and swelling and have Vertisolic features such as cracks and slickensides, but disruption does not occur to the extent that it overrides the diagnostic horizons of the other orders (Expert Committee on Soil Survey, unpublished literature).

Another area of interest is the movement of water through these soils. Soils with high clay content contain a significant amount of water adsorbed onto the clay particles. Under adsorbed conditions, a large portion of the soil water becomes immobile, and thus water movement through the soil can no longer be described by conventional relationships.

Since soils with vertic properties tend to crack extensively, these soils are especially conducive to rapid downward movement, or macropore flow. Large macropores formed from plant root channels, and other biological activity within the soil (earthworms, ants, etc) also affect the permeability. These biopores tend to be more stable than cracks and fractures because their tubular shape allows them to remain open even when the soils swell and the cracks close upon wetting (Mellanby, 1971; Green and Askew, 1965).

In this study the effects of salinity, groundwater movement, groundwater quality, the number, distribution and age of roots, and the frequency and depth of biopores, cracks and slickensides will be examined in contiguous soil cores to determine how macropore flow is influenced by these physical characteristics.

Objectives

This study was undertaken to analyze the physical and morphological properties of three clay soils under different hydrogeologic influences to determine whether these soils meet the proposed criteria for Vertisols or vertic intergrades of other soil orders in the Canadian System of Soil Classification.

In addition, the study examines the influence of physical features on the permeability of high clay content soils. Two phenomena which affect permeability are addressed: non-Darcian flow and macropore flow.

LITERATURE REVIEW

I. Vertic Properties of Clays

The two distinguishing features of Vertisolic soils are slickensides and microrelief (gilgai). Slickensides are polished, grooved surfaces on soil peds formed from the sliding of one soil mass past another (Dudal and Eswaran, 1988). In terms of soil genesis, slickensides form very rapidly (100-1000 years). Gilgai are micro-knolls and micro-depressions formed due to shrink-swell phenomena of these soils (Dudal and Eswaran, 1988). The distance between the crests of these micro-ridges can be anywhere from 3 to 25 metres or more.

1. Conceptual Models of Vertisolic Development

There have been at least three models developed to explain the movement of soil responsible for the genesis of Vertisols. The most popular model has been the pedoturbation model (Buol et al. 1980). This model proposes that during the period in which the soil cracks, soil from the surface is sloughed into these cracks, at least partially filling them (Fig. 1). When the soil is rewetted, it swells and the pressures exerted on the infilled cracks results in soil displacement and the sequential development of micro-mounds and depressions at the soil surface. The main problem with this model is that the effects of soil infilling cracks ("self-swallowing") should be confined to the depth of profile where cracking occurs. Yet slickenside formation is known to occur below the maximum depth of cracking (typically 2 to 3 m).

The soil mechanics model (Ritchie et al. 1972; Yaalon and Kalmar, 1978) describes soil displacement as the result of unequal wetting, which causes swelling under confinement. When the swelling pressures become greater than internal forces resisting shear, soil displacement produces slickensides at a particular depth range (Fig. 2). White (1967) expected slickensides to rarely form below a depth of two metres because the weight of overlying soil increases the packing and density of the soil, causing resistance to shearing to increase with depth. Blockhuis (1982) and Ahmad (1983) contend that slickensides found at depths below two metres were likely formed during ripening of the sediments, large-scale land slipping, or mass wasting rather than via soil formation (ie. geologic versus pedologic slickensides). The difficulty with this model is that unequal wetting near the soil surface has a limited effect on slickenside formation because low overburden pressure and cracks retard lateral stresses required for slickenside development. Consequently, unequal wetting accounts for slickensides below the maximum depth of cracking but not for the formation of slickensides within 1.5 m of the soil surface (Yaalon and Kalmar, 1978).

The least accepted model, the differential loading model, describes gilgai formation to be the result of clays moving from areas of high to low confining pressure (Paton, 1974). It is hypothesized that low plasticity surface soils with different

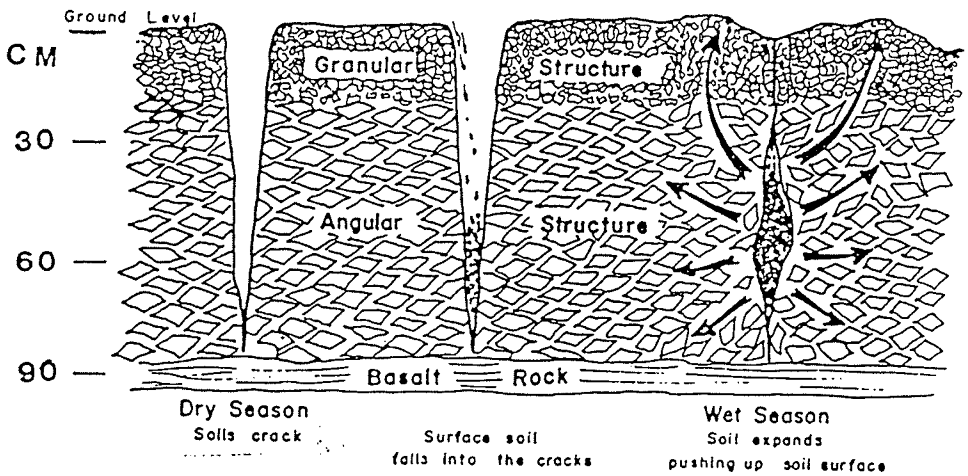

Figure 1. Pedoturbation model (Buol et al. 1980).

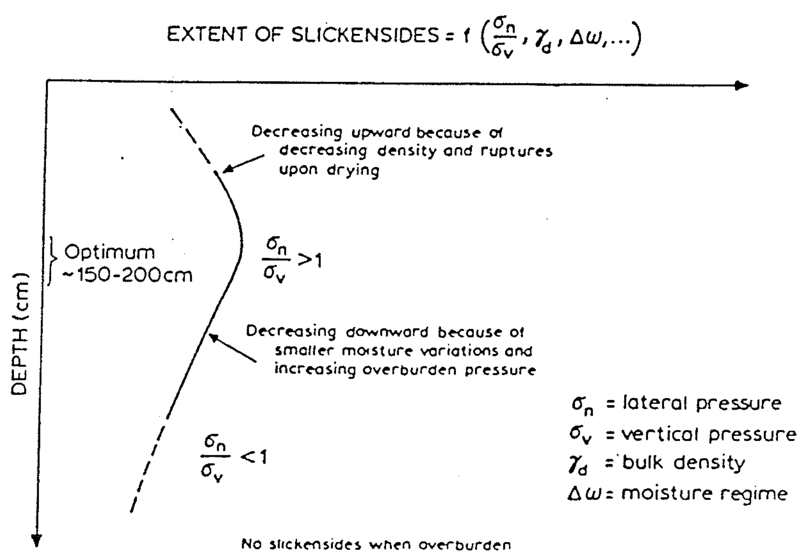

Figure 2. Soil mechanics model (Yaalon and Kalmar, 1978).

thicknesses and densities exert differential pressure on underlying subsoils which are much more plastic. The downfall of this theory is the absence of marked density gradients required for the existence of differential pressure in the soil (Gustavson, 1975).

2. Classification of Vertisols

A new proposal for the Canadian System of Soil Classification currently advocates including a Vertisolic order, which includes heavy-textured soils with high shrink-swell characteristics and a lack of horizon development. The Vertisolic order contains Vertisol and Humic Vertisol great groups, with each great group made up of Orthic, Gleyed and Gleysolic subgroups. In this classification, intersecting slickensides must be present within 1 m from the soil surface, along with a vertoturbic horizon, which displays evident disruption due to shrinking and swelling, and vertical cracks, often containing sloughed-in surface material.

Also included in the proposed classification order are vertic intergrades for the Chernozemic, Luvisolic, Solonetzic and Gleysolic orders. The intergrades all have a slickenside horizon within 1 m of the soil surface, and may have a weak or juvenile vertoturbic horizon. The intergrades contain the prefix "vertic" or "gleyed vertic". It has yet to be determined if all the requirements have been met for Vertic intergrades within the Gray Brown Luvisol, Solonetzic, and Regosolic orders (Soil Classification Working Group, unpublished literature, 1993, 1994).

II. Permeability of Clays

The movement of water through soil is a complex and dynamic process that affects almost every type of land use. Infiltration rates determine the threshold at which surface runoff, and subsequently, water erosion occurs on soil. The ease with which surface waters and any solutes present may reach the groundwater and contribute to groundwater recharge and/or pollution is also affected by infiltration rates.

Hydraulic conductivity and permeability are terms that are used interchangeably, since many of the older reports cited refer to hydraulic conductivity as the coefficient of permeability. More recently published literature distinguish between these two terms. Hydraulic conductivity, K, is the proportionality constant of Darcy's Law and is a function of both the porous medium and the fluid. Hydraulic conductivity has the dimensions length per unit time (m/s). Permeability, or more correctly known as the specific or intrinsic permeability, is a function only of the medium and has the dimensions length^2 (Freeze and Cherry, 1979). Throughout this study, the measurement of the rate of water flow through soils will be referred to as the hydraulic conductivity (Freeze and Cherry, 1979).

A. Non-Darcian Flow

Saturated and unsaturated flow through soils is best described by Darcy's Law. Darcian flow is defined by the mathematical expression:

$$q = K(H_2\text{-}H_1)/L$$

where

q is the flux;

K is the hydraulic conductivity;

$(H_2-H_1)/L$ is the hydraulic gradient.

Darcian flow is a straight-line relationship between flux and hydraulic gradient with the constant slope being defined as the hydraulic conductivity (Hillel, 1982). Darcian flow implies that this line passes through the origin, implying no flow at zero gradient and some flow at any other gradient. Under most circumstances, Darcian behavior adequately explains saturated flow phenomena. However, in soils with high clay content and low hydraulic gradient, flux values may be overestimated by Darcian flow. A portion of the soil water may be tightly held by the clay particles, creating a shell of immobile water. The resulting relationship is known as non-Darcian flow behavior, a deviation from the directly proportional relationship between flux and hydraulic gradient. It is difficult to predict at what hydraulic gradient non-Darcian flow takes effect and by how much it deviates from Darcian flow. In order to accurately predict flow of water and other constituents through soil, it is imperative to understand non-Darcian behavior.

One of the difficulties in testing for non-Darcian flow in media with low permeability is that most laboratory experiments must use gradients much higher than what exists in the field in order to detect a flux that can be measured (Neuzil, 1986).

Neuzil (1994), in his assessment of the permeability of clays and shales, noted that permeability is critical in the analyses of subsurface flow, and that many permeability values are lower than usually assumed. Data now suggest that hydraulic conductivity values for clays and shales commonly assumed to be 10^{-12} to 10^{-9} m/s for porosities less than 0.4 are now more in the range of 10^{-16} to 10^{-10} m/s (Neuzil, 1994). One of the greatest difficulties in determining the permeability of a material is the inability to predict how and where heterogeneity affects large-scale permeability in media.

B. Macropore Flow

The infiltration rate of a soil is influenced by the initial moisture content of the soil and by several inherent properties of the soil. In clay soils, which generally have matrices through which water moves slowly, the presence of several types of relatively large openings, known as macropores, can dramatically increase the rate at which water moves into and through the soil. Darcian flow theory assumes soils are rigid, homogeneous and isotropic - none of which hold for soils with macropores. This preferential movement of free water along large pores through unsaturated soil is known as short-circuiting (Hoogmoed and Bouma, 1980), non-matrix flow (Bouma et. al. 1980) or bypass flow (Bouma, 1991). Preferential flow in saturated soil involving rapid displacement of water from macropores is called hydrodynamic dispersion (Bouma, 1981). Throughout the remainder of the thesis this phenomenon shall be referred to as macropore flow.

Preferential channels occur not only in heavy-textured, swelling soils but also in structured soils of moderately light texture. Gallichand et. al. (1989) found preferential channels near subsurface drain perforations in a weakly structured sandy loam.

Bouma and Dekker (1978) discussed the practical applications of short-circuiting, acknowledging that preferential flow allows the soil surface to remain dry while maintaining a relatively high mechanical stability which is crucial for highly mechanized farming. Short-circuiting is favorable for deep rooted plants because water will be concentrated in the deep cracks along which the roots tend to grow. However, short-circuiting is unfavorable for waste disposal or irrigation of shallow rooted crops. Kluitenberg and Horton (1990) reported that increased soil macroporosity increased the soil's sensitivity to the method of material application. Careful selection of management pracitices must be exercised to avoid rapid transmission of solutes into the groundwater, especially when macropores are present.

Radulovich et. al. (1992), measuring macropore flow in two microaggregated Inceptisols in Costa Rica, found macropore flow to occur in noncapillary interpedal pore space whenever the application rate of water exceeded the infiltration rate of individual microaggregates. This phenomenon appeared to occur commonly in these microaggregated soils because the matrix conductivity values were so much slower than typical rainfall rates for tropical, volcanic and forest soils. With macropore flow playing a larger role in these soils than previously expected, current assumptions regarding nutrient cycling pathways and fertilizer application strategies in tropical soils used for agriculture may need to be revisited and revised.

1. Defining Macropores. Macropores in soil have been studied for many years, but only recently the environmental implications of macropores have been seriously considered. This is because macropores contribute very little to total pore volume, but in terms of total water flux, macropores contribute immensely. Douglas (1986) reported that air filled pore volume occupied on average less than 10% of the total soil volume and functional (continuous) macroporosity occupied less than 0.3% of the total soil volume.

Macropores can be broken down into several types of voids, such as packing voids (simple and compound), vugs, channels and planes. Bouma et al. (1977) distinguished between three main void shapes by comparing the ratios of void area to the square of the void perimeter. Rounded voids (channels) have a ratio greater than 0.04; intermediate-shaped voids (vugs) with a ratio between 0.04 and 0.015, and a ratio less than 0.015 for elongated voids (planes).

There is much speculation among researchers in defining the size at which soil pores are considered macropores. Brewer (1964) defines macropores as voids greater than 75 μm equivalent diameter. Bullock and Thomasson (1979) included pores greater than 60 μm diameter as macropores. Bouma and coworkers (1979) found small pores, 40 μm in diameter, can conduct considerable quantities of water if they provide a continuous path throughout the soil sample. Shipitalo and Protz (1987) classified macropores as pores with an equivalent circular diameter of 200 μm or larger. Attempts have been made to provide a standard range of pore sizes for all soil types (Luxmoore, 1981), but such an approach is not generally accepted because the effects of hysteresis and the continuity and tortuosity of pores do not account for distinctions between large pores in clay soil versus large pores in sandy soil (Skopp, 1981). Beven (1981) also points out that arbitrary boundaries for pore sizes should not be standardized due to the nonequilibrium behavior of macropore flow and because the differences in hydraulic gradient between large and small pores may result in the breakdown of the Darcian concept.

Bouma (1981) suggested that macropores simply be defined as pores which are significantly larger than those which result from the simple packing of the individual soil particles. He also critically examined morphological descriptions of soil pores in order to distinguish between:

- macromorphological data from soil survey descriptions
- macromorphological data from tracing techniques
- micromorphological data from thin sections.

Several authors have noted structural differences within the same soil material yield significantly different flow patterns (Elrick and French, 1966; Cassel et. al. 1974; McMahon and Thomas, 1974). They found that texture alone is not adequate for correlation with hydrodynamic dispersion, but there is a possible rough correlation if texture is used along with structure (planar neck sizes and amount of vertical infiltration along ped faces are factors as well).

Smettem (1986) noted that pore length exerts a large effect on volume flux over the range of macropore diameters commonly encountered in agricultural soils.

Mackie (1987) produced information on the orientation of interconnected soil pores that would be useful for quantifying pore continuity. Photographs were taken at different soil depths to trace the path of pores that had been filled with plaster of Paris.

This data was digitized and displayed in three dimensions on a computer monitor.

Therefore, to adequately understand the influence of macropores on soil infiltration, one must consider not only pore diameter, but also the length, continuity and orientation of the macropores.

2. Effect of Shrinkage Cracks. In Greece, on calcareous, alluvial soils with extensive cracking, Kosmas et. al. (1991) measured cracks more than 7 cm wide and more than 1.5 m deep in the dry season. They found decreasing the moisture content by a small amount in the 7-13% range could more than double bypass flow. If the initial soil moisture content increased, bypass flow decreased markedly.

Dasog and Shashidhara (1993) compared crack volume per unit area, or index of cracking intensity, of different crops after harvest (chickpea, wheat, sorghum, sunflower, safflower) with fallow on Vertisolic soils in India. The volume of the cracks were directly measured by infilling cracks with sand. Cracks were longer and narrower in the fallow treatment than in the cropped treatments, and only in the sorghum and safflower plots were the cracks significantly deeper than in fallow. However, because of the deep-rooting, efficient moisture extraction of safflowers, crack volume was highest in safflower plots (445 m^3/ha) and lowest in fallow plots (234 m^3/ha). Overall, it was estimated that the crack space could accommodate 223-44 mm of rainfall, facilitating moisture recharge in otherwise slowly permeable soils.

Wopereis and others (1994), worked on soil in a rice-growing area that had previously been cracked and puddled (soil was mixed with water by plowing, harrowing and levelling to create a soft medium for transplanting). They observed cracks 10 to 30 mm wide, up to 65 cm deep, which allowed the vast majority of the infiltrating water to bypass the bulk soil.

Bronswijk (1988) discusses the effect of swelling and shrinkage on water simulation models for clay soils. By having macropore flow account for 28% of the fate of precipitation, the results are a drier topsoil, a higher groundwater table with very rapid response after precipitation events, and a higher drain outflow than if macropore flow did not occur.

3. Effect of Plant Roots. Tippkotter (1983) examined tubular macropores 0.1-1 mm in diameter in loess soils located in Germany. He discovered a direct correlation between the location of macropores 100-400 μm in diameter and the depth of rooting (2.15 m). Ants and earthworms were also responsible for the formation of tubular macropores, but ants could not be found below 1 m depth, nor earthworms below 1.5 m depth. Based on his findings, the author noted that tubular pores formed by roots should have the following characteristics:

- diameters similar to roots present or in the recent past
- dendritic character
- side channels smaller in diameter than main channels
- constant angles between side and main channels, close to 90°
- lateral spurs of subsidiary pores caused by root hairs
- tapering diameters of perennial roots

The management history of the soil, primarily the extent to which tillage is employed and the selection of crop rotation strategies, influence the growth of roots in the soil. Groenvelt et. al. (1984) examined the suitability of a soil to accommodate growing roots based on existing pore space for unobstructed root growth, and obstruction imposed by the soil matrix. The two treatments measured were continuous corn (five years) and a forage rotation (three years forages, two years corn). In the long term, roots could face fewer overall obstructions in the forage plots than in continuous corn plots.

Examination of root systems reveal growing plant roots tend to follow pathways of least resistance (Jarvis and others, 1987). Living plant roots seem to either fill the larger pores or cause them to decrease in size by rearranging soil grains during growth. After the roots have died and decayed, the remaining macropores are most important in solute transport at high gradients (Gish and Jury, 1983).

Macropores in the form of root channels can transport large volumes of water, but the effectiveness of these macropores is determined by the quantity of water conducted and how often water is conducted. Bouma et al. (1981), working with cores of 55% clay covered by a grass crop with a 20 cm effective rooting depth, conducted infiltration experiments using irrigation events of various intensities, durations and scheduling patterns. Higher moisture content at the soil surface resulting after an initial shower induced more rapid surface ponding and more short-circuiting in a subsequent shower.

4. Effect of Earthworms. Zachmann and others (1987) observed on a silt loam soil macropores were less continuous in tilled plots than those under no-till, resulting in more bypassing of water to greater depths under no-till. Increased infiltration under no-till is

also due to increased earthworm activity, whose survival is much higher when tillage does not occur, especially for earthworm species which are both surface and subsurface dwellers. Furthermore, earthworm activity which produces burrows open to the soil surface is more than doubled when crop residues are left on the surface rather than incorporated.

Ehlers (1975) found earthworm channels 2-11 mm in diameter reaching depths as great as 80 cm, and observed any channel not connected to the soil surface did not contribute to water infiltration. Conducting channels in untilled soil had a maximum infiltration rate of 1 mm/min, but occupied only 0.2% of the pore volume.

Jones et. al. (1993) added two earthworm species (*Lumbricus terrestris* L. and *Lumbricus rubellus* L.) to septic tank filter fields. The earthworm species produced channels 2.3 mm and 8.4 mm in diameter respectively, which, as demonstrated on soil columns, increased effluent fluxes from $1.9\text{-}2.9 \times 10^{-6}$ m/s to $4.8\text{-}12.4 \times 10^{-6}$ m/s within 80 days.

Similar to macropores formed from plant roots, the effectiveness of earthworm channels as flow pathways depends largely on the nature of the rainfall event. Edwards et. al. (1993) observed atrazine movement with water through earthworm burrows to be greatest when high-intensity rainfall occurred shortly after atrazine application. Atrazine movement was greatly reduced by any delay in rainfall and low-intensity rainfall events prior to high-intensity events that produced percolate.

5. Effect of Tillage Practices. The influence of various tillage practices on several

environmental aspects is an area where macropore flow plays a key role. Management practices such as reduced tillage or zero tillage have been demonstrated to have several benefits for soil conservation. Logan and others (1987) define conservation tillage as a variety of reduced tillage practices that leave 30% or more crop residue on the soil surface at the time of planting. With reduced tillage, the presence of macropores at the soil surface increases, and along with less incorporation of chemicals there is greater potential for infiltration and chemical leaching. Isensce et. al. (1990) measured pesticide residue levels in groundwater and found residue levels 2 to 50 times higher under no-till than under conventional till, due to the increased occurrence of preferential transport.

Given the risk of increased leaching potential and groundwater contamination under no-till conditions, tillage may be an effective means of reducing macropore flow. Carter (1988) found "a greater proportion of the tillage-induced macropores under moldboard plowing, compared with direct drilling, were isolated pores or non-functional in regard to water transmission". Similarly, Wopereis and others (1994) looked at shallow (0-50 mm) surface tillage as a means of reducing bypass flow water losses in rice-growing areas where soils crack over highly permeable subsoil. By making the cracks discontinuous, water losses were reduced by 45-60%.

Mwendera and Feyen (1993) concluded infiltration into freshly tilled soils was best described by exponentially decaying functions with the process controlled by conditions and properties at the soil surface.

Although zero tillage prevents the destruction of macropores near the soil surface, more pronounced effects of compaction on zero tillage tend to offset an increase in macroporosity. Shipitalo and Protz (1987) found the macroporosity of no-till Ap horizons of a silt loam soil in corn for seven consecutive years was approximately half of that for conventional till Ap horizons. Compared to macropores under conventional till, the macropores in the no-till plots were smaller in mean pore size, more elongated, less tortuous and oriented parallel to the soil surface rather than randomly oriented. An increase in burrowing earthworm activity below the Ap horizon in the no-till pedon, resulting in 2-9 times more bioporosity than under conventional till, may counteract the loss of macroporosity in its surface horizon.

Instances have been noted where infiltration rates under conventional tillage are considerably higher than under zero tillage. Pikul, Jr. et. al. (1990) measured spring infiltration rates in the Pacific Northwest to be 9.2 mm/h in no-till, 22.3 mm/h in chiseled stubble and 23.5 mm/h in paraplowed stubble. In the chiseled treatment, macroporosity decreased from 20% at 7.6 cm depth to less than 1% at 25.4 cm. The paraplowed treatment decreased to a minimum of 6.9% at 12.7 cm, then increased to a maximum of 17.2% at 25.4 cm. The no-till treatment had a macroporosity less than 1% throughout the profile. Consequently, it is crucial to determine the amount of effective, continuous macroporosity present in a soil regardless of the type of tillage practice in use.

In summary, tillage can either increase or reduce preferential transport depending on the conditions of the horizon to be tilled. If tillage breaks up a horizon of continuous macropores, preferential transport is reduced; if tillage breaks up a compacted surface layer, preferential transport is increased.

6. Macropore Flow and Solute Movement. Nitrate-nitrogen and leachable pesticides must be managed carefully to prevent leaching and groundwater contamination due to macropore flow. Under saturated conditions, such as during a heavy rainfall or irrigation event, solutes in the macropore volume were lost much more rapidly than those in the micropore volume. However, under less than saturated conditions, such as a light rain, solutes moved into the soil matrix, reducing their potential for transport. It was determined that if leachable solutes have more time to diffuse into the soil matrix and be utilized, there is less chance of these solutes leaching down the soil profile by a heavy rain (Steenhuis and Muck, 1988; Shipitalo et. al. 1992).

Kosmas et. al. (1991) found the amount of nitrate leached in the bypass water was small (0.01-1.8% of that present in soil cores), particularly if the nitrates were allowed to diffuse into the soil peds before irrigation began. Rainfall timing was also an important factor in pesticide movement, with the greatest leaching losses of pesticide residues occurring when rain fell shortly after pesticide application (Isensce and coworkers, 1990).

Lund et. al. (1974) concluded that profile characteristics such as particle size distribution, organic matter content, cation exchange capacity and how these factors vary with depth are highly significant in determining nitrate concentration in the 1.8-8 m depth. The presence of duripans and accessibility to groundwater are also major factors determining the likelihood of groundwater contamination. Isensce and others (1990) found pesticide residue levels two to four times higher in unconfined groundwater than in confined groundwater.

7. Using Tracers to Study Infiltration. Tracing techniques identify flow into macropores which starts as soon as the application rate of water exceeds the infiltration rate of the soil; therefore one expects a higher application rate to induce an earlier macropore flow response. Other indicators of preferential flow are coatings of clay along the walls of larger pores and mottling patterns on the walls of pores. Under unsaturated conditions, iron is reduced on the pore walls but is oxidized some distance from the pore as water moves from the pore to the aerobic soil matrix (Veneman et al., 1976; Verpraskas and Bouma, 1976). Tracers also distinguish between flow inside different types of macropores. For example, flow of water into tile drains in heavy clay soils followed only planar voids and not root channels. This knowledge was extremely important in implementing the proper management decisions for effective tile drainage of this soil (Bouma, 1981).

Bouma et. al. (1977) emphasized the need to use dyes to characterize pore continuity which influences K_{sat}. Thin section analysis provides no indication of macropore continuity and cannot determine whether a macropore contributes to flow. Flow through macropores is governed by "pore necks" so that flow occurs along the walls of macropores without filling the entire pore. Since these "pore necks" can occur anywhere along the pore, estimating K_{sat} from a thin section at the bottom of a pore may give unrealistically high values.

Shortly thereafter, Bouma et. al. (1979) attempted to estimate the sizes of the "pore necks" in the flow system. "Pore necks" are assumed to determine K_{sat}, based on the strong effect the variability in the width of the "necks" has on water flow. The active voids (stained voids) contributed less than 1% of the volumetric makeup of the soil, but affected the flow so extensively that calculated K_{sat} values were only close to measured K_{sat} values when continuous vertical pores greater than 100 μm in diameter were absent.

Logsdon et. al. (1990) used methylene blue as an indicator of macropore continuity. Pores greater than 0.4 mm in equivalent diameter ranged from 100 to over 3000 per square meter (0.1-2% of the total area). Based on the descriptions of biopore area, cracks, soil structure and soil texture the authors could estimate K_{sat} within a range out of eight defined classes (Nowland, 1981).

Diab et. al. (1988) compared two tracers, methylene blue and oxygen-18 (^{18}O), in monitoring preferential flow. The soil horizon they studied was a Bt horizon (Soil Taxonomy), consisting of a silty clay loam prismatic brown matrix 54 - 80 or 90 cm below the surface. Within the matrix were subvertical grey, silt loam tongues surrounding the prisms, consisting of many very fine to coarse tubular and vesicular pores. Methylene blue is transferred in saturated conditions in the field and in undisturbed cores, and is a good indicator of functional porosity. ^{18}O monitors the actual behavior of water under natural conditions. In a degraded and leached soil, ^{18}O revealed mean water transfer was ten times faster in the "tongues" (preferential paths) than in the Bt matrix, even though some of the tongues were non-functional. Methylene blue tracing showed functional porosity under saturated conditions was comprised only of the coarser and more continuous macroporosity inside the tongues. Compared to the soil matrix, these tongues had a lower clay content and lower cation exchange capacity.

Priebe and Blackmer (1989) surface-applied ^{15}N-labelled urea to undisturbed 20 cm diameter by 50 cm long soil cores at field capacitiy, then applied ^{18}O-labelled water to simulate a 25 mm rainfall event. Significant amounts of labelled water and urea were present in the first increment of effluent sampled, and labelled urea and water moved much deeper and was more dispersed in all of the soil cores than expected. Yet these rapid flow values were considered to be underestimates of the true values for two reasons: the small sample size provided little opportunity for lateral flow or the effects of microrelief, and the cement casing used to surround the cores may have blocked some of the macropores.

Bouma and Dekker (1978) conducted methylene blue tracer studies on four dry soils with different macrostructures under a variety of rainfall volumes and intensities. The number of colored bands increased with increasing rain intensity at any given applied water volume, and with an increase in the applied water volume at any given intensity. Increasing rainfall intensity or rainfall volume increases the contact area between soil and the water infiltrating through large pores, but this contact area was never more than 2% of the total pore volume.

An experiment was conducted by Booltink and Bouma (1991) using undisturbed soil cores and transducer tensiometers. Tensiometers within a few millimeters of macropores reacted quickly then showed a drying pattern after the rainfall. By contrast, tensiometers inside soil peds reacted slowly and showed continued wetting after the rainfall had ended, due to the internal catchment of water at the bottom of discontinuous macropores and the redistribution of water that followed as a result.

Zachmann and others (1987) found Br^- tracer movements deeper than 19 cm was most frequent under no-till treatments with worms and residues present.

Other tracers which have been used effectively are Acid-Red 1, an anionic, water-soluble dye which moves slightly slower than water (Ghodrati and Jury, 1990), and Lissamine green, or Acid Green 50 (Jarvis and others, 1987).

8. Voids in Thin Section. Brewer (1964) noted that different types of macropores have different degrees of effectiveness during water movement: planar voids or cracks may close upon swelling whereas tubular worm and root channels may remain open. Different types of macropores present throughout a soil profile may be examined using thin sections.

Thin sections are 0.02 mm thick slides or polished blocks of soil. They do not provide a continuous picture of soil morphological changes with depth, and they require expensive technology and expertise. Dyes and tracers must be used when preparing thin sections to examine the functional porosity and pore continuity of each sample (Bouma, 1981). Thin section preparation and analysis was discussed by Murphy and coworkers (1977), using the method described by Bascomb and Bullock (1974).

Bullock and Thomasson (1979) compared macroporosity described through image analysis to results from water retention measurements. Water retention experiments measure the diameter of the smallest exit point of the pore, whereas image analysis determines the maximum diameter of the pore. The greatest discrepancy between the two methods occurs in soils with many large pores made up of narrow exit necks.

On a silt loam soil, 9% slope and in no-till corn since 1960 in Ohio, Edwards and others (1988) found the number of pores was inversely proportional to pore diameter and increased with increasing depth. Mean pore diameter was 1-2 mm at all observed depths, and pores larger than 0.4 mm diameter occupied about 1.4% of the total area. Pore counts of those greater than 0.4 mm in diameter ranged from 3369-21 151/m^2 at 2.5 cm depth to 5673-28 966/m^2 at the 30 cm depth. The overall average pore count was 14 576/m^2, 160 of which were larger than 5 mm diameter.

9. K_{sat} and Types of Flow. Bouma (1991) explains the differences in notation for various flow phenomena. K_{sat} is saturated hydraulic conductivity, or the flux at a hydraulic gradient of unity and zero pressure when all pores are completely filled with water. K_{unsat}, in contrast, is unsaturated hydraulic conductivity, which is measured at a given suction when only micropores are filled with water. In addition to these two notations, there is $K_{(sat)}$, which differs from K_{sat} in that only the small pores are saturated while water runs down the walls of the macropores without filling them entirely. $K_{(sat)}$ is also measured at unit hydraulic gradient and zero pressure, but the values obtained for $K_{(sat)}$, in which the soil is not completely saturated, are very different from the values measured for K_{sat}. In fact, in soils with continuous macropores, K_{sat} may have a wide range of values and may not be accurately defined.

Bouma (1982) recognized the following problems in interpreting K_{sat} measurements for saturated soil horizons with continuous macropores:

- due to the shrinking and swelling of clay soils, K_{sat} continuously changes in these soils

- the effect of macropore continuity patterns results in K_{sat} being a function of sample size

- underlying or overlying horizons can dramatically influence the measured flux of a particular soil horizon

- when infiltration occurs through a variety of light surface crusts, the fluxes can have a wide range of values at saturation

For these reasons it is much easier to treat the flow system through macropores separately from the one through the soil matrix. The flow contribution of macropores can be found by subtracting the K_{sat} value of the soil matrix from the K_{sat} of the entire soil.

Lee and others (1985) measured saturated hydraulic conductivity (K_{sat}) on four sites in southern Ontario, each with a different soil texture, using three different measuring techniques: an air entry permeameter, a Guelph Permeameter (constant head well permeameter) and a falling head permeameter. At each site, there was a significant difference between some or all methods used to measure K_{sat}. These values varied increasingly with an increase in clay content, with values ranging over three orders of magnitude for a clay soil. The authors summarize the optimum situations for using each technique: the falling head permeameter is preferred for obtaining soil matrix dominated flow in a structured soil; in situations where a combination of macropore and matrix dominated flow is desired, the Guelph Permeameter is the instrument of choice; and the air entry or Guelph permeameters are best for estimating macropore dominated flow through a structured soil.

Lauren et. al. (1987) found K_{sat} measurements obtained in the laboratory were neither reliable nor comparable with attached soil cylinders measured in the field because of the increased short-circuiting occurring in the detached samples.

Clothier and Smettem (1990) observed on a fine sandy loam soil with large connected macropores, hydraulic conductivity changed three orders of magnitude from a tension of -100 mm to zero tension (saturation). The authors suggest a combination of lab and field measurements in order to most accurately define the saturated and unsaturated hydraulic properties of soil.

Bouma and others (1989) used soil morphological descriptions to determine which of several sample volumes gave the optimal sample volume for K_{sat} measurements in heterogeneous soil materials. Measuring horizontal areas made up of both materials gave a K_{sat} which was successfully estimated by approximating the cross-sectional area of materials and their proportional contributions to K_{sat}.

The "field saturated" hydraulic conductivity (K_{fs}), as measured with a Guelph Permeameter by Paige and Hillel (1993), is one to three orders of magnitude less than K_{sat} as determined by the other methods because of factors such as entrapped air, anisotropic conditions, smearing of the well walls, and the sensitivity of this method to hysteresis according to antecedent moisture conditions and discontinuous macroporosity.

Koppi and Geering (1986) demonstrated the effectiveness in using a quick-setting epoxy resin to provide an unsmeared soil surface; infiltration rates were 2.5 - 6 times more rapid than cut and smeared surfaces.

McKeague et. al. (1982) provided estimates of K_{sat} based on soil morphology observations and compared them with measured K_{sat} values from an air entry permeameter from 78 soil horizons of various textures. Soil morphology observations included texture, structure, porosity (including counts of biopores), consistency and density of the horizons. The estimates of K_{sat} were classified into one of eight classes which related specific soil morphological features to a range of K_{sat} (Nowland, 1981). The predictability of K_{sat} when based on soil morphology was remarkably high. 45% of the horizons had the same estimated class as the measured class, and 87% of the horizons were estimated to be within one class of their measured class. For the horizons with high K_{sat} values, the major contributing factors were abundant biopores, textures coarser than loamy fine sand, and fine to medium blocky structure. The major difficulties of this method were estimating the effectiveness of biopores and the K_{sat} of tilled near-surface horizons.

10. Modelling Macropore Flow. Steenhuis et. al. (1990) developed a model for macropore flow in the vadose zone to simulate solute movement. It involved a linear approximation of hydraulic conductivity as a function of water content that identifies pore groups in which water moves at distinct velocities.

Smettem and Collis-George (1985) studied macropore flow on a native pasture soil (dark brown, fine sandy loam) and introduced the following equation to describe macropore volume fluxes:

$$v = aR^b$$

where v is the flow in cm^3/s, R is pore radius in cm, and a and b are constants.

Hosang (1993) developed a two-phase model for preferential flow of water through soils. The first phase described redistribution and low infiltration of water into soil (matrix flow), while the second phase modelled heavy infiltration which produces macropore flow.

METHODOLOGY

A. Description of Sites and Samples

Sixteen contiguous core samples, obtained in 1991, from a hazardous waste management site in the rural municipality of Montcalm (NE 2-3-1E) were examined. Properties such as texture, color, and mottling were determined. In addition, features such as roots, biopores, slickensides, carbonates and salt deposits were described and their distribution measured with respect to depth. The soils were described according to The Canadian System of Soil Classification (Expert Committee on Soil Survey, 1987) and the Manual for Describing Soils in the Field for Manitoba Soils (Canada-Manitoba Soil Survey, 1992).

Two additional contiguous cores were sampled in September, 1993 for analysis of the pore water. One core was sampled at the waste management site (NE 2-3-1E) on the Red River series (UMA Engineering Report, 1991). This is a lacustrine clay (Red River clay) with hydrologic properties characteristic of a regional recharge area. The other core sample was taken near the town of Warren, MB, from an area where the groundwater was known to be saline (SW 35-13-2W) on the Dencross series (Canada-Manitoba Soil Survey, unpublished literature). At this site, the soil is a silty clay with hydrology evident of regional groundwater discharge (Betcher, 1980).

These locations were selected because of their contrasting hydrologic regimes; the first site is a regional recharge site, whereas the second site is a regional discharge site. Contrasting hydrologic regimes should provide insight into the degree of influence groundwater and salinity have on the development of Vertisolic features and the permeability of clay soils.

The contiguous cores were obtained using a truck-mounted, split spoon sampler, approximately 62 mm in diameter. After drilling was complete, the holes were backfilled with bentonite pellets to 1-2 m below the surface and then backfilled with soil to the surface. The cores obtained in 1993 were double wrapped in plastic and transported back to the laboratory on a sheet of plywood fixed with small wooden slabs to hold the cores stationary. The cores were refrigerated in the laboratory to minimize evaporation. The physical properties according to depth were recorded as before and subsamples were immediately frozen for nitrate content determination. Various sections from each core were analyzed for stable isotopes (tritium) in the groundwater, soil moisture content, saturated hydraulic conductivity, micromorphology and carbon-14 content of roots found at depth in the subsoils.

Notation used on these samples consisted of:

- site name (Montcalm or Warren)
- year retrieved (1991 or 1993)-abbreviated '91 or '93
- location or test hole # - abbreviated TH
- depth of subsample (in meters)
  (eg. Montcalm '91 TH 16 0-0.8)

Twelve cores, approximately 35 mm in diameter, were sampled from the Black Lake Series to a depth of 0.8-1.2 m using a Giddings soil sampler and probe. Samples were collected on four different types of crop rotation/tillage practices observed over two growing seasons: alfalfa-alfalfa/no tillage, alfalfa-wheat/alfalfa removed by tillage, wheat-wheat/zero tillage, and continuous summerfallow/conventional tillage.

B. Determination of K_{sat} in the Field

Management practices, such as the frequency of tillage and type of cropping patterns, have been shown to dramatically affect the infiltration of a soil (Groenvelt et. al., 1984; Zachmann et. al., 1987; Shipitalo and Protz, 1987). A Guelph Permeameter was used in the field to investigate the effect of management and management history on saturated hydraulic conductivity (K_{sat}) of a Black Lake series (Cumulic Regosol). The investigation site was the Department of Plant Science research plots (The Point) on the University of Manitoba campus. The work was conducted during the summers of 1993 and 1994. Two replicates of four different treatment plots (alfalfa, summerfallow, and zero-till wheat, before and after alfalfa) were measured using a Guelph Permeameter at three depths (25, 50 and 75 cm). Soil samples were collected at 25, 50 and 75 cm depths for moisture content and bulk density. The loose samples were oven dried at 105°C and volumetric water content was calculated.

One of the difficulties of measuring K_{sat} in a fine textured soil was the occasional development of negative pressure, which resulted in water from the bore hole moving into the Guelph Permeameter rather than into the soil. In order to reduce the possibility of negative pressure developing, a spike tooth roller rather than a wire brush was used to clean the walls of the bore hole and reduce the likelihood of smearing and creating a soil layer that inhibits water movement. It was discovered later that a J-cloth produced more uniform bubbling and also prevented soil particles from clogging the outlet. The large reservoir on the Guelph Permeameter was covered with aluminum foil to provide shade and minimize temperature and pressure changes due to heating by the sun.

C. Determination of K_{sat} in the Laboratory

Laboratory determinations of K_{sat} were performed on the soils at the Montcalm and Warren sites in order to discover whether non-Darcian behavior occurs in these clay soils. It was also desirable to compare K_{sat} values from the laboratory with those obtained in the field from previous studies.

A total of five subsoil samples were used to determine the water flux at a range of hydraulic gradients. Samples from above and below the water table from the two sites were used in this experiment. Each core sample (approx. 62 mm diameter) was placed into a plexiglass sleeve (approx. 58 mm inside diameter) using a cutting head placed over the plexiglass sleeve on a hydraulic press, which shaved off the outer diameter of the cores. Both faces of each sample were cut with a thin wire (guitar string) to give a flat surface with minimal smearing. The ends of the sample were covered with cloth, porous plastic screens and plexiglass endplates, then fastened with three bolts and six wingnuts (Fig. 3). The endplates have an opening in the center which allows water to enter the sample via plastic tubing. To saturate the samples, the cores with sleeves and endplates

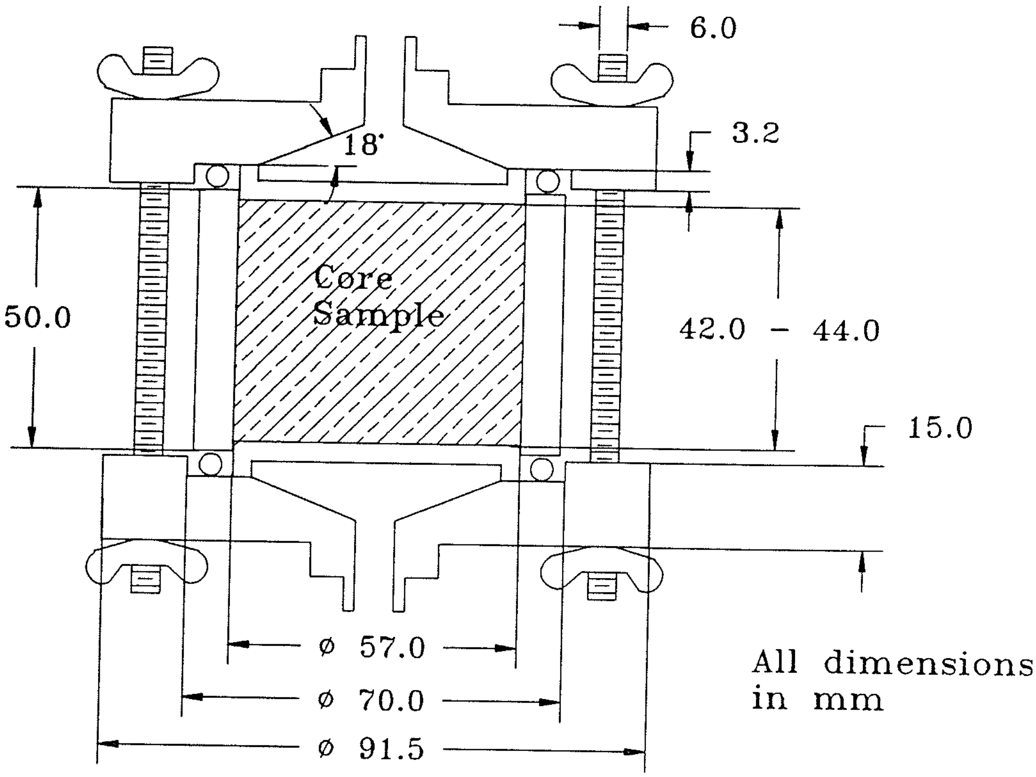

Figure 3. Sample holder for laboratory K_{sat} determination (modified after Karthigesu, 1994).

were placed in a chamber connected to a vacuum pump. The chamber was filled with enough water to completely submerge the samples. To eliminate any ionic strength effects on aggregate stability, groundwater was used to saturate the samples. Groundwater was retrieved from the same site as the soil samples and from as close to the same depth as the soil samples as possible to ensure that the solute content and pore chemistry of the samples closely modelled field conditions. The samples were placed under vacuum in submerged conditions for two to three weeks to remove any dissolved air. Once saturated, the samples were removed from the vacuum chamber. Any bubbles remaining in the ends of the samples were sucked out using a syringe with a rubber tube. The endplates were each connected to plastic tubing filled with distilled, de-aired water which served as the inflow and outflow for water moving through the sample once connected to the flow meter. The inflow tube was connected to the top of the samples to simulate percolation of surface waters.

Saturated hydraulic conductivity was determined in the laboratory. Soil samples were placed in a controlled temperature (20°C$\pm$0.2) insulated box. Temperature was continuously monitored using a thermistor and a computer for data storage.

The plastic tubing connected the sample to two capillary tubes, 0.8 mm in diameter, which were filled with water (Figs. 4 and 5). A small bubble of immiscible red dye was placed in the capillary to detect movement (Fig. 6). Two adjustable burets were used to establish a gradient. Water was pushed into one end of the sample and forced out the other. Water flow caused the bubbles in the capillary tubes to move a given distance in a specified amount of time. From this information, a value for the flux

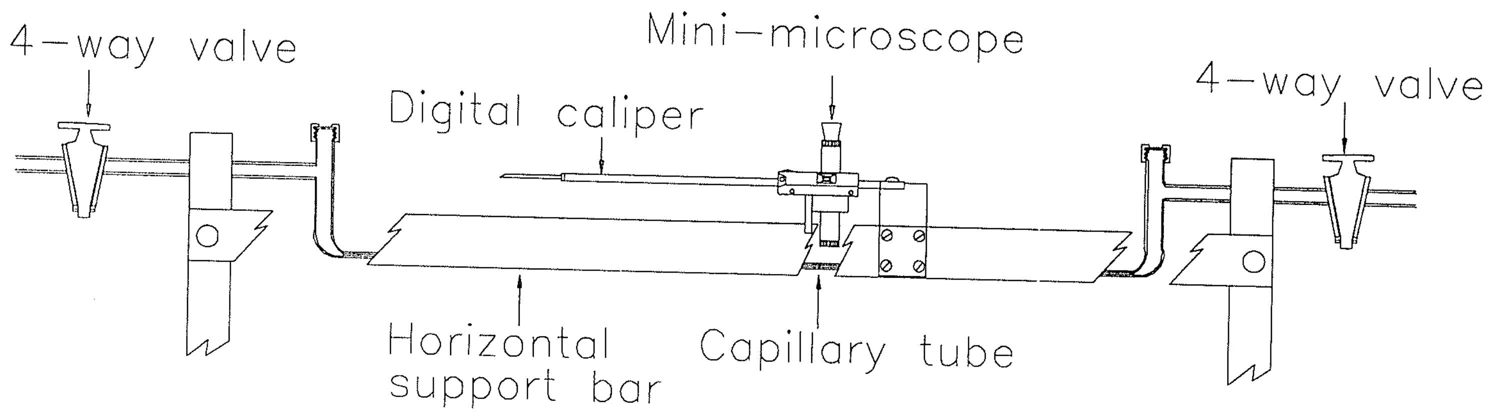

Figure 4. Side view of capillary tube apparatus (Karthigesu, 1994).

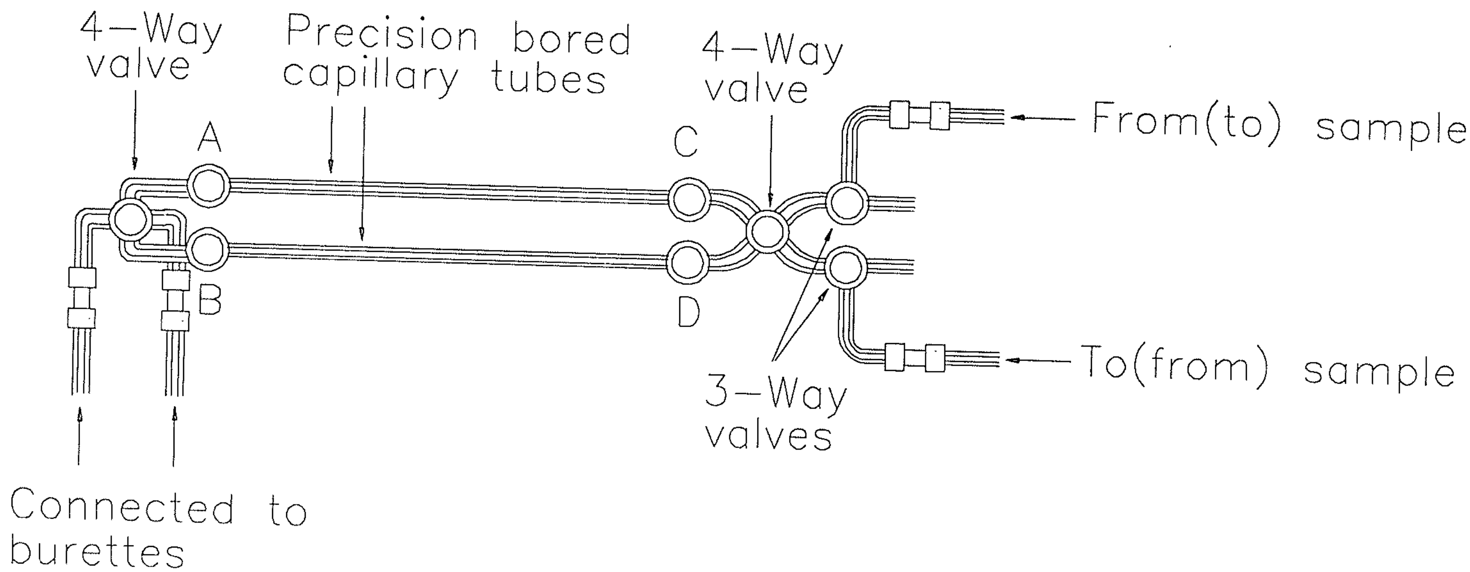

Figure 5. Top view of capillary tube apparatus (Karthigesu, 1994).

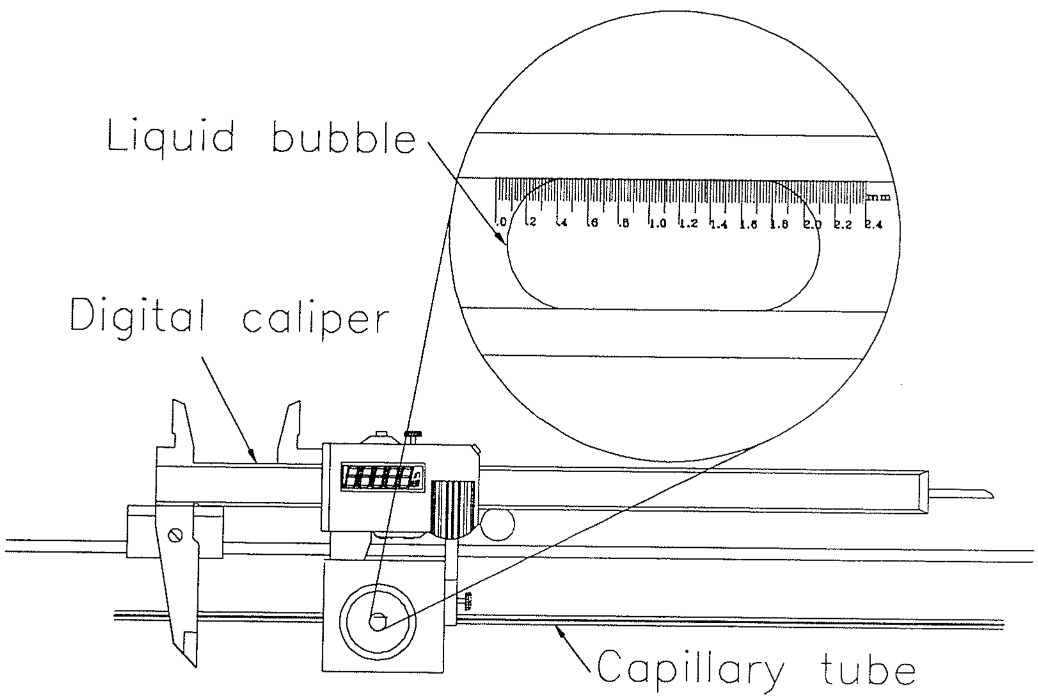

Figure 6. Detection of bubble movement in capillary tube (Karthigesu, 1994).

at the inflow and outflow was determined.

The capillary tubes were frequently rinsed with distilled, de-aired water, usually once a day. Rinsing prevented foreign particles such as dust or microbial growth from reducing flow through the capillary tubes, which would underestimate flow through the sample.

Rinsing was required when bubble movement was hesitant, due to increased friction between the bubble and capillary wall, when the bubbles disintegrated, and when reduced flow between replicates at a given hydraulic gradient occurred. To remedy this condition, the capillary tubes were filled with CLR (phosphoric acid), left overnight, and thoroughly washed with clean water the next morning. Because the dye in the bubbles was broken down by CLR, the bubbles were removed with a syringe and replaced with new ones after rinsing. In extremely dirty situations, as with caked on residues, CLR was added and a fine thread composed of a series of knots was pulled through the capillary tubes using fishing line to dislodge any particles adhering to the capillary walls.

K_{sat} of the first sample tested (Montcalm '91, TH 1, 43.5 ft) was measured at gradients of 0.6, 0.8, 1.0, 1.2, 1.5, 2.0, 5.5, 8.0, 12.0, and 16.0. This sample was slightly longer than the other samples (44 mm) because, unlike the subsequent samples, no spacers were included to provide additional room between the endplate and cover for the syringe during air bubble removal.

Bubbles would often move in the same direction in both capillary tubles at low gradients, indicating that the sample was adsorbing water. This problem was due to wide temperature fluctuations in the laboratory which made constant temperature control in the sample chamber difficult. Hence, it was doubtful that additional measurements at lower gradients would have been possible under these conditions. To remedy the problem of temperature fluctuations, the entire apparatus was placed into an environmental chamber under a relatively constant temperature of 20°C. The environmental chamber eased the workload of the smaller sample chamber temperature regulator so that sample chamber temperatures only varied between 19.7 - 20.1°C.

K_{sat} of the second sample (Montcalm '91, TH 8, 5-7.5 ft) was measured at gradients of 0.4, 0.6, 0.8, 1.0, 1.2, 1.5, 2.0, 5.0, 8.0, 12.0, 16.0, and 20.0. Measuring low-gradient flow which approached the threshold gradient (i_o) (Fig. 7) of the apparatus (0.4-0.45) was difficult because the resistance to flow in the capillary tubes was too large to allow flow to occur (Dixon, 1995). To remedy this problem a pressure transducer was connected to the flow meter to monitor the actual hydraulic head that was imposed on the sample. Preliminary use of the transducer showed interference from the capillary bubbles of dye which made it difficult to acheive stable transducer readings. Friction between the bubbles and the capillary walls resulted in back and forth, piston-type movement of the bubbles, which resulted in erratic, pulsating readings on the transducer. A wetting agent was contemplated to reduce the friction between the bubbles and the capillary walls, but this was not attempted for fear of adverse effects on the solubility of the bubbles and possible contamination of the sample. To overcome this, the bubbles and some of the water in the capillary tubes were removed, leaving an air-water interface whose meniscus could be traced by the microscopes. With air now introduced into the capillary tubes, the pressure transducer could then be used to indicate the amount of head

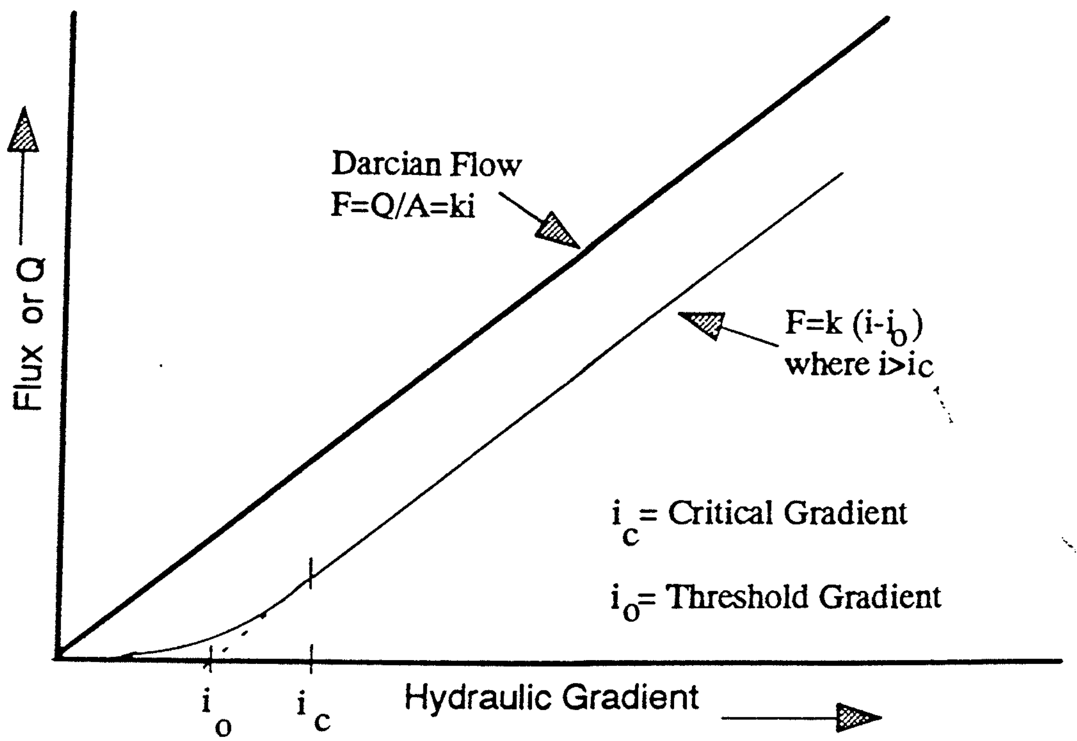

Figure 7. Flux-hydraulic gradient relationships typically reported (Yong and Warkentin, 1975).

to which the sample was subjected. Gradients of 0.2, 0.3, 0.4, 0.8, 1.0, 1.2, 1.5, 2.0, and 3.0 were measured with the pressure transducer on this sample.

The third sample to be measured (Warren '93, 0.2-0.9 m) contained numerous biopores and had a higher silt content. One or both of these factors resulted in transmission of water too quickly and at inconsistent pressures to be measured by the capillary flow meter. Instead, a simple falling head permeameter was constructed, with the sample connected to a reservoir of distilled, de-aired water filled to a given height. The outflow was open to the atmosphere and positioned at a height just below that of the water level in the reservoir in order to establish a gradient and initiate flow. Gradients of 0.2, 0.3, 0.4, 0.6, 0.8, 1.0, 1.2, 1.5, 2.0, 3.0, and 5.0 were imposed in increasing and decreasing order. It was determined that each drop of water formed at the end of the outflow tube weighed 0.05 grams (and thus occupied a volume of 0.05 cm^3). The flux was calculated as:

$$q = v/(At) \times 100$$

where

q = flux (m/s)
v = volume of water drop (cm^3)
A = cross-sectional area of sample (cm^2)
t = time (s)

Unlike the other three samples measured, this saturated flow experiment was performed outside the environmental chamber at room temperature (approximately 24°C).

Unfortunately, the flow of water through the other three samples did not always move smoothly at gradients less than two. Because the samples were probably not completely saturated and thus had not yet reached equilibrium, absorption of water would periodically occur. As a result, water in the inflow and outflow capillary tubes would flow in the correct direction for a short time, but at some point the air-water meniscus in one or both of the capillary tubes would slow down and begin to flow in the reverse direction. There were times when this pulsating action of the meniscii could not be visually detected but was displayed by the transducer as a series of cyclic high and low readings. This was sometimes remedied by leaving the apparatus to flow undisturbed for one to three days, until flow was in the correct direction. Another helpful strategy was to begin the flow measurements with the meniscii at the centre portion of the capillary tubes to minimize disruption of the air columns. Unequal lengths of air columns between inflow and outflow may affect pressure readings measured by the transducer. A repeating cyclic pattern indicated that the water passing through the sample required a certain force to overcome the resistance imposed by the apparatus as well as the soil sample itself. Any air trapped within the sample may be compressed and display elastic forces, as may be the case for the plastic tubing connecting the sample to the glass capillary tubes. Therefore, the water must overcome a repeating cycle of increased resistance to flow followed by a period of low resistance. This phenomena could explain the piston-type movement, recorded by the transducer.

The transducer is very sensitive to vibrations and jarring movements, so to minimize reading fluctuations, foam was placed under the transducer and the capillary tube apparatus. Occasional fluctuations in transducer pressure readings still occurred due to bumping of the apparatus while taking measurements and from closing the door on the environmental chamber. Foreign material tends to collect at the ends of the capillary tubes and impede movement of the air/water columns in this area. Also, not all water is effectively removed when producing an air column in a capillary tube. Thus, thin films of water remaining on the walls of the capillary tubes may coalesce to form water drops in the air-filled portion of the capillary tubes which produce erroneous measurements by the pressure transducer. Therefore, care must be taken to ensure water is kept out of the air-filled portion of the capillary tube so that the air column remains as one long, continuous bubble. A syringe or a piece of J-cloth with wire were effective tools for water removal.

Usually six measurements of net meniscus movement in the capillary tubes were timed in order to calculate the rate of flow through the sample at a particular gradient. To do this, the cross-sectional areas of the sample and the capillary tube must be known. The values calculated from the outflow capillary tube were plotted on a graph of the log of hydraulic flux versus the log of hydraulic gradient. Similar plots of flux-gradient relationships have been presented by Sri Ranjan and Karthigesu (1992), Sri Ranjan and Gillham (1991), Dixon et al. (1993a) and Karthigesu (1994). Interpretation of these data was based on Darcy's Law of water flow. If a series of K_{sat} measurements for a given sample yielded a straight line with a slope of one, then Darcy's Law was obeyed. If, at the lower gradients, the series of points deviated from this line, then Darcy's Law overestimated low gradient flow in clay soils, which is known as non-Darcian behavior.

D. Electrical Conductivity/Soluble Salt Content

The amount and type of salts in the Montcalm and Warren soils were measured to characterize the hydrologic regime of each soil. The presence of salts also provides clues to the soil's moisture status and potential for downward flow of water.

Eleven samples of the cores obtained in 1993 from the two sites were made into saturated pastes and filtered under suction in order to measure the electrical conductivity of each filtrate. The filtrate samples were further prepared (diluted if necessary, treated with $La_2 0_3$) to measure the concentration of cations (Ca^{++}, Mg^{++}, Na^+) and anions ($SO_4^=$, Cl^-, HCO_3^-) using atomic adsorption for the cations and titrations for the anions.

E. Thin Section Analysis

The core samples were examined in thin section to determine if near surface slickensides are formed by similar means as slickensides at depth.

Thin sections of eleven samples from both the Montcalm and Warren sites were prepared. The samples were saturated with acetone to remove the pore water. Once this was complete, the samples were impregnated with resin to form hard blocks of soil. The blocks were cut and polished into thin slides that can be viewed under a microscope or image analyzer to examine soil fabric and pore characteristics. The samples analyzed were:

Table 1. Samples used for thin section analysis.

Site and Year	Depth (m)	Pedologic/Geologic features*
Montcalm '93	0.2	slickenside @ 30°
Montcalm '91 TH 2	3.8	biopores, root, fractures
Montcalm '93	4.8 - 5.5	2 slickensides @ 45, 60°
Montcalm '91 TH 8	4.9	slickenside @ 65°
Montcalm '91 TH 3	6.4	slickenside @ 40o
Montcalm '91 TH 1	13.1	slickenside @ 35°
Warren '93	0.1	slickenside @ 45°
Warren '93	0.3 - 0.4	2 slickensides @ 40, 25°
Warren '93	1.0	matrix, carbonates, salts
Warren '93	4.0 - 4.1	clay/till interface
Warren '93	5.4 - 5.5	till/sandy till interface

*pedologic features refers to those features which are found within a 1 m deep control section

Thin sections were observed under plane polarized light (PPL) and cross-polarized light (XPL) for the number and type of voids, type of fabric, orientation of fabric, illuviation of clay, and types of minerals present (Douglas, L. A. 1990; Stoops and Eswaran, 1986; Fitzpatrick, 1984).

An image processing system (ImageX), developed by Dr. L. Lamari of the Department of Plant Science, University of Manitoba, was utilized to photograph the thin sections under plane light and to calculate the percent area occupied by voids (porosity). Each slide was placed on a light table (orientation arrow pointing down so that image is right-side up on the viewing screen) and viewed through a 100 mm macro camera lens approximately 15 - 20 cm above the slide. The image of the slide was projected onto a computer screen where it was frozen and the percent void space calculated.

F. Isotope Analysis of Pore Water

Tritium analysis of pore water is used to distinguish between waters of different ages, which provides information on the hydrologic regime and the recharge potential (penetration of recent water) in a given soil (UMA Engineering Ltd., 1992).

Eight samples were measured to determine the tritium content, and thus the relative age, of the pore water. The samples analyzed were:

- Montcalm 0.2-1.0 m	- Warren 0.0-0.9 m
- Montcalm 2.8-3.2 m	- Warren 2.3-3.1 m
- Montcalm 3.3-3.9 m	- Warren 3.1-3.7 m
- Montcalm 5.5-6.2 m	- Warren 6.1-6.5 m

Enough sample water was extracted from each sample to completely fill a 125 mL plastic bottle. The technique used by the Environmental Isotope Laboratory to detect and quantify tritium is known as liquid scintillation counting (LSC), which has a lower limit of detection of approximately six tritium units (Drimmie et al. 1991.)

The analysis involved various treatment pathways according to the conductivity of the sample and whether or not those samples with low conductivity are clear and colorless. Distillation (if necessary) separates the salts from the water sample. The sample was mixed with a low level tritium cocktail (Canberra-Packard Pico-fluor LLT) which had a high carrying capacity for water and low background characteristics. The laboratory standard contained tritium reference material diluted with background water from a well with radiocarbon activity older than 3500 years and a conductivity less than 0.3 dS/m (Mary Ellen Patton, technician, Environmental Isotope Laboratory, University of Waterloo, personal communication).

The isotope to be traced was tritium (^{3}H), measured in tritium units (TU) which is one tritium atom present for every 10^{18} atoms of hydrogen (^{1}H) present. The half-life of tritium was measured to be 12.3 years. Therefore, rainwater prior to 1952 was estimated to contain 5-20 TU (Payne, 1972). Groundwater recharged before 1953 would have 2-4 TU. Modern (post-1953) rainwater was measured between 50-100 TU (Solomon and Sudicky, 1991). Consequently, groundwater samples in which tritium levels were greater than 5-10 TU would be considered "modern" (post-1953).

G. Determination of Age of Roots Using ^{14}C Analysis

Roots were carbon dated to determine the depth of rooting by modern plants.

Roots at depths well below the expected root zone for annual crops or native grasses were found in two samples. One of the samples was a dense till sample from SW 14-9-12E, approximately 3.5-3.7 m below the surface. Carbon dating of the roots was conducted from this sample.

RESULTS AND DISCUSSION

I. Physical Features

A. Results - Montcalm Site

In the sixteen test cores from the Montcalm site, the texture was commonly heavy clay, with occasional silt lenses which resulted in a silty-silty clay texture within 2 m from the surface. Slickensides were found throughout the mapped area at various depths (0.9 to 13.1 m) with greatest occurrence between 4 to 11 m below the surface (Fig. 8). Average angle of the slickensides was between 22 and 45 degrees, which remained relatively constant regardless of depth (Fig. 9). Extremes in slickenside inclination varied from 15 to 65 degrees from the horizontal. Gravimetric moisture content varied from air dry (11%) to saturation (60%), with the majority of the soil samples at a moisture content of approximately 45 per cent.

Evidence of mottling in the form of iron and manganese staining was most common around the 2 m depth. Carbonates were concentrated in silt lenses usually within 2 m of the soil surface. Testing with dilute hydrochloric acid found carbonates present in trace amounts below this depth. Overall salt content at the Montcalm site was low, with electrical conductivities (EC) from various cores and depths less than 1.3 dS/m (Table 2).

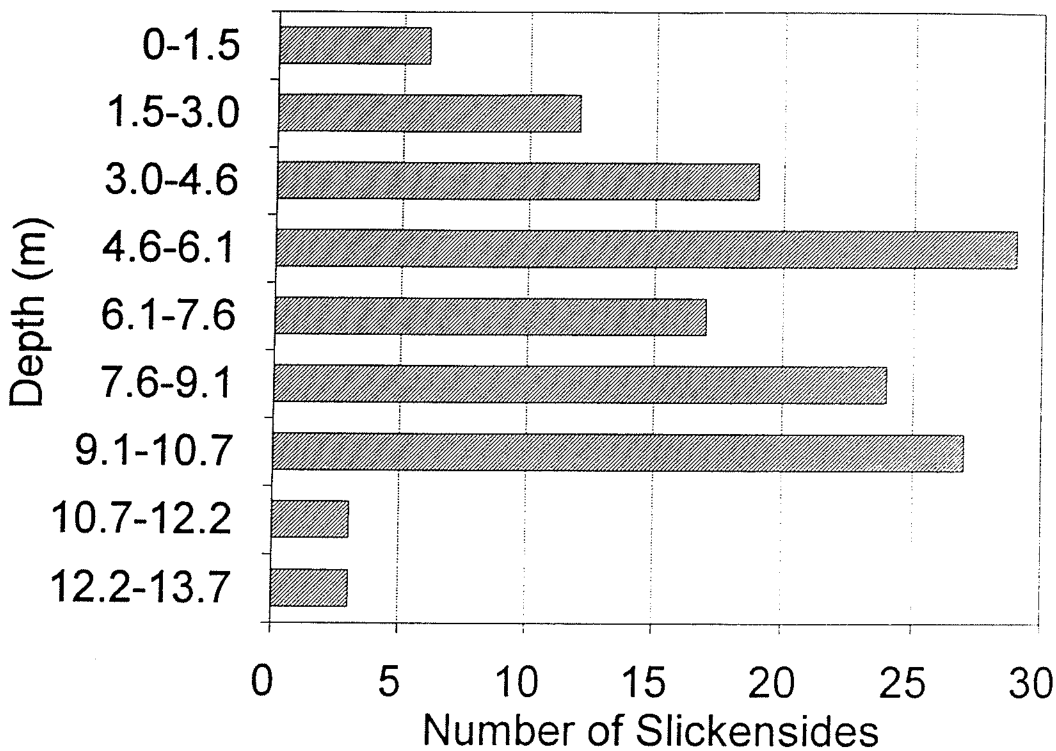

Figure 8. Distribution of slickensides at Montcalm site.

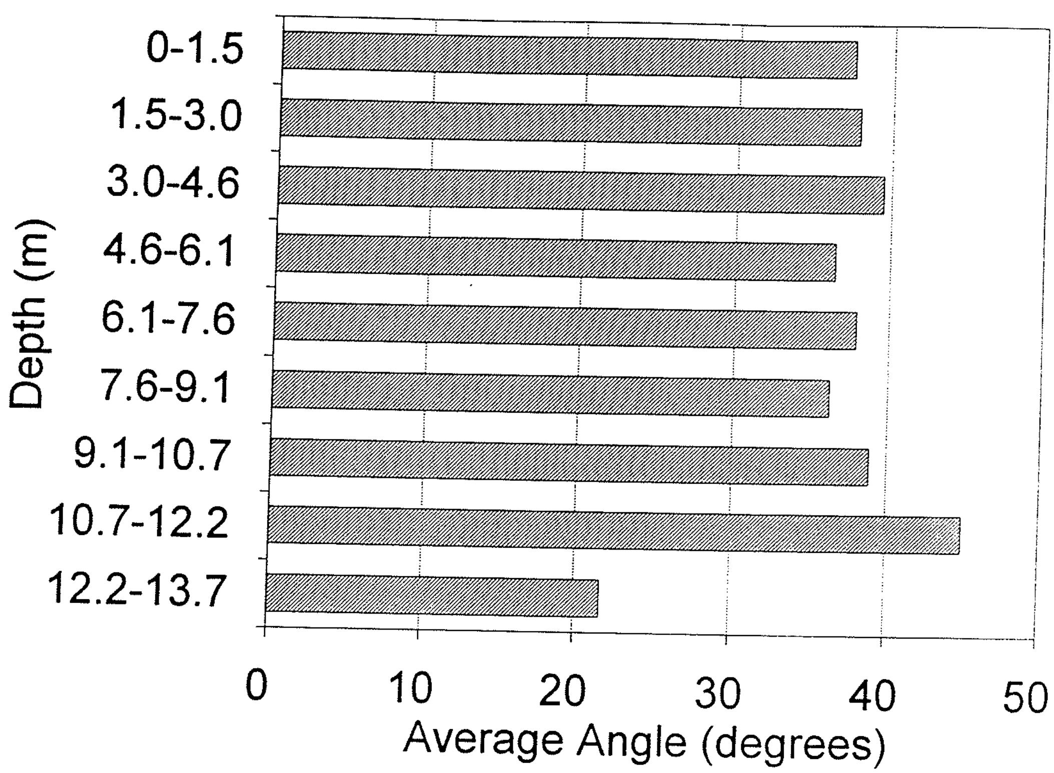

Figure 9. Average slickenside angle at various depth intervals at Montcalm site.

Table 2. Soluble salt analysis from the two sites.

Sample #	Site	Depth	Conductivity (dS/m)	Ca++	Mg++	Na+	Total Cations (meq/L)	SO4=	Cl-	HCO3-	Total Anions (meq/L)
1	Montcalm	surface	0.7	3.5	1.6	1.3	6.4	N/A	0.7	N/A	N/A
2	Montcalm	1.5	0.5	2.3	0.9	1.6	4.8	1.0	0.3	3.5	4.8
3	Montcalm	3.2	0.6	2.4	1.0	2.7	6.1	5.8	0.3	0.0	6.1
4	Montcalm	5.8	1.3	4.9	1.7	5.7	12.3	11.6	0.7	0.0	12.3
5	Montcalm	8.2	1.2	6.3	1.4	5.9	13.6	10.5	0.9	2.2	13.6
6	Montcalm	11.5	1.0	4.2	1.1	4.3	9.6	4.2	1.0	4.4	9.6
7	Montcalm	13.0	1.1	7.0	1.3	4.5	12.8	7.1	1.3	4.4	12.8
8	Warren	surface	15.7	19.3	55.7	101.4	176.4	66.4	106.1	3.9	176.4
9	Warren	1.5	17.8	57.4	69.9	96.5	223.8	96.7	124.0	3.1	223.8
10	Warren	3.2	12.9	28.7	37.7	65.1	131.5	55.4	73.0	3.1	131.5
11	Warren	5.0	6.1	10.3	13.1	50.8	74.2	26.4	44.8	3.0	74.2
12	Warren	5.8	5.8	9.9	7.7	46.6	64.2	23.3	38.0	2.9	64.2

Occasionally, salt deposits (gypsum) were found in old root channels; other samples contained small salt precipitates throughout the soil matrix.

Roots, when present, occurred from the soil surface to depths of 6.5 m. Generally, root abundance decreased sharply after 20 cm and again after 1.5 m. In some instances, no roots could be found in an entire soil core. Root growth was most restricted in those cores which contained high carbonates and prominent mottles within the top 1 m of the soil profile. Old root channels filled with gypsum, sodium sulfates and sometimes partially decayed root material were found at 3-5 m depths in four of the cores.

A brief summary of the core sample from Montcalm in 1993 showed the following:

- slickensides were found much closer to the surface than previous samples
- average angle of the slickensides was 42 degrees
- moisture content was approximately 35% in the top 2 m, and increased to an average moisture content of 55% for the subsoil (Fig. 10a)
- weakly calcareous in the top 1 m, and except for small, occasional carbonate lenses in the subsoil, carbonates decreased with depth
- evidence of mottling below 2 m
- electrical conductivity less than 1.5 dS/m at all depths
- roots were found in the top 130 cm, the bulk of which located in the top 35 cm
- nitrate-nitrogen less than 3 ppm throughout the profile.

Micromorphological analysis revealed features most indicative of slickenside development occurred at depths between 3.8 and 6.4 m (Figs. 11 and 12). Above 3.8 m slickenside development was restricted because of large proportion of silt and the calcareous nature of the material. Below 6.4 m (Fig. 13) slickenside features were less common than above, suggesting that these forces were not strong enough to produce

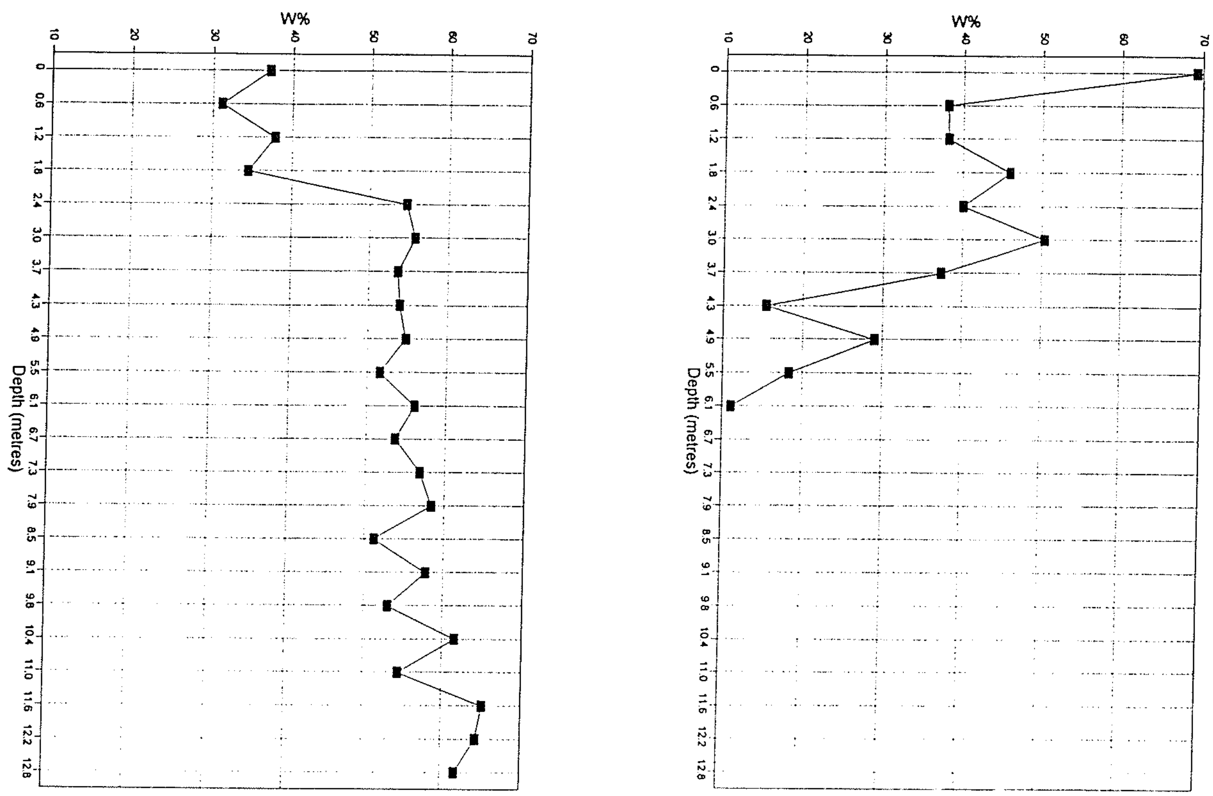

Figure 10. Gravimetric moisture content of continuous cores.
a) Montcalm '93 b) Warren '93

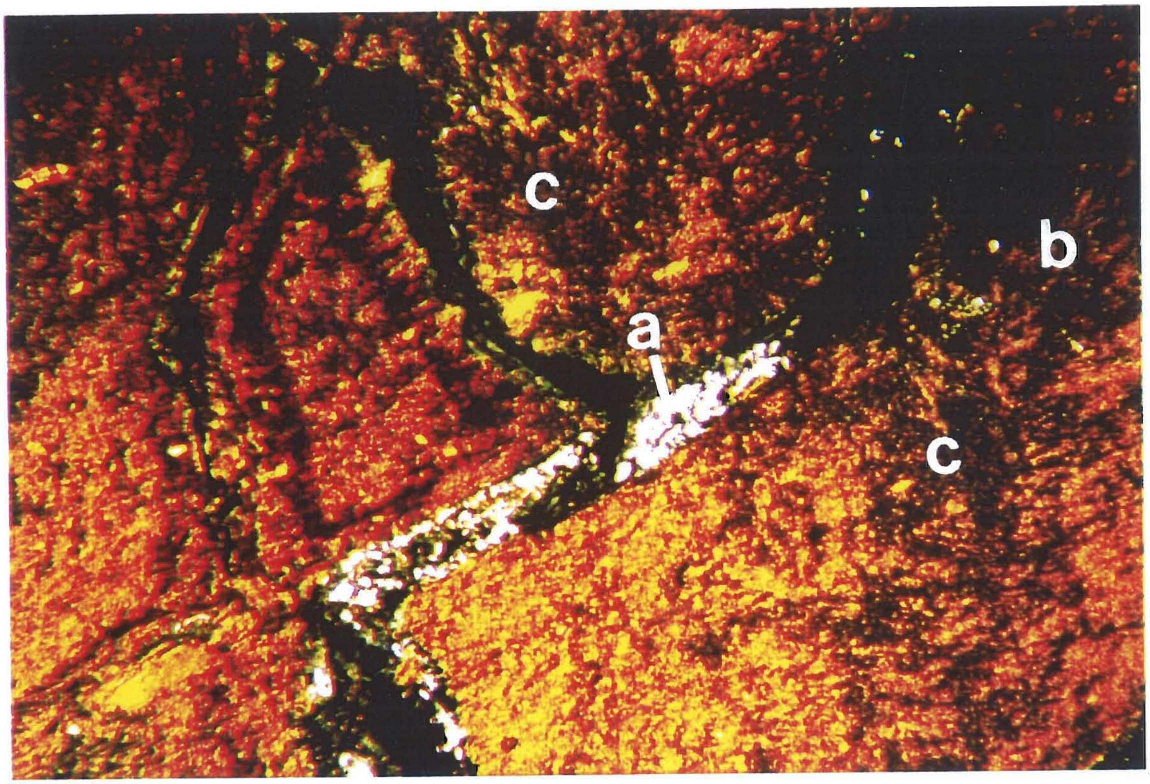

Scale: 5 cm = 0.1 mm

Figure 11. Sample 9351 @ 3.8 m depth under cross-polarized light (XPL). Montcalm '91 - biopores, roots, fractures

Birefringent plasma clay oriented preferentially, approximately 30° from horizontal; distinct circular regions fine to coarse grains of gypsum; nodules in close association to pore space filled with gypsum crystals (formed *in-situ*) - may be replacement features (**a**); occasional quartz of sand size; highly weathered mica remnants in clay material; straight, horizontal channels with craze planes found near surface; reddish-brown to black Fe/Mg oxide accumulations in upper portion of slide (**b**) - diffuse, very rare concretions; diffuse mottles Fe oxides; also few reduced regions (light gray) (**c**).

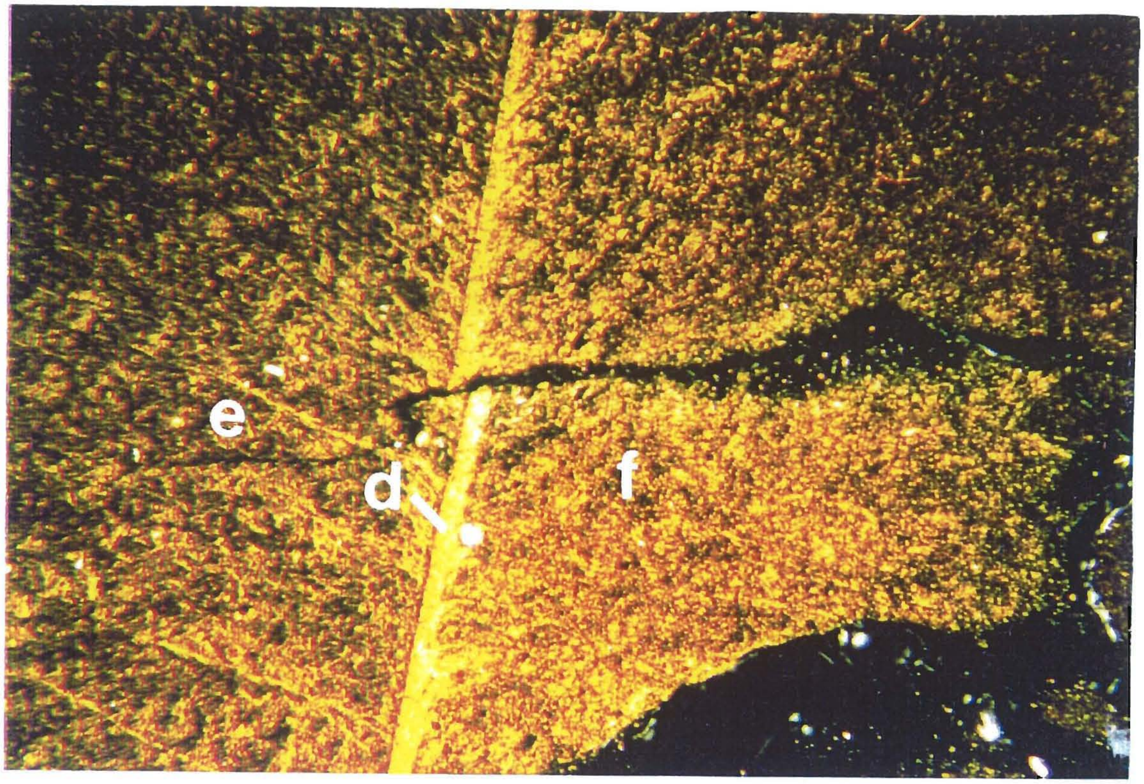

Scale: 5 cm = 0.1 mm

Figure 12. Sample 9353 @ 6.4 m depth under XPL.
Montcalm '91 - slickenside with 40°∠

All clay (slide orientation unknown - assume horizontal view); birefringent band (**d**) due to swelling appears as plane closed due to plasma expansion between two blocks of clay (**e, f**); probable shear plane - orientation of clays different on both sides of plane - pressure involved and possibly directed in different directions because of orientation - could possibly be slickenside feature (but these usually associated with pores) - more likely shear plane as portions can be matched up - probably the result of sediment being laid down, very little to no weathering of mineral grains and high calcareous quality suggests little soil formation; highly calcareous, very weak intersecting fabric, less strongly pronounced than in Sample 9352 (Appendix C).

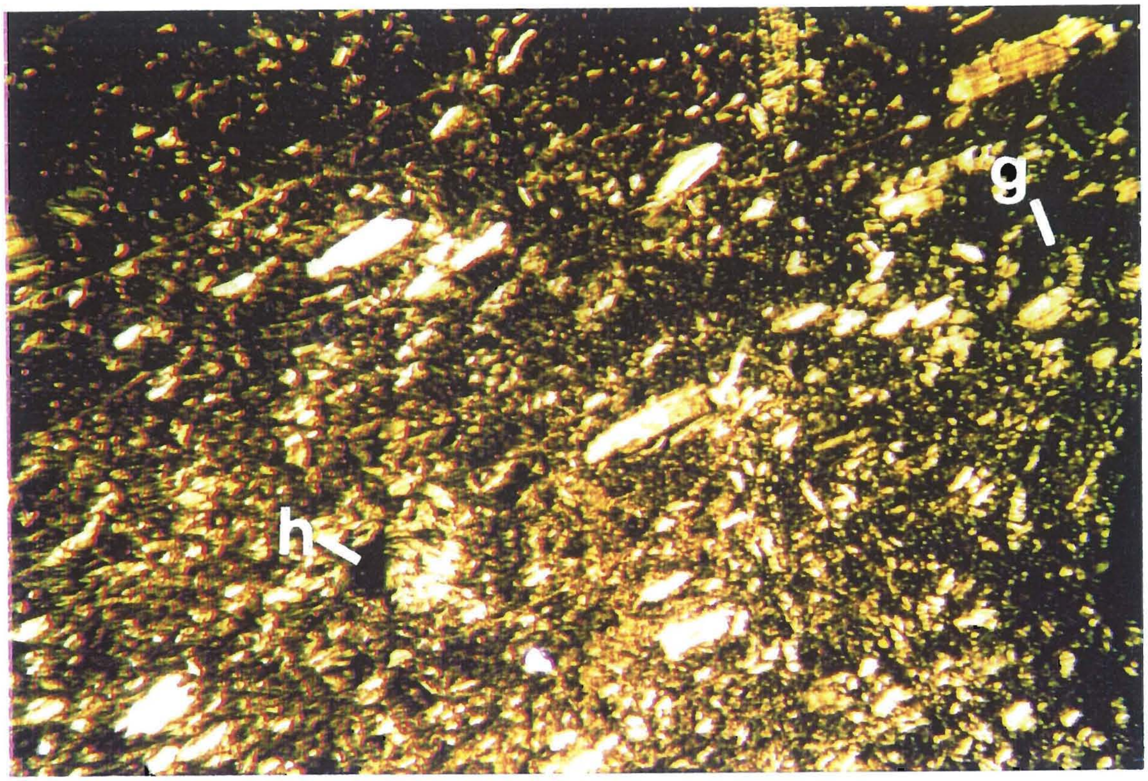

Scale: 5 cm = 0.1 mm

Figure 13. Sample 9355 @ 13.1 m depth under XPL.
Montcalm '91 - slickenside with 35°∠

Artifact from resin/epoxy of slide appears in shape of root (**g**); black deposit on soil material is Mn (**h**), probably replacing deposit of organics when sediments laid down; more crystals than in previous samples - fine sand and silt; some inclusions of silt/sand sized material; no change in texture from Sample 9354 (Appendix C) - calcareous; sediment (fragments of micas, clay nodules) very oriented, suggesting possible mixing of sediments by water; superimposed onto this sediment some stress planes (thin) crossing through at 25 - 30° to horizontal; large pores (probably cracks) resulting from shrinkage of sample after sampling (expect sample to be fairly compact).

(See Appendix C for remaining micromorphology descriptions).

shearing and thus create slickenside features. A less dynamic moisture status (ie. a continuously saturated environment) may explain the reduced occurrence of slickenside features at depths below 6.4 m. Within this depth range there are features such as birefringent clay, oriented in a specific direction from the horizontal, with stress features indicative of shrinking, swelling and shearing.

Isotope analysis of ^3H revealed that "modern" (post-1953) pore water was present to a depth of 3.2 m below the soil surface (Table 3). With the exception of slickensides slightly closer to the surface, this core is typical of the others previously sampled.

The presence of roots and "modern" water well into the soil profile, coupled with few soluble salts and carbonates, indicates an active zone of extensive downward movement of water and groundwater recharge.

B. Results - Warren Site

The core sample from the Warren site had a clay-clay loam texture from the surface to a depth of 4.1 m, where till was found. The till had a loamy texture with increased sand content at 5.4 m depth. Bedrock was encountered at a depth of 6.5 m.

This core contained few slickensides which were confined to the top metre of the profile, with an average angle of 34 degrees. Moisture content decreased sharply from 69% at the surface to 20% in the till at 4.3 m depth (Fig. 10b, page 56). Silt, sand and gravel content was much higher in the subsoil (1-4 m depth) at Warren than at Montcalm. The surface 20 cm was moderately calcareous, which decreased only slightly in the subsoil and increased again in the till and bedrock. Mottles were observed at 1.5 m and continued to the bedrock. Electrical conductivity was very high at the surface (15.7 dS/m) and decreased gradually with depth to a conductivity of 5.8 dS/m in the bedrock. Micromorphological analysis found no evidence of slickensides because of the high silt content, calcareous nature of the material, and lack of birefringent, oriented clay (Figs. 14 and 15). ^{3}H isotope analysis indicated that "modern" (post-1953) water was located within the top 90 cm of the soil profile. Roots were observed only in the top 90 cm of the soil. Nitrate-nitrogen was less than 3 ppm throughout the entire profile. These physical features showed that even though the Warren soil had a coarser texture than the Montcalm soil, downward movement was more restricted in the Warren soil because of the upward movement of saline groundwater into the soil profile.

Table 3. Isotope analysis of groundwater from both sites.

Montcalm		Warren	
Depth (m)	TU	Depth (m)	TU
0.2 - 1.0	29±8	0 - 0.9	29±8
2.8 - 3.2	11±8	2.3 - 3.1	0
3.3 - 3.9	0	3.1 - 3.7	0
5.5 - 6.2	0	6.1 - 6.5	0

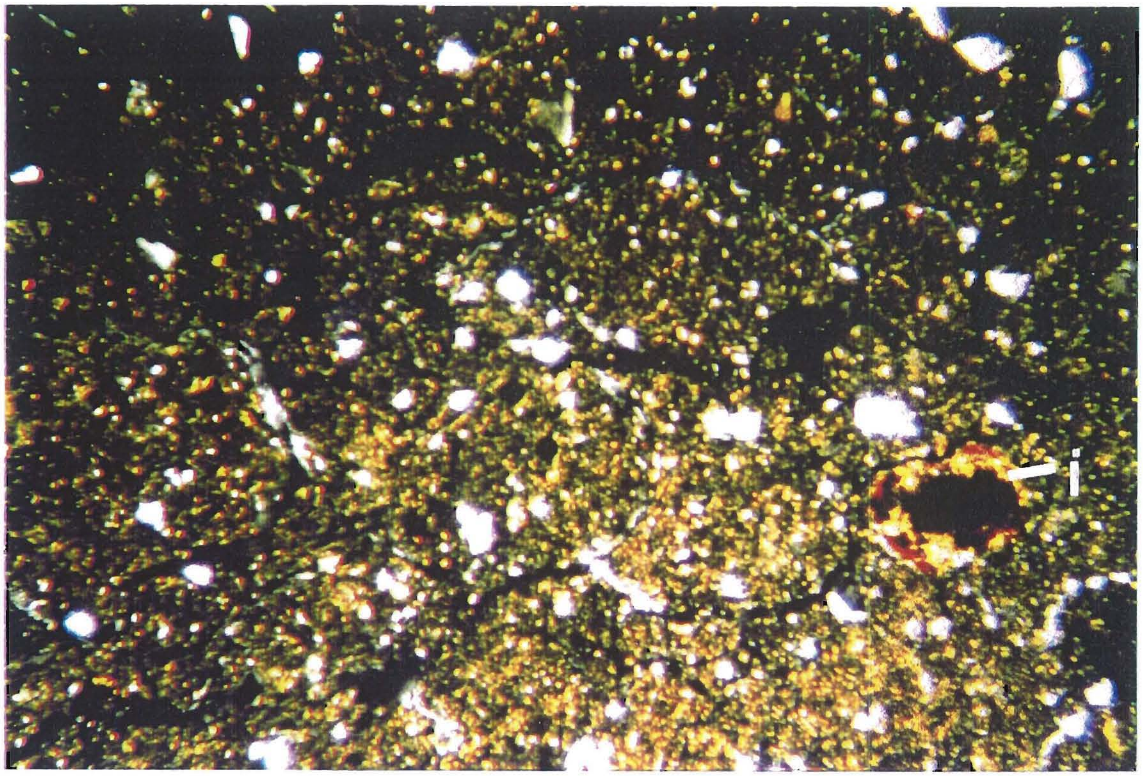

Scale: 5 cm = 0.1 mm

Figure 14. Sample 9356 @ 0.1 m depth under XPL.
Warren '93 - slickenside with 45°∠

Granular structure; granular units tend to be very rounded which may suggest some movement (likely tillage); moderately calcareous; remnants of root material; very organic rich; Fe/Mn oxide concretions (**i**); granic-porphyroskelic fabric with granic dominates; smaller, more numerous voids (very interconnected vugs and channels) because of granular structure.

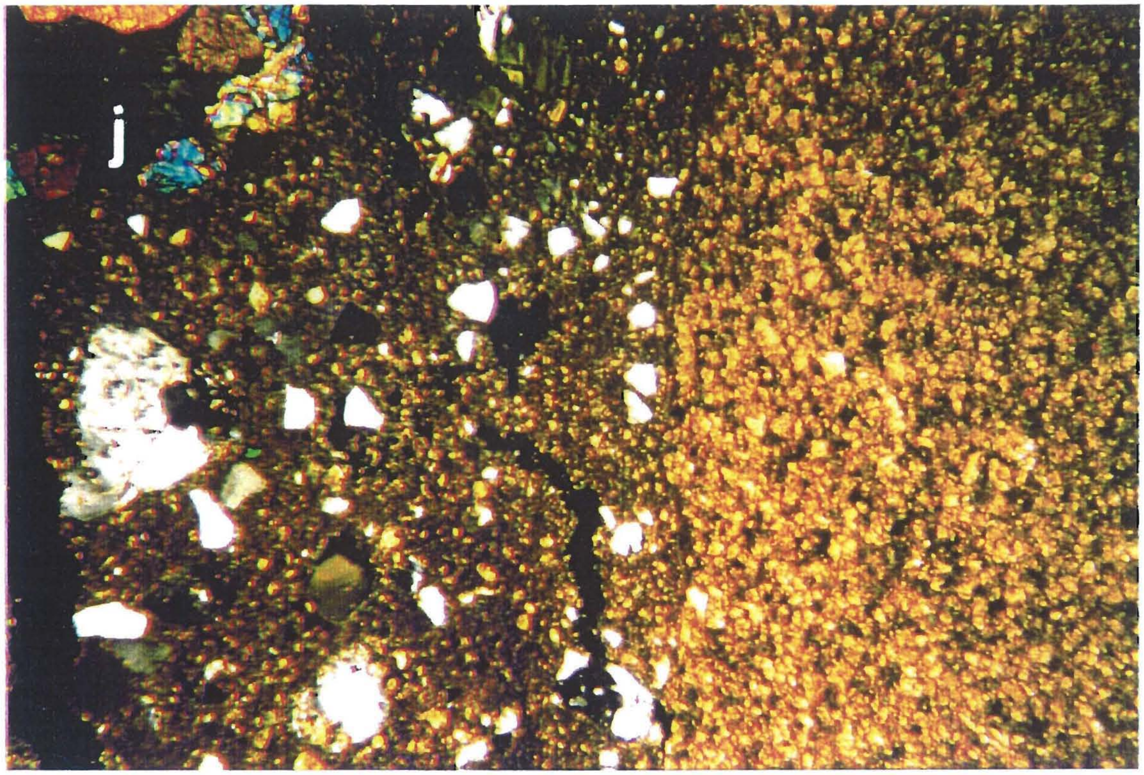

Scale: 5 cm = 0.1 mm

Figure 15. Sample 9359 @ 4.0 m depth under XPL.
Warren '93 - clay/till contact

Porphyric fabric; sample contains more sediment than soil (unsorted); highly birefringent because almost entirely calcareous; calcareous sand/gravel mixture (more sand grains than above samples); lithorelic (**j**) (many colors under XPL) - fragments of granite contain feldspar, quartz, olivine; possible evidence of twinning in feldspar - some lithorelics are calcareous, bioclastic (fossils), limestone; no evidence of slickensides - very little clay only in rare occurrences means this material will never get slickensides.

(See Appendix C for remaining micromorphology descriptions).

C. Discussion

The depth at which many of the slickensides occurred in the Montcalm soil was much deeper than previously predicted by several researchers (Dudal and Eswaran, 1988; Yaalon and Kalmar, 1978; White, 1967). Furthermore, the average angle of the slickensides does not change noticeably with depth, contrary to predictions by Dudal and Eswaran (1988). Based on the core analysis, it appears that the presence of small amounts of salts, carbonates and silt does not directly inhibit slickenside formation, as long as montmorillonitic clay remains the dominant fraction. Groundwater movement, wetting and drying cycles and degree of swelling appear to be the most probable dominant factors determining the location of slickenside formation.

The presence of slickensides at depth raises some interesting scenarios. The formation of slickensides at depths greater than two metres must occur by some means other than the pedoturbation model (Buol et al. 1980). Reduced soil colors indicate that the average depth of oxidation/reduction in these clays is 5.5 m. The fact that slickensides were mapped well below this depth (Fig. 8, page 52), in the presence of blue/grey mottles, indicates that they can form and have formed in a continuously saturated environment. This scenario would eliminate shrink-swell processes as a factor of their development. Thus their origin must be attributed to other geologic processes. The uniformity of texture, as indicated by a uniform moisture content (Fig. 10a, page 56) with depth would tend to minimize the effects of natural differential loading as a factor in slickenside formation.

A possible mechanism that could create an environment conducive to slickenside formation involves the overall hydraulic gradients of the area. The long term downward drainage typical of groundwater recharge could promote greater dewatering than replenishment from incoming water. Yuen (1995) discussed the various shrinkage phases of clays during desaturation. Structural shrinkage was the first type of shrinkage undergone by a saturated clay. Structural shrinkage involved the removal of water from "stable volume" macropores, in which the resulting water volume loss was greater than the decrease in soil volume.

The greatest amount of cracking and volume change occurred during normal shrinkage, the shrinkage phase where the decrease in soil volume was equal to the volume of water lost. During this stage water was removed from the "variable volume" pores of aggregates, which remained fully saturated while they decreased in volume.

Residual shrinkage, similar to structural shrinkage, occurred when water was lost from "stable volume" micropores. At this stage, volume change associated with water loss was greater than the observed volume change in the soil due to the entry of air into the pores.

The final stage, known as the no shrinkage phase, was encountered as soil particles reached their densest configuration. Any subsequent loss of water was equal to an increase in air volume.

This typical series of shrinkage phases (Figure 16) may assist in our understanding of slickenside formation. Stresses induced by collapse of the interstitial

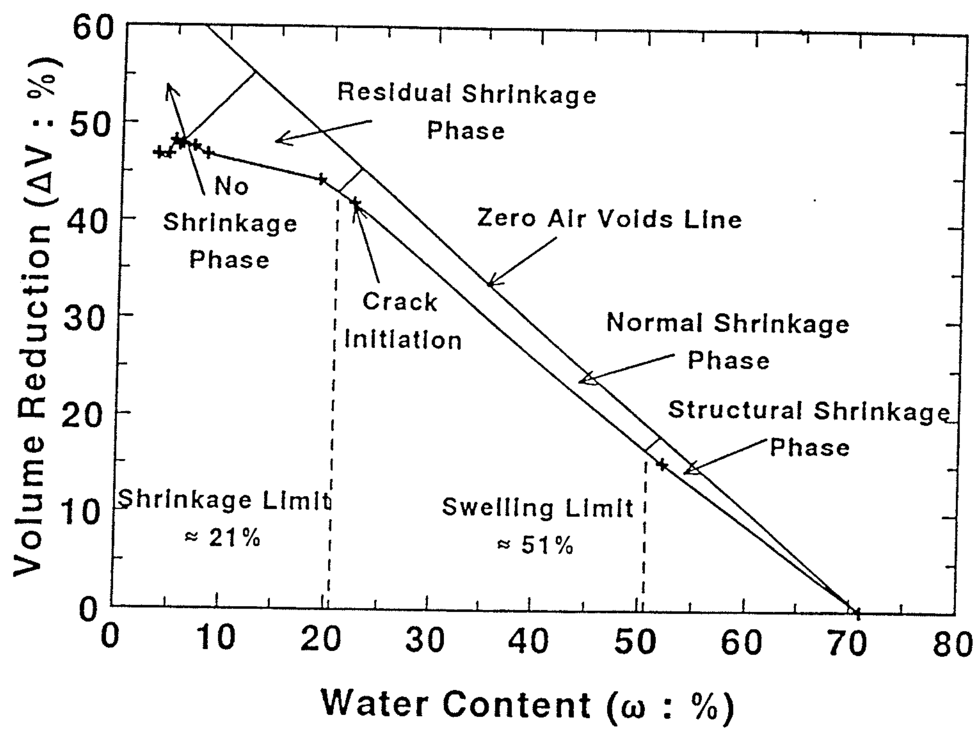

Figure 16. Typical shrinkage curve and shrinkage phases of a swelling soil (Yuen, 1995).

("variable volume") pores through drainage and normal shrinkage could result in development of stress-induced slickensides. This stress-induced origin may be analogous to those developed as a function of the "ripening of sediments" referred to by Ahmad (1983). In this case the formation of slickensides would be a one time event with their subsequent preservation as a natural characteristic of these materials. The lower pore water pressures in downward gradient environments may also explain the absence of slickensides in clay sediments containing relatively higher pore water pressures in upward gradient environments as occur at the Warren sample site.

Yuen (1995) also noted that after shrinkage and re-wetting of Lake Agassiz clays, volumes of the clay specimens were 15% lower than initial volumes, and their diameters were 4% smaller than their initial diameters. It was apparent from these observations that cracks formed *in-situ* in these clays do not fully heal. The formation of these cracks may be a factor in serving as planes of weakness for slicknside development (Ahmad, 1983) or as cracks which may be infilled and produce slickensides as described by the pedoturbation model (Buol et al. 1980). Micromorphological analysis of thin sections from cores taken from each site was inconclusive in distinguishing between slickensides formed near the soil surface and at depth. Since the thin sections display only a fraction of the entire soil sample, the chances of having the face of a slickenside show up on a thin section sample were remote. However, some of the thin sections did show evidence of conditions conducive to slickenside development. Evidence such as birefringent clay, stress features due to shrinking and swelling, shear planes and re-orientation of clays in various regions suggest slickensides could develop at these depths.

The presence of slickensides is related to the physical and chemical characteristics of the clay. Based on the micromorphology of the thin sections and the physical characteristics of the soils of the Montcalm profiles, the levels of silt and calcite were not too high to impede slickenside development (Fox, 1995, personal communication). The Warren profile, on the other hand, was not expected to have any slickensides present because of the high content of coarse, calcareous material present in the subsoil. Visual analysis of the cores may have identified features that appeared to be slickensides but may have actually been stress and shear features caused by tillage or by removal of the core from the drill sampler. Some of these features originally referred to as slickensides did not completely intersect the soil core and did not have a flat surface, even though they were shiny in appearance.

The occurrence of slickensides at the Montcalm site at such great depths is also a counter argument against the direct correlation between slickensides and development of surface gilgai (Buol et. al. 1980). Unfortunately gilgai features are not evident at either site, probably due to cultivation and landscaping.

D. Soil Classification Based on Vertic Properties

Based on the physical evidence of the cores, clay soils at both the Montcalm and Warren sites could be classified as either Humic Vertisols or vertic intergrades of other soil orders, depending on the degree of near surface shrinking and swelling that is evident in these soils. Both soils have slickensides within 1 m of the surface, even though they have different hydrologic regimes. Isotope analysis indicates contrasting hydrologic regimes between the two sites since the movement of "modern" (post-1953) pore water into the soil is limited to the top metre of the profile at the Warren site, even though this soil has a coarser texture than the soil at the Montcalm site. Restricted movement of meteoric water into the soil is characteristic of a high water table. The upward gradients of groundwater and salts at the Warren site may restrict slickenside formation because the soil moisture content remains high (near saturation). Slickenside occurrence is much more extensive at the Montcalm site where the water table is lower and near-surface moisture conditions are more dynamic.

E. Implications for Management

1. Engineering. Slickensides may be indicative of a long-term recharge zone in the soil that has had unsaturated regions in the subsoil at some time in order to have shrinking and swelling of the clay once the soil was rewetted. Slickensides may provide clues as to the relative stability of the soil and the potential for formation of preferential pathways in the soil.

Placing certain clay soils in an order separate from more coarse textured soils identifies a difference in engineering properties. These soils have unique characteristics which affect their suitability for waste management and the size of loads they can withstand in the form of roads and buildings.

2. Agriculture. Clay soils which possess vertic properties, once classified under the Chernozemic, Luvisolic, Gleysolic or Solonetzic Orders, may now meet criteria for a Vertisolic Order. Many of these soils are now classified under the Vertisolic order because of the presence of slickensides and a vertoturbic horizon that overrides the identification of other diagnostic horizons. Creating a new order for soils with well-developed vertic properties also acknowledges the differences in soil formation, leaching potential and shrink-swell potential from soils of other orders. Placing these soils in a different order may further distinguish them from other soils used for agricultural purposes. It has been realized that clay soils require special management practices for fertilization, tillage, seeding depth, and erosion control.

The creation of a Vertisolic Order with vertic intergrades in other orders would make a distinction between clay soils that have a high shrink-swell potential and clay soils which do not. In the case of agricultural soils, the Vertisolic Order would separate high shrink-swell clay soils used for agriculture from the coarser-textured agricultural soils. These distinctions should make it easier to develop recommendations for management more suited to the heavy clay soil types.

II. Macropore Flow Phenomenon

The Red River and Dencross soils studied in the previous section were used in the laboratory to measure K_{sat}. The area sampled at the Montcalm site was seeded to sunflowers in 1993. In previous years, the soil had been seeded to traditional crops such as cereals and canola. In contrast, the Warren site had been seeded to a mixture of salt tolerant grasses with sod-seeded alfalfa. K_{sat} was measured on these two soils to compare water movement in soils with different physical properties and contrasting hydrologic regimes. A Black Lake soil was included in the study to assess the effect of crop rotation/tillage on K_{sat} in a given soil.

The Black Lake Series (well drained Cumulic Regosol) had a silty clay-clay texture, non-saline, few localized carbonates, and no slickensides found within 1.2 m of the soil surface. Soil structure and distribution of roots and cracks varies spatially and with cropping practice (Appendix B).

A. Guelph Permeameter Field Measurements

1. Results. Figure 17 depicts the saturated hydraulic conductivity of a Black Lake Series (log scale) as affected by depth and crop rotation/tillage practice. At 25 cm depth, average hydraulic conductivity on the alfalfa-alfalfa plots was nearly two orders of magnitude higher than any of the other crop rotations. Hydraulic conductivities of all other crops tested differed little from each other. The increased flow rate through the

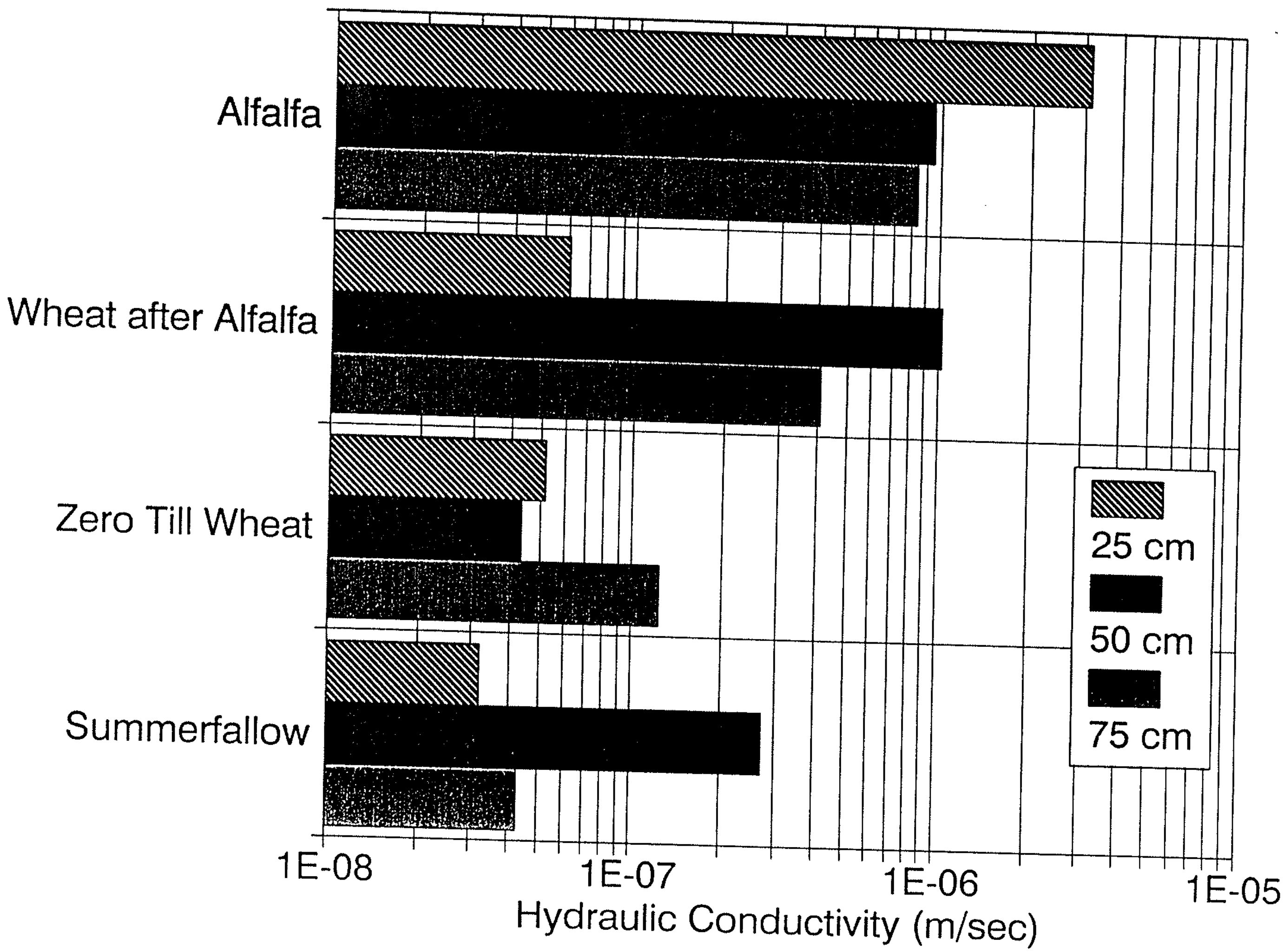

Figure 17. Saturated hydraulic conductivity from various treatments at three depths.

soil is the result of numerous shrinkage cracks more than 1 cm wide at the soil surface which extend well into the soil below the 25 cm depth. This clay soil consists dominantly of montmorillonite, which is responsible for the extensive cracking under dry conditions. The high demand for water by the alfalfa crop is also responsible for the production of the shrinkage cracks, as this treatment consistently displayed lower water contents than the other treatments. Biopores and root channels are expected to be more numerous and more effective in the alfalfa-alfalfa rotation than in the other treatments because of the absence of disruptive tillage practices.

At 50 cm depth, the alfalfa-alfalfa and alfalfa-wheat rotations had soil hydraulic conductivities approximately one to two orders of magnitude greater than the rotations which have not recently been seeded to alfalfa. No explanation at this time could describe the low K_{sat} value for zero till wheat at 50 cm other than the natural variability of the experiment.

At 75 cm below the soil surface, there is a gradual decline in K_{sat} among the different crop rotations/tillage practices. Roughly an order of magnitude separates the maximum and minimum values for this depth. Such a trend may be explained by the decrease in root channel and biopore activity at this depth from a large tap root system to a fibrous root system to a system with no recent roots at all.

It should be noted that the summerfallow treatment served as a long-term check and may not accurately represent agriculture practices in which summerfallow is practiced every second year or on a less frequent rotation.

2. Discussion. Based on the saturated hydraulic conductivity values, it is apparent that macropore flow, and subsequently rapid infiltration, is most likely to occur on the alfalfa-alfalfa rotation or the alfalfa-wheat rotation. Alfalfa, with its perennial growth habit, deep-rooted tap root system, and high demand for water, coupled with no tillage during its establishment, is responsible for the development of effective, stable macropores. Surface-applied fertilizers, pesticides and manures must be applied with care on sites with extensive macropore development. The potential for macropore flow to occur is not limited to only alfalfa sites, but also for other sites in which alfalfa has been extensively used in recent crop rotations. Subsoil and groundwater contamination are possible on soils with well-developed macropore networks. Excess surface moisture conditions could dissolve contaminants and carry them downward in the macropores towards the groundwater.

Since zero tillage takes several years to establish its effects of increased infiltration, hydraulic conductivity on this site remains low, similar to the summerfallow site. These types of management show little evidence of macropore flow, and surface ponding and/or runoff are more likely to occur. In these instances, erosion control, drainage and salinity prevention are the management practices that need to be addressed because the infiltration capability of soils with few or no macropores is easily exceeded.

In order to model the effects of macropore flow, measurements of soil matrix flow need to be conducted in conjunction with total flow values as determined using the Guelph Permeameter. The author suggests future research utilize both a Guelph Permeameter and a tension infiltrometer or falling head permeameter to determine the relative contributions of matrix flow and macropore flow to total flow. This research could aid in developing a model that can predict the hydraulic conductivity of a soil based on its porosity and structure.

B. Saturated Flux Versus Hydraulic Gradient

Darcy's Law is written in the form:

$$q = K (H_2 - H_1)/L$$

where

q is the flux;
K is the hydraulic conductivity;
$(H_2 - H_1)/L$ is the hydraulic gradient.

This can be translated into a relationship where the flux is directly proportional to the hydraulic gradient, with the hydraulic conductivity serving as a constant of proportionality. Therefore, if water moving through a saturated sample obeys Darcy's Law, the plot of saturated flux versus hydraulic gradient for the sample in question yields a straight line with a slope of one.

Dixon (1995) pointed out that there may be instances when the flux-hydraulic conductivity relationship deviates from Darcy's Law (slope $\neq$ 1) but eventually returns to a Darcian relationship (Figure 18). The shift in the location of the 1:1 relationship is interpreted as the change in the pore space available for flow. The cause of this phenomena may be similar to the change the "variable volume" of pores during normal shrinkage, as described by Yuen (1995). In this instance, however, the change in pore volume is due to the amount of structured water present, which influences the effective

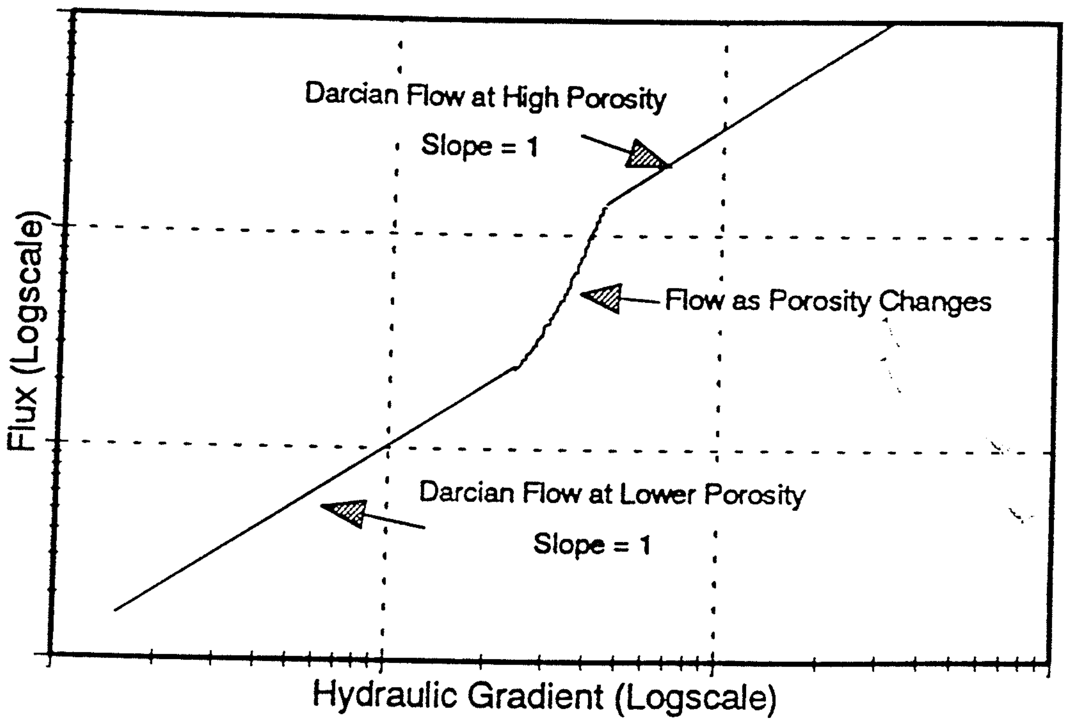

Figure 18. Theoretical plot of log-flux versus log-hydraulic gradient (Dixon, 1995).

pore size of the specimen (Karthigesu, 1994).

1. Results. Figure 19 is a plot of the log of flux versus the log of hydraulic gradient conducted on a sample from one of the drill logs at the Montcalm site. This sample most vividly displays the effects of low-gradient flow on the flux in clay soils. At hydraulic gradients greater than one, flux values at each gradient were nearly identical, regardless of whether the gradient was increasing or decreasing. This series of measurements at gradients greater than one form a very straight line relationship, as predicted by Darcy's Law. Linear regression analysis of these points produced an R^2 value greater than 0.99 and a slope of approximately 1.2. However, at hydraulic gradients of one or lower, there was a greater discrepancy between increasing and decreasing gradient flux values. Therefore, the critical hydraulic gradient (i_c) for this sample occurs at a hydraulic gradient of 1.0 (Yuen, 1995). Measurements of K_{sat} at gradients less than one produced a downward deviation from the straight line relationship with slope = 1 predicted by Darcy's Law. This non-Darcian behavior was attributed to the formation of a hydration shell in close proximity to clay particles. The attraction of clay particles for water molecules results in a portion of the soil water becoming immobile during low-gradient flow, and therefore water movement through the soil is less than what Darcy's Law predicts (Karthigesu, 1994). Thus if low-gradient flow occurs in the field in the absence of macropore flow, flux values could be up to an order of magnitude lower than those predicted by Darcy's Law.

Average flux relationships of all four samples tested are depicted in Figure 20.

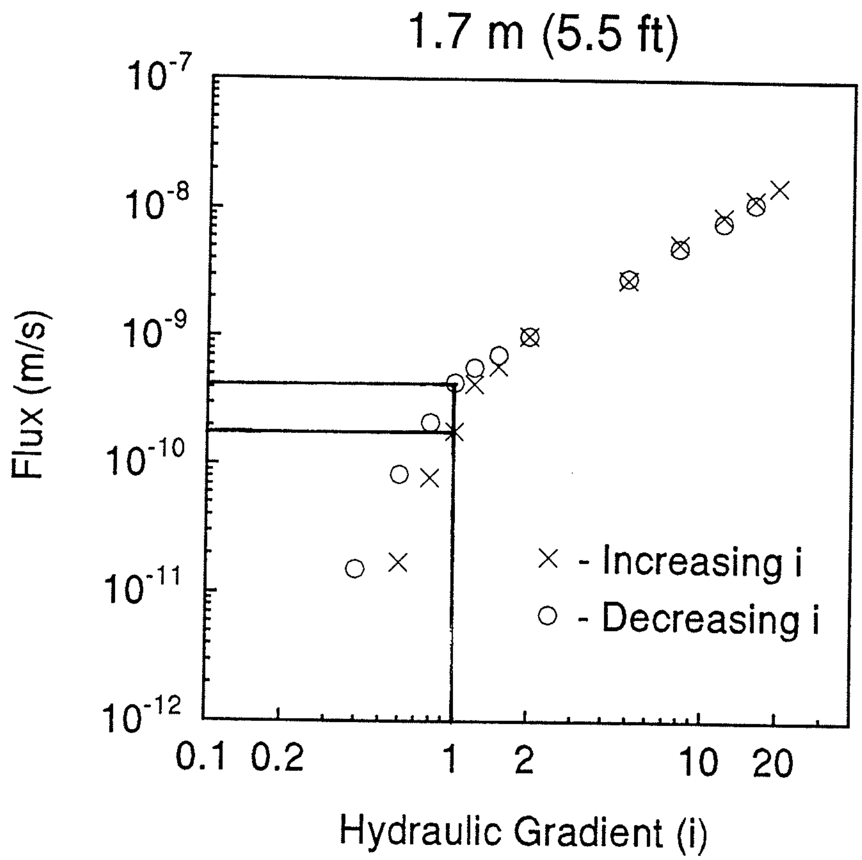

Figure 19. Flux versus hydraulic gradient in sample from above the water table at Montcalm site.

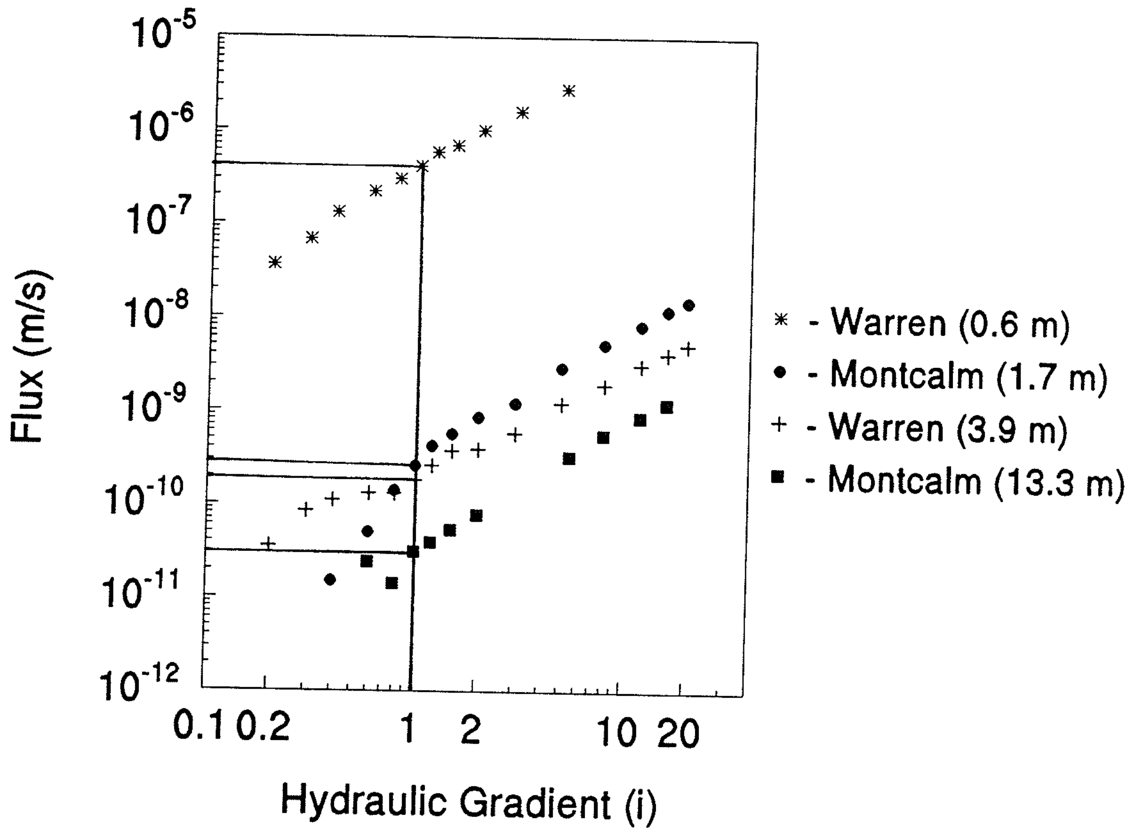

Figure 20. Flux versus hydraulic gradient for samples in laboratory K_{sat} determination.

There appears to be a trend of decreasing hydraulic conductivity with increasing depth, which is expected since root and faunal activity (macropore production) also decrease with depth. All samples appear to closely follow a Darcian relationship at high gradients, but flux values, below critical hydraulic gradients of 1.0 - 1.5, deviate from this relationship and variability of the measurements increases. Samples from the Warren site have higher flux values than the Montcalm samples (Fig. 20, page 79), due to increased macroporosity. This was confirmed by particle size analysis (pipette method), in which there were no significant differences between the samples. (Refer also to Appendix A).

Table 4. Average particle size analysis for samples in laboratory K_{sat} determination.

Site	Depth (m)	% Sand	% Silt	% Clay
Warren	0.6	1.5	15.5	83.0
Montcalm	1.7	6.0	15.0	79.0
Warren	3.9	14.0	20.0	66.0
Montcalm	13.3	0.5	20.5	79.0

2. Discussion. The saturated hydraulic conductivity (m/s) obtained in the lab were compared with those obtained in the field from previous engineering and soil survey reports on the sites. Hydraulic conductivities at the Montcalm site were calculated *in-situ* using the rising head test described by Hvorslev (1951). The values obtained from this test were approximately 10^{-10}m/s from various depths in the clay (UMA Engineering Ltd., 1991). Hydraulic conductivities at the Warren site varied from 10^{-6} to 10^{-8} m/s within 1 m of the soil surface to approximately 10^{-10} m/s in the clay to 10^{-8} m/s in the till (Fitzgerald, 1993).

Laboratory measurements of hydraulic conductivity closely resembled the field measurements of each sample measured at high gradients in this instance. The effects of temperature differences, sample size, sample disturbance during collection and continuity/discontinuity of pores may result in discrepancies between field and laboratory K_{sat} values.

C. Measurement of Salts Present in the Soil

Electrical conductivities of the samples and the relative quantities of anions and cations in each sample are displayed in Table 2 (page 54). Overall salt content at the Montcalm site was low, with electrical conductivities (EC) from various cores and depths less than 1.3 dS/m.

Salt content at the Warren site was very high at the surface. An electrical conductivity of 15.7 dS/m was measured, which decreased gradually with depth to a conductivity of 5.8 dS/m in the bedrock.

D. Thin Section Analysis

Analysis of the percent porosity of various thin sections provided clues to the rate of flow through specific portions of the soil. However, care must be taken in assessing potential flow based on the porosity of thin sections. If the pores are not continuous to the soil surface or if they tend to narrow off at "pore necks", then flow potential through these areas of the soil could be overestimated. Caution must also be excercised in distinguishing a native pore or channel in the thin section from an air bubble or crack that forms as a result of thin section preparation.

A comparison of the porosity of the surface samples from both sites (Montcalm at 0.2 m and Warren at 0.1 m) showed similar pore shapes and configurations with little difference in percent void area - 21% and 15% respectively. The pores in both samples consist largely of interconnected vugs and channels (Fig. 21).

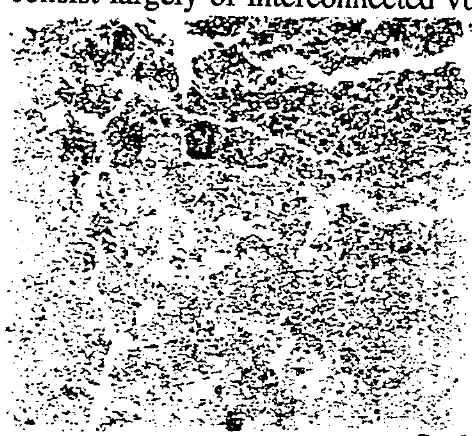

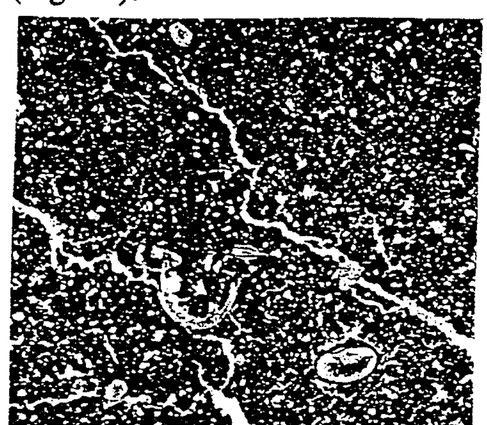

Scale: 1 cm = 1.3 mm

Fig. 21a. Sample 9350
Montcalm @ 0.2 m
20.8% void area

Fig. 21b. Sample 9356a
Warren @ 0.1 m
14.6% void area

Trends which appeared in the Montcalm profile indicated that porosity was highest in areas where plant roots and root channels, biopores and fractures were evident. These features coincided with noticeable structural development - usually weak to moderate, fine to medium subangular blocky structure (Manual for Describing Manitoba Soils in the Field, Canada-Manitoba Soil Survey, 1992). Areas of low porosity and massive structure were commonly found at depths where slickenside activity was greatest.

In the Warren profile trends were more difficult to distinguish. It was difficult to interpret because certain light-colored minerals may have been classified as voids. Porosity may have been overestimated because of the abundance of light-colored minerals. Highest porosity was located at depths of high biological activity; lowest porosity occurred in the till which contained considerable amounts of varved clay that showed evidence of distortion due to sediment pressures.

Table 5. % Area Occupied by Voids as Calculated by Image Analyzer
(Note: Successive measurements from the same sample are taken at increasing depth).

Sample	Site	Depth (m)	% Void Area
9350	Montcalm	0.2	20.8
9351	Montcalm	3.8	23.7
9352	Montcalm	4.9	3.3
9353	Montcalm	6.4	4.5
9354	Montcalm	5.2	18.1
9355	Montcalm	13.1	10.8
9356a	Warren	0.1	14.6
9356b	Warren	0.1	15.9
9357	Warren	0.6	33.6
9358a	Warren	1.2	22.3
9358b	Warren	1.2	11.1
9358c	Warren	1.2	13.0
9358d	Warren	1.2	8.7
9359a	Warren	4.1	11.2
9359b	Warren	4.1	13.8
9359c	Warren	4.1	10.2
9359d	Warren	4.1	27.9
9360a	Warren	5.5	9.3
9360b	Warren	5.5	13.8
9360c	Warren	5.5	28.4
9360d	Warren	5.5	0.6
9360e	Warren	5.5	8.8

(See Appendix D for remaining images).

E. Determination of Age of Roots Using ^{14}C Analysis

Roots from a dense till sample from SW 14-9-12E were carbon dated. Essentially none of the carbon-14 present in the roots had undergone radioactive decay. The relative age of the roots were measured to be 108.41 ± 0.71 per cent modern. This indicates that these roots found approximately 3.5-3.7 m below the surface are relatively young (less than 50 years old) and slow-growing. Therefore, it is possible for roots of modern plant species to penetrate into dense subsurface materials over time. Potential for leaching of materials through dense materials via root channels is greater than initially assumed.

F. Implications for Management

The results of measuring K_{sat} in the field on a soil series under various crop rotations/tillage practices verifies that management and recent history of management practices strongly influence the infiltration rate of a clay soil. It is unclear whether management practices, such as growing alfalfa, would dramatically increase the hydraulic conductivity of a coarse textured soil; however, for fine textured soils, in which water movement could be greatly restricted because of low matric hydraulic conductivities, the ability to increase macro hydraulic conductivity by more than an order of magnitude using different crop rotations and tillage practices demonstrates the need for responsible management of these soils. Not only must the inherent properties and production capabilities of a soil be considered, but also the past and present management practices imposed on the soil.

If the infiltration and drainage of these soils is to be improved, then it would be advisable to reduce or eliminate tillage and establish perennial crops with deep, extensive root systems and a high demand for water, such as alfalfa. Susceptibility to erosion of any kind will be low and infiltration will be increased. These types of effects could be established on a reduced scale using perennial grasses or continuous cropping with zero tillage. The risk of this type of management is that with increased infiltration comes a higher potential for leaching of surface-applied substances, such as pesticides, fertilizers and manures. Care and proper timing in applying these amendments to the soil must be exercised even for some time after the establishment of crops and practices that initially improved the infiltration of the soil.

In order to reduce the effects of leaching, practices that limit the initiation of macropore flow should be implemented. Logan and others (1987) suggested the implementation of more effective methods to limit macropore flow, such as point injection of fertilizer and the lifting and replacing of mulch during pesticide application to incorporate chemicals without incorporating residues. By injecting the fertilizer solution directly into the soil matrix, leaching as a result of macropore flow will be greatly reduced. Another means of preventing leaching in soils with low residue crops is through the use of wide-blade cultivators (noble plows). This tillage practice cuts off some the root channels and other macropores from the soil surface, as well as providing chemical-free weed control and maintaining adequate residue cover for erosion control. For crops that produce large quantities of residue, such as cereals, conventional tillage methods that incorporate some of the residue while disrupting macropore continuity are adequate.

If these soils are to be used as impermeable barriers for waste confinement, then management practices must be employed that will impede infiltration in favor of localized runoff and containment. Addition of soil amendments that favor dispersion of soil colloids, compaction, tillage, removal of excess water and establishment of shallow-rooted plants all contribute towards minimal leaching in these soils. The risk in implementing the above practices is the increased risk of soil erosion by water, since the bulk of the water is not entering the soil, but leaving as surface runoff. Erosion control measures other than plant cover may be used to maintain a low leaching potential, such as artificial covers and structures which hold the soil in place.

The difficulty in managing clay soils as either well-drained soils or impermeable barriers is the lack of confidence in assessing the actual hydraulic conductivity of the entire soil due to the spatial variability that occurs in these soils. Regardless of the management practices employed, the leaching potential of the soil is dependent on the size, continuity and number of channels present in the soil. Since a contaiminant needs only one continuous macropore to travel through in a significant quantity to reach the groundwater, the focus in analyzing the leaching potential of soils must shift from finding the average rate of infiltration to determining the worst case scenario - the maximum possible rate of infiltration. To determine such a rate, the maximum rate of macropore formation and how long such macropores can serve as effective transmission pathways under various management practices must be known. Further study must be conducted on resilience of various types of macropores under several management practices. Development of non-distructive means of measuring macropore formation under various types of tillage/cropping practices would be the ideal procedure for studying this phenomena. For example, if it were possible to discover or synthesize an inert, non-toxic tracer whose mobility was similar to water or constituents we wish to study, tests to identify macropore networks would be greatly simplified.

CONCLUSIONS

I. Vertic Properties

The purpose of this study was to compare several properties of two clay soils from the Red River Basin, one from a groundwater recharge area and the other from a discharge area, to determine whether these soils would meet criteria for Vertisolic soils. The presence of both a slickenside horizon and a prominent vertoturbic horizon are required to classify soils under the Vertisolic order.

The presence of slickensides in both soils confirmed that these soils could be classified either as Humic Vertisols or Vertic Black. Whether these soils are classified in the Vertisolic order or as vertic intergrades of other orders depends on the degree of expression of the vertoturbic horizon. Evidence of horizon disruption in the form of tonguing was recognized in the Red River soil (UMA Engineering Ltd., 1991). Therefore, the Red River soil could be classified as a Humic Vertisol. However, the Dencross soil, due to lack of distinct slickensides present in the profile and due to shallow cracking would be classified as a Vertic Rego Black.

The cores of the Black Lake series did not contain any slickensides, nor was there evidence of deep vertical cracking (pedoturbation). It was expected that this soil would remain in its present classification as a Cumulic Regosol.

More research is needed to develop a model which better explains the genesis of slickensides at depths greater than 2 m, the effects of slickensides on gilgai development and the effects of other factors such as groundwater movement on slickenside development.

II. Macropore Flow Phenomenon

Based on the saturated hydraulic conductivities observed in Black Lake, Red River and Dencross soils, there is potential for macropore flow to occur in clay soils near the surface as a result of recent and ongoing management practices, such as crop rotations and frequency of tillage. Alfalfa stands exhibit the strongest potential for macropore flow of all the observed management practices, with near-surface saturated hydraulic conductivity values more than an order of magnitude greater than the other treatments. These effects of alfalfa on soil porosity and hydraulic conductivity were evident one year after the alfalfa crop was removed and may remain for some time beyond one year.

In this study it has become apparent that measurement and prediction of hydraulic conductivity in clay soils is more difficult than for coarser textured soils. Measurements of low-gradient matrix flow in clay soils were lower than predicted by Darcy's Law. Macropore flow does not result in a deviation from Darcy's Law, but rather an upward shift of the 1:1 straight-line relationship, when compared to a similar soil in which macropores are absent. Flow was higher than that expected for a clay soil at all gradients, as a result of the presence of macropores.

To adequately assess the risk of groundwater contamination on a particular soil, all factors that influence macropore development and bypass flow must be considered. Table 6 is a generic guide in assigning an overall risk for a soil based on several soil properties. Many of the boundary conditions which define whether the risk is low, moderate or high were arbitrarily assigned, and therefore could be subject to testing and revision. In addition, not all properties carry equal importance in risk assessment. For instance, texture would be more important to consider than slickensides, because coarse-sized separates would contribute more to rapid movement of materials than numerous slickensides formed in heavy clay soils under confining pressures. Research and testing is suggested to develop weighting factors for the individual properties. The purpose of this table was to ensure that several soil properties were considered before making any recommendations pertaining to the management of these soils where groundwater contamination could occur.

Table 6. Risk assessment of soils as impermeable barriers to groundwater contamination based on several properties.

Property		Low Risk	Moderate Risk	High Risk
Texture		$K_{sat} \leq 10^{-8}$ m/s	K_{sat} 10^{-8} - 10^{-5} m/s	$K_{sat} \geq 10^{-5}$ m/s
Clay Mineralogy		low shrink-swell	-	high shrink-swell
Moisture		saturated	near field capacity	near wilting point
Salts	a) type	-	monovalent salts that favor dispersion	divalent salts that favor flocculation
	b) EC to 120 cm	> 8 dS/m	4 - 8 dS/m	0 - 4 dS/m
Cracks/Fissures	a) abundance	soil peds remain as intact core	some soil peds fall apart from core	peds fall apart; core loses shape
	b) continuity	< 30 cm long	30 - 100 cm long	> 100 cm long
Biopores	a) abundance*	-	few/plentiful	abundant
	b) continuity	-	< 100 cm long	≥ 100 cm long
Roots	a) abundance*	few	plentiful	abundant
	b) continuity	< 30 cm long	30 - 100 cm long	> 100 cm long
Slickensides	a) depth	> 4 m below surface (geologic)	2 - 4 m below surface	< 2 m below surface (pedogenic)
	b) angle	< 45° (horizontal movement favored)	-	> 45° (vertical movement favored)
	c) number	< 5/m^2	5 - 10/m^2	> 10/m^2
Depth to Water Table		> 2 m below surface	-	< 2 m below surface
Stable Isotopes in Groundwater		"modern" water confined within 3 m of surface (slow recharge)	"modern" water confined within 1 m of surface (discharge)	"modern" water relatively unconfined (rapid recharge)
Micromorphology	a) fabric	fine	-	coarse
	b) orientation	none	around pores and cracks only	highly oriented

*Refer to Manual for Describing Soils in the Field for Manitoba Soils. Canada-Manitoba Soil Survey, 1992.

There are many factors that require a more complete understanding in order to quantify and accurately predict water movement through soil with macropores.

One of the difficulties in measuring hydraulic conductivity in soil with macropores is spatial variability (Neuzil, 1994). Depending whether the Guelph Permeameter, or any apparatus used to measure *in-situ* hydraulic conductivity, intersects a macropore or is confined within the soil matrix, the value of the hydraulic conductivity of the soil may vary by one or two orders of magnitude. Thus, depending on the intensity of macropores present in the soil, hydraulic conductivity may change within a few centimeters across the soil. As a result, average values for hydraulic conductivity may have little significance. Similarly, in micromorphological analysis of thin sections, the area observed is very small compared to the area of the entire soil core. Therefore, even within the soil core, spatial variability limits the reliability with which thin sections may be used to determine the porosity of the soil or the presence of slickensides or other vertisolic properties in the soil. What is needed is a more accurate method for measuring and predicting flow through clay soils that accounts for the tremendous influence of spatial variability. To evaluate risk for contamination, it may be more important to find the maximum hydraulic conductivity of the soil rather than an average hydraulic conductivity.

The resilience of tubular channels (biopores, root channels) in clay soils is an important factor affecting macropore flow. Pores developed from bio-activity remain open below the plow layer and may serve as effective transmission pathways even if the soil is relatively moist. Unlike planar shrinkage cracks, the tubular shape of these pores resists closure as the soil is wetted and swells (Brewer, 1964). Knowing the lifespan of tubular pores would have implications for the long term hydraulic conductivity of the soil.

The field and laboratory experiments both revealed a decrease in hydraulic conductivity with increasing soil depth. This indicates that macropore pathways terminate gradually at some point in the soil, usually in the oxidized zone above the water table. Discontinuities in macropore pathways can also occur as a result of tillage and slickenside activity. To what degree macropore discontinuities affect flow through macropores needs to be observed more closely (Ehlers, 1975; Logsdon et al. 1990). This could determine if breaks in macropore pathways of various sizes at various depths are more effective than others in reducing macropore flow.

The nature of the liquid being transmitted through the soil must also be addressed when assessing flow rates. Temperature and its influence on the viscosity of the liquid must be considered. If the liquid was something other than water, then factors such as solubility in water, polarity, and relative stability in oxidizing and reducing conditions to accurately predict rate of movement through a given soil.

Finally, there is a great deal yet to be learned about flow through macropores. It is a challenging concept in that a fraction of the total number of pores is responsible for the majority of fluid transmission. The difficulties in measuring and predicting flow rates through clay soils with macropores require more understanding of the complex nature of the soil and a new appreciation for managing clay soils, both in an agricultural and in an environmental setting. Clay soils should no longer be assumed to be impermeable barriers; they should be managed responsibly with the realization that these soils can also allow potential contaminants to be leached to the groundwater.

BIBLIOGRAPHY

Ahmad, N. 1983. Vertisols. pp 91-119 in L.P. Wilding, N.E. Smeck, and G.F. Hall, eds. Pedogenesis and soil taxonomy. II. The soil orders. Elsevier Publ., Amsterdam.

Bascomb, C. L. and Bullock, P. 1974. In: Soil Survey Laboratory Methods, Avery, B. W. and Bascomb, C. L. (Eds.) Sample preparation and stone content. Soil Surv. Gt. Br. Tech. Monogr. 6, Harpenden, p. 5-13.

Betcher, R. 1980. Groundwater Availability Study Report No. 13, Winnipeg Map Sheet 62-H. Manitoba Department of Natural Resources, Water Resources Branch.

Beven, K. J. 1981. Micro-, meso-, macroporosity and channeling flow in soils. Soil Sci. Soc. Am. J. 45:1245.

Blockhuis, W.A. 1982. Genesis of Vertisols. in Vertisols and Rice Soils of the Tropics, Symposia papers II. pp 23-47. 12th Intl. Soil Sci Soc Congr. New Delhi, India.

Booltink, H. W. G. and Bouma, J. 1991. Physical and morphological characterization of bypass flow in a well-structured clay soil. Soil Sci. Soc. Am. J. 55:1249-1254.

Bouma, J. 1991. Influence of soil macroporosity on environmental quality. Adv. Agron. 46:1-37.

Bouma, J. 1982. Measuring the hydraulic conductivity of soil horizons with continuous macropores. Soil Sci. Soc. Am. J. 46:438-441.

Bouma, J. 1981. Soil morphology and preferential flow along macropores. Agric. Water Manage. 3:235-250.

Bouma, J., Dekker, L. W. and Muilwijk, C. J. 1981. A field method for measuring short-circuiting in clay soils. J. Hydrol. 52:347-354.

Bouma, J. and Dekker, L. W. 1978. A case study of infiltration into dry clay soil. Geoderma 20:27-51.

Bouma, J., Jongerius, A., Boersma, O., Jager, A., and Schoonderbeek, D. 1977. The function of different types of macropores during saturated flow through four swelling soil horizons. Soil Sci. Soc. Am. J. 41:945-950.

Bouma, J., Jongerius, A. and Schoonderbeek, D. 1979. Calculation of saturated hydraulic conductivity of some pedal soils using micromorphometric data. Soil Sci. Soc. Am. J. 43:261-265.

Bouma, J., Jongmans, A. G., Stein, A. and Peek, G. 1989. Characterizing spatially variable hydraulic properties of a boulder clay deposit in The Netherlands. Geoderma 45:19-29.

Bouma, J., Paetzhold, R. F. and Grossman, R. B. 1980a. Application of hydraulic conductivity measurements in soil survey. Soil Cons. Service USDA. Soil Survey Investigation Rep., Washington, DC, 12 pp.

Brewer, R. 1964. Voids. pp. 179-204 in: Fabric and mineral analysis of soils. John Wiley & Sons. Inc. New York.

Bronswijk, J. J. B. 1988. Effect of swelling and shrinkage on the calculation of water balance and water transport in clay soils. Agric. Water Manage. 14:185-193.

Bullock, P. and Thomasson, A. J. 1979. Rothamsted studies of soil structure, II. Measurement and characterization of macroporosity by image analysis and comparison with data from water retention measurements. J. Soil Sci. 30:391-413.

Buol, S.W., Hole, F.D. and McCracken, R.J. 1980. Soil Genesis and Classification, 2nd ed. Iowa University Press, Ames, Iowa.

Canada-Manitoba Soil Survey, 1992. Manual for Describing Soils in the Field for Manitoba Soils.

Carter, M. R. 1988. Temporal variability of soil macroporosity in a fine sandy loam under moldboard ploughing and direct drilling. Soil Tillage Res. 12:37-51.

Cassel, D. K., Krueger, T. H., Schroer, F. W. and Norum, E. B. 1974. Solute movement through disturbed and undisturbed soil cores. Soil Sci. Soc. Am. Proc. 37:36-38.

Clothier, B. E. and Smettem, K. R. J. 1990. Combining laboratory and field measurements to define the hydraulic properties of soil. Soil Sci. Soc. Am. J. 54:299-304.

Dasog, G. S. and Shashidhara, G. B. 1993. Dimension and volume of cracks in a Vertisol under different crop covers. Soil Sci. 156(6):424-428.

Diab, M., Merot, Ph. and Cumri, P. 1988. Water movement in a Glossaqualf as measured by two tracers. Geoderma 43:143-161.

Dixon, D. A. 1995. Towards an understanding of water structure and water movement through dense clays. Ph. D. Thesis, Dept. of Civil Engineering, University of Manitoba, Winnipeg, Canada.

Dixon, D. A., Gray, M. N., Lingnau, B., Graham, J. and Campbell, S. L. 1993a. Thermal expansion testing to determine the influence of pore water structure on water flow through dense clays. 46th Canadian Geotechnical Conference, Saskatoon, SK. September, 1993.

Douglas, J. T. 1986. Macroporosity and permeability of some soil cores from England and France. Geoderma 37:221-231.

Douglas, L. A. 1990. Soil Micromorphology: A Basic and Applied Science. Elsevier Science Publishers, New York.

Drimmie, R. J., Heemskerk, A. R. and Johnson, J. C. 1991. Tritium Analysis. Technical Procedure 1.0, Rev 02, Environmental isotope laboratory: 32 pages. Department of Earth Sciences, University of Waterloo.

Dudal, R. and Eswaran, H. 1988. in L.P. Wilding and R. Peuntes (eds.), Vertisols: Properties, Classification and Management. Texas A&M University Press.

Dunn, G. H. and Phillips, R. E. 1991. Macroporosity of a well-drained soil under no-till and conventional tillage. Soil Sci. Soc. Am. J. 55:817-823.

Edwards, W. M., Norton, L. D. and Redmond, C. E. 1988. Characterizing macropores that affect infiltration into non-tilled soil. Soil Sci. Soc. Am. J. 52:483-487.

Edwards, W. M., Shipitalo, M. J., Owens, L. B. and Dick, W. A. 1993. Factors affecting preferential flow of water and atrazine through earthworm burrows under continuous no-till corn. J. Environ. Qual. 22:186-193.

Ehlers, W. 1975. Observations of earthworm channels and infiltration on tilled and untilled loess. Soil Sci. 119:242-249.

Elrick, D. E. and French, L. K. 1966. Miscible displacement patterns on disturbed and undisturbed soil cores. Soil Sci. Soc. Am. Proc. 30:153-156.

Expert Committee on Soil Survey, 1987. The Canadian System of Soil Classification, 2nd ed. Agric. Can. Publ. 1646. Supply and Services Canada, Ottawa.

Fenton, M., Moran, S. R., Teller, J. T. and Clayton, L., 1983. Quaternary stratigraphy and history in the southern part of the Lake Agassiz Basin. Geological Association of Canada, Special Paper 26, pp. 49-74.

Fitzgerald, M. 1993. Soil Salinity assessment, monitoring and prediction study. Warren, Manitoba. Internal report.

Fitzpatrick, E. A. 1984. Micromorphology of Soils. Chapman and Hall, New York.

Freeze, R. A. and Cherry, J. A. 1979. Groundwater. Prentice-Hall, Inc., Englewood Cliffs, N. J.

Gallichand, J., Lagacé, R. and Callier, M. 1989. Thin section study of soil materials near perforations in corrugated subsurface drains. Geoderma 43:337-347.

Ghodrati, M. and Jury, W. A. 1990. A field study using dyes to characterize preferential flow of water. Soil Sci. Soc. Am. J. 54:1558-1563.

Gish, T. J. and Jury, W. A. 1983. Effect of plant roots and root channels on solute transport. Trans. ASAE 26(5):440-451.

Green, R.D. and Askew, G.P. 1965. Observations on the biological developments of macropores in soils of Rommey Marsh. J. Soil Sci. 16(2):342.

Groenvelt, P. H., Kay, B. D. and Grant, C. D. 1984. Physical assessment of a soil with respect to rooting potential. Geoderma 34:101-114.

Gustavson, T.C. 1975. Microrelief (gilgai) structures on expansive clays of the Texas Coastal Plain - their recognition and significance in engineering construction. Geol. Circ. 75-7. Bur. of Ecol. Geol., The Univ. of Texas, Austin, Texas.

Hillel, D. 1982. Introduction to Soil Physics. Academic Press, San Diego.

Hoogmoed, W. D. and Bouma, J. 1980. A simulation model for predicting infiltration into cracked clay soil. Soil Sci. Soc. Am. J. 44:458-461.

Hosang, J. 1993. Modelling preferential flow of water in soils - a two-phase approach for field conditions. Geoderma 58:149-163.

Hvorslev, M. J. 1951. Time Lag and Soil Permeability in Groundwater Observation, U. S. Army Corps of Engineers, Waterways Experiment Station, Vicksburg, Mississippi, Bul. No. 36, pp. 1-50.

Isensce, A. R., Nash, R. G. and Helling, C. S. 1990. Effect of conventional versus no-tillage on pesticide leaching to shallow groundwater. J. Environ. Qual. 19:434-440.

Jarvis, N. J., Leeds-Harrison, P. B. and Dosser, J. M. 1987. The use of tension infiltrometers to assess routes and rates of infiltration in a clay soil. J. Soil Sci. 38:633-640.

Jenny, H. 1980. The Soil Resource - Origin and Behavior. Springer-Verlag New York Inc.

Jones, L. A., Rutledge, E. M., Scott, H. D., Wolf, D. C. and Teppen, B. J. 1993. Effects of two earthworm species on movement of septic tank effluent through soil columns. J. Environ. Qual. 22:52-56.

Karthigesu, T. 1994. Validity of Darcy's Law for low-gradient saturated flow through bentonite and sand mixtures. M. Sc. Thesis. Dept. of Agricultural Engineering, University of Manitoba, Winnipeg, Canada.

Kluitenberg, G. J. and Horton, R. 1990. Effect of solute application on preferential transport of solutes in soil. Geoderma 46:283-297.

Koppi, A. J. and Geering, H. R. 1986. The preparation of unsmeared soil surfaces and an improved apparatus for infiltration measurements. J. Soil Sci. 37:177-181.

Kosmas, C., Moustakas, N., Kallianou, C. and Yassoglou, N. 1991. Cracking patterns, bypass flow and nitrate leaching in Greek irrigated soils. Geoderma 49:139-152.

Lauren, J. G., Wagenet, R. J., Bouma, J. and Wosten, J. H. M. 1987. Variability of saturated hydraulic conductivity in a Glossaquic Hapludalf with macropores. Soil Sci. 145:20-28.

Lee, D. M., Reynolds, W. D., Elrick, D. E. and Clothier, B. E. 1985. A comparison of three field methods for measuring saturated hydraulic conductivity. Can. J. Soil Sci. 65:563-573.

Logan, T. G., Davidson, M. J., Baker, J. L. and Overcash, M. R. (editors), 1987. Effects of Conservation Tillage on Groundwater Quality - Nitrates and Pesticides. Lewis Publishers.

Logsdon, S. D., Allmaras, R. R., Wu, L., Swan, J. B. and Randall, G. W. 1990. Macroporosity and its relation to saturated hydraulic under different tillage practices. Soil Sci. Soc. Am. J. 54:1096-1101.

Lund, L. J., Adriano, D. C. and Pratt, P. F. 1974. Nitrate concentrations in deep soil cores as related to soil profile characteristics. J. Environ. Qual. 3:78-82.

Luxmoore, R. J. 1981. Micro-, meso- and macroporosity of soil. Soil Sci. Soc. Am. J. 45:671.

Mackie, L. A. 1987. Production of three-dimensional representations of soil macropores with a microcomputer. Geoderma 40:275-280.

McCurdy, M. and McSweeney, K. 1993. The origin and identification of macropores in an earthen-lined dairy manure storage basin. J. Environ. Qual. 22:148-154.

McKeague, J. A., Wang, C. and Topp, G. C. 1982. Estimating saturated hydraulic conductivity from soil morphology. Soil Sci. Soc. Am. J. 46:1239-1244.

McMahon, M. and Thomas, G. W. 1974. Chloride and titrated water flow in disturbed and undisturbed soil cores. Soil Sci. Soc. Am. Proc. 38:727-732.

Mellanby, K. 1971. The Mole, Collins, London.

Murphy, C. P., Bullock, P. and Turner, R. H. 1977. The measurement and characterization of voids in soil thin sections by image analysis, I. Principles and techniques. J. Soil Sci. 28:498-508.

Mwendera, E. J. and Feyen, J. 1993. Tillage and rainfall effects on infiltration and predictive applicability of infiltration equations. Soil Sci. 156(1):20-27.

Neuzil, C. E. 1994. How permeable are clays and shales? Water Resour. Res. 30(2):145-150.

Neuzil, C. E. 1986. Groundwater flow in low-permeability environments. Water Resour. Res. 22(8):1163-1195.

Nowland, J. L. 1981. Soil water regime classification. pp. 64-74 in J. H. Day (ed.) Proc. 3rd Meeting, Expert Committee on Soil Survey. Ottawa, 2-6 Mar. 1981. Agriculture Canada, Ottawa.

Paige, G. B. and Hillel, D. 1993. Comparison of three methods for assessing soil hydraulic properties. Soil Sci. 155(3):175-189.

Paton, T.R. 1974. Origin and terminology for gilgai in Australia. Geoderma 11:221-242.

Payne, B. R. 1972. Isotope Hydrology. Adv. Hydrosci., 8:95-138.

Pikul, Jr., J. L., Zuzel, J. F. and Ramig, R. E. 1990. Effect of tillage-induced macroporosity on water infiltration. Soil Tillage Res. 17:153-165.

Priebe, D. L. and Blackmer, A. M. 1989. Preferential movement of oxygen-18-labelled water and nitrogen-15-labelled urea through macropores in a Nicollet soil. J. Environ. Qual. 18:66-72.

Radulovich, R., Sollins, P., Baveye, P. and Solorzano, E. 1992. Bypass water flow through unsaturated microaggregated tropical soils. Soil Sci. Soc. Am. J. 56:721-726.

Ritchie, J.T., Kissel, D.E. and Burnett, E. 1972. Water movement in undisturbed swelling clay soil. Soil Sci. Soc. Am. Proc. 36:874-879.

Shipitalo, M. J., Edwards, W. M., Dick, W. A. and Owens, L. B. 1992. Rainfall intensity affects transport of water and chemicals through macropores in no-till soil. Soil Sci. Soc. Am. J. 54:1530-1536.

Shipitalo, M. J. and Protz, R. 1989. Chemistry and micromorphology of aggregation in earthworm casts. Geoderma 45:357-374.

Shipitalo, M. J. and Protz, R. 1987. Comparison of morphology and porosity of a soil under conventional and zero tillage. Can. J. Soil Sci. 67:445-456.

Skopp, J. 1981. Comment on 'Micro-, meso- and macroporosity of soil'. Soil Sci. Soc. Am. J. 45:1246.

Smettem, K. R. J. 1986. Analysis of water flow from cylindrical macropores. Soil Sci. Soc. Am. J. 50:1139-1142.

Smettem, K. R. J. and Collis-George, N. 1985. The influence of cylindrical macropores on steady-state infiltration in a soil under pasture. J. Hydrol. 79:107-114.

Soil Survey Staff, 1975. Soil Taxonomy: a basic system of soil classification for making and interpreting soil surveys. USDA Agr. Handb. 346. U.S. Gov't. Print. Office, Washington, DC, 754 pp.

Soil Survey Staff, 1987. Keys to Soil Taxonomy (third printing). SMSS Technical Monograph No. 6, Ithaca, NY.

Soloman, D. K. and Sudicky, E. A. 1991. Tritium and helium-3 isotope ratios for direct estimation of spatial variations in groundwater recharge. Water Resources Res. 27:2309-2319.

Sri Ranjan, R. and Gillham, R. W. 1991. Non-linear electro-osmotic and hydraulic flow phenomena in saturated clays. Can. Soc. Agricultural Engineering, Agriculture Institute of Canada Annual Meeting, Frederecton, N. B., July, 1991.

Sri Ranjan, R. and Karthigesu, T. 1992. Validity of conventional hydraulic conductivity measurement methods for clayey soils. Proc. 35th Annual Meeting Manitoba Society of Soil Science, Winnipeg, January 6-7, pp. 104-108.

Steenhuis, T. S. and Muck, R. E. 1988. Preferred movement of nonadsorbed chemicals on wet, shallow, sloping soils. J. Environ. Qual. 17:376-384.

Steenhuis, T. S., Parlange, J. Y. and Adreini, M. S. 1990. A numerical model for preferential solute movement in structured soils. Geoderma 46:193-208.

Stoops, G. and Eswaran, H. 1986. Soil Micromorphology. Van Nostrand Reinhold Company Inc., New York.

Tippkotter, R. 1983. Morphology, spatial arrangement and origin of macropores in some Hapludalfs, West Germany. Geoderma 29:355-371.

UMA Engineering Ltd. 1992. Manitoba Hazardous Waste Management Corporation. R. M. of Montcalm Detailed Site Evaluation - Additional Groundwater Chemistry and Isotope Studies.

UMA Engineering Ltd. 1991. Manitoba Hazardous Waste Management Corporation. R. M. of Montcalm Detailed Site Evaluation.

Veneman, P. L. M., Vespraskas, M. J. and Bouma, J. 1976. The physical significance of soil mottling in a Wisconsin toposequence. Geoderma, 15:103-118.

Vepraskas, M. L. and Bouma, J. 1976. Model studies on mottle formation simulating field conditions. Geoderma, 15:217-230.

White, E. M. 1967. Subsoil structure genesis: theoretical consideration. Soil Sci. 101:135-141.

Wopereis, M. C. S., Bouma, J., Kropff, M. J. and Sanidad, W. 1994. Reducing bypass flow through a dry, cracked and previously puddled rice soil. Soil Tillage Res. 29:1-11.

Yaalon, D.H. and Kalmar, D. 1978. Dynamics of cracking and swelling clay soils: displacement of skeletal grains, optimum depth of slickensides, and rate of intra-pedonic turbation. Earth Surface Processes 3:31-42.

Yong, R. N. and Warkentin, B. P. 1975. Soil properties and behavior, developments in geotechnical engineering. Elsevier, New York, N. Y.

Yuen, K. 1995. The effects of freeze-thaw weathering, drying-wetting weathering and changes in pore fluid chemistry on the hydraulic conductivity of Lake Agassiz clay. M. Sc. Thesis, Dept. of Civil Engineering, University of Manitoba, Winnipeg, Canada.

Zachmann, J. E., Linden, D. R. and Clapp, C. E. 1987. Macroporous infiltration and redistribution as affected by earthworms, tillage and residue. Soil Sci. Soc. Am. J. 51:1580-1586.

Appendix A - Drill Log Examination

Test Hole	Depth (m)	Effervescence* (10% HCl test)	Moist Color	Mottles^	Slickensides (location, angle)	Texture	Structure^^	Roots***	Porosity^^^	Salts	Notes
1	0-0.8	W (0-0.1 m)	10YR2/1	FFD-10YR6/6	-	SiC	M MC SB	F F I	A F/VF, fractures	-	
		M (0.1-0.35 m)	10YR4/3								
1	0.8-1.5	M	10YR4/3	CFD-10YR5/6	-	SiC	M C SB	VF F/VF I	A F/VF, fractures	-	
1	1.5-2.3	V	10YR4/3	CMP-5YR5/8	-	SiC	W FM SB	-	A F/VF, fractures	-	brown-black stains in upper 15 cm
1	2.3-3.0	W	2.5Y4/2	FFD-10YR5/6	-	SiC	SL - MA	-	F F/VF, fractures	-	
1	3.0-3.8	V	2.5Y2.5/2	FFD-2.5Y5/6	35 cm, 50	C	SL - MA	-	F F/VF, fractures	-	
1	3.8-4.6	V	2.5Y2.5/2	FFP-5YR3/4	-	C	SL - MA	-	F F/VF, fractures	-	
1	4.6-5.3	V	5Y3/2	-	-	C	SL - MA	-	VF VF, fractures	-	hor fractures every 8-10 cm
1	5.3-6.1	V	5Y3/2	FFP-10YR5/6	-	C	SL - MA	-	VF VF, fractures	white carbonates	
1	6.1-6.9	V	5Y3/2	-	-	C	SL - MA	-	VF VF, fractures	white carbonates	
1	6.9-7.6	V	5Y3/2	-	-	C	SL - MA	-	VF VF, fractures	white carbonates	
1	7.6-8.4	V	5Y3/2	-	-	C	SL - MA	-	VF VF, fractures	white carbonates	
1	8.4-9.1	V	5Y3/2	-	-	C	SL - MA	-	few fractures	white carbonates	
1	9.1-9.9	V	5Y3/2	-	-	C	SL - MA	-	few fractures	white/orange carb	
1	9.9-10.7	V	5Y3/2	-	-	C	SL - MA	-	fractures	-	
1	10.7-11.4	V	5Y3/2	-	-	C	SL - MA	-	few fractures	-	
1	11.4-12.2	V	5Y3/2	-	-	C	SL - MA	-	few fractures	-	
1	12.2-13.0	V	5Y3/2	-	-	C	SL - MA	-	few fractures	-	
1	13.0-13.7	V	5Y3/2	-	18 cm, 35	C	SL - MA	-	few fractures	-	

Test Hole	Depth (m)	Effervescence* (10% HCl test)	Moist Color	Mottles^	Slickensides (location, angle)	Texture	Structure^^	Roots***	Porosity^^^	Salts	Notes
2	0-0.8	N/O	N/O	N/O	-	N/O	N/O	F F I (0-15cm) VF F I (>15cm)	F VF	-	
2	0.8-1.5	N/O	N/O	N/O	-	N/O	N/O	-	VF VF	-	
2	1.5-2.3	N/O	N/O	N/O	15 cm, 20 45 cm, 30	N/O	N/O	-	ext hor fractures	-	small sand lenses
2	2.3-3.0	N/O	N/O	N/O	25 cm, 25	N/O	N/O	-	ext vert fractures	-	small sand lenses
2	3.0-3.8	N/O	N/O	N/O	-	N/O	N/O	F FM(root ch)	VF VF, fractures	salts in r.c.& matrix	
2	3.8-4.6	N/O	N/O	N/O	-	N/O	N/O	VF FM(root ch)	VF VF, fractures	salts in r.c.& matrix	
2	4.6-5.3	N/O	N/O	N/O	30 cm, 15	N/O	N/O	-	fractures	white salts in matrix	
2	5.3-6.1	N/O	N/O	N/O	40 cm, 45	N/O	N/O	-	hor fractures	some salts-matrix	
2	6.1-6.9	N/O	N/O	N/O	40 cm, 40	N/O	N/O	-	few hor fractures	some salts-matrix	
2	6.9-7.6	N/O	N/O	N/O	-	N/O	N/O	-	few hor fractures	some salts-matrix	
2	7.6-8.4	N/O	N/O	N/O	50 cm, 40 55 cm, 30	N/O	N/O	-	few hor fractures	some salts-matrix	
2	8.4-9.1	N/O	N/O	N/O	20 cm, 40 30 cm, 30	N/O	N/O	-	-	gray salts-matrix	
2	9.1-9.9	N/O	N/O	N/O	20 cm, 30 35 cm, 25	N/O	N/O	-	-	gray salts-matrix	
2	9.9-10.7	N/O	N/O	N/O	-	N/O	N/O	-	hor fractures	some salts-matrix	
2	10.7-11.4	N/O	N/O	N/O	-	N/O	N/O	-	hor fractures	some salts-matrix	
2	11.4-12.2	N/O	N/O	N/O	40 cm, 60	N/O	N/O	-	hor fractures	some salts-matrix	
2	12.2-13.0	N/O	N/O	N/O	-	N/O	N/O	-	hor fractures	gray & orange-matrix	
2	13.0-13.7	N/O	N/O	N/O	-	N/O	N/O	-	hor fractures	gray salts-matrix	

Test Hole	Depth (m)	Effervescence* (10% HCl test)	Moist Color	Mottles^	Slickensides (location, angle)	Texture	Structure^^	Roots***	Porosity^^^	Salts	Notes
3	0-0.8	N/O	N/O	N/O	-	N/O	N/O	F F I (0-20cm) VF F I (>20cm)	F F I fractures	-	
3	0.8-1.5	N/O	N/O	N/O	-	N/O	N/O	-	VF F I fractures	-	
3	1.5-2.3	N/O	N/O	N/O	-	N/O	N/O	-	VF VF I fractures	-	
3	2.3-3.0	N/O	N/O	N/O	55 cm, 50	N/O	N/O	-	hor/vert fractures	-	
3	3.0-3.8	N/O	N/O	N/O	25 cm, 45	N/O	N/O	F F I(root ch)	ext fractures	-	
3	3.8-4.6	N/O	N/O	N/O	20 cm, 40 25 cm, 30 40 cm, 40	N/O	N/O	F F I(root ch)	ext fractures	-	
3	4.6-5.3	N/O	N/O	N/O	10 cm, 40	N/O	N/O	VF F I (r c)	ext fractures	-	
3	5.3-6.1	N/O	N/O	N/O	15 cm, 35 25 cm, 50 50 cm, 45	N/O	N/O	-	ext fractures	-	
3	6.1-6.9	N/O	N/O	N/O	-	N/O	N/O	-	few hor fractures	-	
3	6.9-7.6	N/O	N/O	N/O	-	N/O	N/O	-	few hor fractures	-	
3	7.6-8.4	N/O	N/O	N/O	-	N/O	N/O	-	few hor fractures	-	
3	8.4-9.1	N/O	N/O	N/O	-	N/O	N/O	-	few hor fractures	-	
3	9.1-9.9	N/O	N/O	N/O	20 cm, 50	N/O	N/O	-	few hor fractures	-	
3	9.9-10.7	N/O	N/O	N/O	15 cm, 20	N/O	N/O	-	few hor fractures	-	
4	0-0.8	W (0-0.1 m) V (>0.1 m)	2.5Y2/0(0-25cm 10YR3/1(>25cm)	FFF-10YR3/3	-	C	M FM SB (0-35cm) SL - MA (>35cm)	P FM I(0-25cm) F FM I(>25cm)	A F I (0-25cm) P F I (>25cm)	white salts @ roots	small cracks present
4	0.8-1.5	M (0-0.2 m) S (0.2-0.3 m)	2.5Y4.5/4	FFF-10YR4.5/4	-	SiC	SL - MA	-	F F I	-	

Test Hole	Depth (m)	Effervescence* (10% HCl test)	Moist Color	Mottles^	Slickensides (location, angle)	Texture	Structure^^	Roots***	Porosity^^^	Salts	Notes
4	1.5-2.3	S	2.5Y4/2(clay) 2.5Y7/4(silt)	FMP-10YR4/6	-	SiC	SL - MA	-	F F I	-	Fe, Mn deposits
4	2.3-3.0	V	10YR4/2	CMP-10YR4/6	-	SiC	SL - MA	-	VF F/VF I	-	vert(0-20) & hor(>20cm) fractures
4	3.0-3.8	V	2.5Y4/2	CMP-10YR4/6	40 cm, 35	SiC	SL - MA	-	F F/VF I	-	Fe, Mn deposits in r.c.
4	3.8-4.6	V	2.5Y4/2	CMP-10YR4/6	-	SiC	SL - MA	-	VF F/VF I	-	Fe, Mn deposits
4	4.6-5.3	V	5Y3/1	FFP-10YR4/6	-	SiC	SL - MA	-	VF VF I	few white salts inped	
4	5.3-6.1	V	5Y3/1	-	40 cm, 20	SiC	SL - MA	-	-	salts inped	
4	6.1-6.9	V	5Y3/1	-	35 cm, 45	SiC	SL - MA	VF VF I@38cm	VF VF I	salts inped	
4	6.9-7.6	V	5Y3/1	-	-	SiC	SL - MA	-	VF VF I	salts inped	horizontal fracture at 25 cm
4	7.6-8.4	V	5Y3/1	-	-	SiC	SL - MA	-	VF VF I	salts inped	
4	8.4-9.1	V	5Y3/1	-	-	SiC	SL - MA	-	-	salts inped	
4	9.1-9.9	V	5Y3/1	-	45 cm, 55	SiC	SL - MA	-	-	salts inped	
4	9.9-10.7	V	5Y3/1	-	-	SiC	SL - MA	-	VF VF I	salts inped	hor and vert fractures
5	0-1.5	N/O	N/O	N/O	-	N/O	N/O	-	VF VF I	-	
5	1.5-3.0	N/O	N/O	N/O	-	N/O	N/O	-	VF VF I	-	mottles, silt
5	3.0-4.6	N/O	N/O	N/O	-	N/O	N/O	-	VF VF I	white salts @ 14ft.	silt
5	4.6-6.1	N/O	N/O	N/O	-	N/O	N/O	-	VF VF I	white & gray salts	
5	6.1-7.6	N/O	N/O	N/O	40 cm, 20 55 cm, 40 85 cm, 30	N/O	N/O	-	-	white & gray salts	

Test Hole	Depth (m)	Effervescence* (10% HCl test)	Moist Color	Mottles^	Slickensides (location, angle)	Texture	Structure^^	Roots***	Porosity^^^	Salts	Notes
5	7.6-9.1	N/O	N/O	N/O	15 cm, 45	N/O	N/O	-	hor fractures	white & gray salts	
					80 cm, 40						
5	9.1-10.7	N/O	N/O	N/O	25 cm, 40	N/O	N/O	-	-	white & gray salts	
					30 cm, 25						
					55 cm, 25	N/O	N/O				
5	10.7-12.2	N/O	N/O	N/O	55 cm, 25	N/O	N/O	-	hor fractures	white & gray salts	
					100 cm, 50						
5	12.2-13.7	N/O	N/O	N/O	75 cm, 15	N/O	N/O	-	hor fractures	white & gray salts	
					95 cm, 15						
6	0-1.5	W (0-0.1 m)	10YR2/1	-	-	C	M FM SB	P F I	A F I	-	
		S (0.1-0.5 m)	10YR5/3	FFD-10YR4/6	-	SiL	W FM SB	-	A F I	-	
		S (0.5-1.0 m)	5Y4/3	FFD-10YR4/6	-	SiC	M MC SB	-	A F I	-	
		W (>1.0 m)	5Y4/2	CFD-10YR4/6	100 cm, 30	SiC	SL - MA	-	P F I	-	Fe, Mn deposits
6	1.5-2.3	M (1.5-1.7 m)	2.5Y4/4	CMP-10YR5/6	10 cm, 30	Si	M FM SB	-	F F I	-	mottles, carb. deposits on slickenside
		V (>1.7 m)	5Y4/2			SiC	SL - MA		VF VF I,fractures		
6	2.3-3.0	V	5Y4/2	CMP-2.5Y4/4	25 cm, 40	SiC	SL - MA	root channels	VF VF I	-	Fe, Mn deposits in root channels
6	3.0-3.8	V	5Y3/1	MMP-2.5Y4/4	-	SiC	SL - MA	F M I	F VF I	-	Fe, Mn deposits in root channels
6	3.8-4.6	V	5Y3/1	MMP-2.5Y4/4	-	SiC	SL - MA	F F I	F F/VF I	few white salts	root channels w/some roots
6	4.6-6.1	V	5Y3/1	CMP-N4/	100 cm, 25	SiC	SL - MA	-	F VF I	-	gleying at 80 cm
					105 cm, 20						

Test Hole	Depth (m)	Effervescence* (10% HCl test)	Moist Color	Mottles^	Slickensides (location, angle)	Texture	Structure^^	Roots***	Porosity^^^	Salts	Notes
6	6.1-7.6	V	5Y3/1	-	100 cm, 45	SiC	SL - MA	-	VF VF I		many horizontal fractures
6	7.6-9.1	V	5Y3/1	FMPgley 5B4/1 (80cm)	55 cm, 45	SiC	SL - MA	-	-	few white salts	
					70 cm, 40						
6	11.4-12.2	V	5Y3/1	-	-	SiC	SL - MA	-	-	few white salts	
6	11.4-13.0	V	5Y3/1	-	-	SiC	SL - MA	-	-	few white salts	
6	13.0-13.7	V	5Y3/1	-	-	SiC	SL - MA	-	-	few white salts	
7	0-1.5	N/O	N/O	N/O	-	N/O	N/O	-	-	-	
7	1.5-3.0	N/O	N/O	N/O	-	N/O	N/O	-	F F I fractures	-	mottles, silt
7	3.0-4.6	N/O	N/O	N/O	-	N/O	N/O	-	VF VF I fractures	white salts-matrix	
7	4.6-6.1	N/O	N/O	N/O	25 cm, 30	N/O	N/O	-	-	white salts-matrix	
					35 cm, 30						
7	6.1-7.6	N/O	N/O	N/O	20 cm, 30	N/O	N/O	-	hor fractures	few white/grey-matrix	
7	7.6-9.1	N/O	N/O	N/O	25 cm, 40	N/O	N/O	-	few hor fractures	few white/grey-matrix	
					35 cm, 45						
					85 cm, 35						
7	9.1-10.7	N/O	N/O	N/O	25 cm, 25	N/O	N/O	-	hor fractures	few white/grey-matrix	
					80 cm, 45						
					85 cm, 45						
					100 cm, 50						

Test Hole	Depth (m)	Effervescence* (10% HCl test)	Moist Color	Mottles^	Slickensides (location, angle)	Texture	Structure^^	Roots***	Porosity^^^	Salts	Notes
8	0-0.8	N/O	N/O	N/O	-	N/O	N/O	F VF I	F F I	-	
8	0.8-1.5	N/O	N/O	N/O	-	N/O	N/O	-	F F I	-	
8	1.5-2.3	N/O	N/O	N/O	-	N/O	N/O	-	F F I fractures	-	
8	2.3-3.0	N/O	N/O	N/O	30 cm, 50	N/O	N/O	-	hor fractures	-	
8	3.0-3.8	N/O	N/O	N/O	35 cm, 30	N/O	N/O	-	hor fractures	-	
					45 cm, 35						
8	3.8-4.6	N/O	N/O	N/O	-	N/O	N/O	-	VF VF I fractures	-	
8	4.6-5.3	N/O	N/O	N/O	25 cm, 25	N/O	N/O	-	-	few white/grey-matrix	
					40 cm, 65					few white/grey-matrix	
8	5.3-6.1	N/O	N/O	N/O	35 cm, 40	N/O	N/O	-	-	few white/grey-matrix	
8	6.1-6.9	N/O	N/O	N/O	15 cm, 55	N/O	N/O	-	hor fractures	few white/grey-matrix	
8	6.9-7.6	N/O	N/O	N/O	-	N/O	N/O	-	few hor fractures	few white/grey-matrix	
8	7.6-8.4	N/O	N/O	N/O	-	N/O	N/O	-	few hor fractures	few white/grey-matrix	
8	8.4-9.1	N/O	N/O	N/O	-	N/O	N/O	-	few hor fractures	few white/grey-matrix	
8	9.1-9.9	N/O	N/O	N/O	-	N/O	N/O	-	few hor fractures	few white/grey-matrix	
8	9.9-10.7	N/O	N/O	N/O	-	N/O	N/O	-	few hor fractures	few white/grey-matrix	
9	0-2.5	N/O	N/O	N/O	-	N/O	N/O	F F I	F F I	-	
9	2.5-5.0	N/O	N/O	N/O	-	N/O	N/O	F F I (0-20cm)	F F I	-	
9	5.0-7.5	N/O	N/O	N/O	-	N/O	N/O	-	F F I	-	
9	7.5-10.0	N/O	N/O	N/O	-	N/O	N/O	-	F F I hor fractures	-	
9	10.0-12.5	N/O	N/O	N/O	-	N/O	N/O	-	hor fractures	-	
9	12.5-15.0	N/O	N/O	N/O	-	N/O	N/O	root/r.c(35cm)	few hor fractures	-	
9	15.0-17.5	N/O	N/O	N/O	-	N/O	N/O	-	few hor fractures	v.few salts-matrix	

Test Hole	Depth (m)	Effervescence* (10% HCl test)	Moist Color	Mottles^	Slickensides (location, angle)	Texture	Structure^^	Roots***	Porosity^^^	Salts	Notes
9	17.5-20.0	N/O	N/O	N/O	35 cm, 40	N/O	N/O	-	few hor fractures	v.few salts-matrix	
9	20.0-22.5	N/O	N/O	N/O	-	N/O	N/O	-	hor fractures	-	
9	22.5-25.0	N/O	N/O	N/O	-	N/O	N/O	-	few hor fractures	-	
9	25.0-27.5	N/O	N/O	N/O	35 cm, 40	N/O	N/O	-	few hor fractures	few white/grey-matrix	
9	27.5-30.0	N/O	N/O	N/O	20 cm, 20	N/O	N/O	-	few hor fractures	few white/grey-matrix	
9	30.0-32.5	N/O	N/O	N/O	15 cm, 50	N/O	N/O	-	few hor fractures	few white/grey-matrix	
9	32.5-35.0	N/O	N/O	N/O	10 cm, 40	N/O	N/O	-	few hor fractures	few white/grey-matrix	
					35 cm, 45						
					40 cm, 40						
10	0-1.5	V-W (0-0.2m)	10YR2.5/1d	-	-	C	M M SB	P M I	F F I	white crystals-matrix	
		W-M (>0.2 m)	2.5Y5/4d	FMP-10YR5/6d (>50cm)		SiC	M C SB	P FM I	A FM I		Fe, Mn deposits
10	1.5-3.0	W (1.5-2.1 m)	2.5Y5/4	MMP-10YR4/6, 7.5YR3/4	-	SiC	W C SB	-	P FM I	-	fine sand, Mn deposits @ ped edges
		V (>2.1 m)	2.5Y4/2	FFD-10YR4/6		SiC	SL - MA			white salts-matrix	few horizontal fractures
10	3.0-4.6	V	5Y3/2	-	90 cm, 30	SiC	SL - MA	-	-	white salts-matrix	
10	4.6-6.1	V	5Y3/1	FFP-10YR5/6	-	SiC	SL - MA	-	-	white salts-matrix	
10	6.1-7.6	V	5Y3/1	-	-	SiC	SL - MA	-	-	white salts-matrix	
10	7.6-9.1	V	5Y3/1	-	-	SiC	SL - MA	-	-	white salts-matrix	horizontal fractures
10	9.1-10.7	V	5Y3/1	-	75 cm, 30	SiC	SL - MA	-	-	white salts-matrix	horizontal fractures
11	0-0.8	M (0-0.3 m)	10YR2/1	-	-	SiCL	M FM SB	P F/VF	A F/VF	-	
		S (>0.3 m)	10YR6/3			SiL	M MC SB	F F/VF	A F/VF		

Test Hole	Depth (m)	Effervescence* (10% HCl test)	Moist Color	Mottles^	Slickensides (location, angle)	Texture	Structure^^	Roots***	Porosity^^^	Salts	Notes
11	0.8-1.5	W	10YR5/3	Mn-10YR4/3d Fe-10YR6/6d	-	Si	M FM SB	F F/VF	A F/VF	-	
11	1.5-2.3	W	10YR5.5/3	MMP-10YR4/4, 10YR5/8	-	SiCL	MS MC SB	VF F/VF	F M/F;A VF	-	
11	2.3-3.0	V	10YR4.5/2	MMP-10YR5/6d	-	SiCL	MS MC SB	root channels	F M/F	-	
11	3.0-3.8	V	10YR4/4	FFD-10YR5/6d	-	SiC	SL - MA	root channels	F F	-	
11	3.8-4.6	V	10YR4/2	FFD-2.5Y4/2d	20 cm, 35	SiC	SL - MA	root channels	F M/F	salts in r.c.&matrix	
11	4.6-5.3	V	2.5Y3/2d	FFD-2.5Y6/8d	40 cm, 35 45 cm, 35	SiC	SL - MA	root channels	F M/F	salts in r.c.&matrix	
11	5.3-6.1	V	2.5Y3/2d	FFF-2.5YR5/6d	40 cm, 37.5	SiC	SL - MA	-	F F	salts in matrix	
11	6.1-6.9	V	2.5Y3/2d	FFF-2.5YR4/6d	15 cm, 35 25 cm, 40	SiC	SL - MA	-	V F	carbonates in matrix	
11	6.9-7.6	V	2.5Y3/2d	FFD-10YR4/4d	40 cm, 40	SiC	SL - MA	-	V F	carb in r.c.&matrix	mottles on outside of core
11	7.6-8.4	V	2.5Y3/2d	-	50 cm, 35 25 cm, 45 45 cm, 35	SiC	SL - MA	-	V F	carb in r.c.&matrix	
11	8.4-9.1	V	2.5Y3/2d	FFD-10YR4/4d	25 cm, 35	SiC	SL - MA	-	V F	carb in r.c.&matrix	mottles on outside of core
11	9.1-9.9	V	2.5Y3/2d	-	25 cm, 35 35 cm, 35	SiC	SL - MA	-	V F; fractures	carb in r.c.&matrix	
11	9.9-10.7	V	2.5Y3/2d	-	30 cm, 40	SiC	SL - MA	-	V F; fractures	carb in r.c.&matrix	
12	0-0.8	N/O	N/O	N/O	-	N/O	N/O	F F I	F F I	-	

Test Hole	Depth (m)	Effervescence* (10% HCl test)	Moist Color	Mottles^	Slickensides (location, angle)	Texture	Structure^^	Roots***	Porosity^^^	Salts	Notes
12	0.8-1.5	N/O	N/O	N/O	-	N/O	N/O	F F I	F F Ihor fractures	-	
12	1.5-2.3	N/O	N/O	N/O	-	N/O	N/O	-	VF VF I fractures	-	
12	2.3-3.0	N/O	N/O	N/O	-	N/O	N/O	-	VF VF I fractures	-	mottles
12	3.0-3.8	N/O	N/O	N/O	-	N/O	N/O	-	VF VF I fractures	-	some sand
12	3.8-4.6	N/O	N/O	N/O	10 cm, 40 25 cm, 35	N/O	N/O	-	VF VF I fractures	-	
12	4.6-5.3	N/O	N/O	N/O	-	N/O	N/O	-	ext. fractures	white salts-matrix	
12	5.3-6.1	N/O	N/O	N/O	55 cm, 20	N/O	N/O	-	few fractures	white/grey - matrix	
12	6.1-6.9	N/O	N/O	N/O	35 cm, 35	N/O	N/O	-	few fractures	white/grey - matrix	
12	6.9-7.6	N/O	N/O	N/O	30 cm, 40	N/O	N/O	-	few fractures	white/grey - matrix	
12	7.6-8.4	N/O	N/O	N/O	30 cm, 35 35 cm, 45 45 cm, 30	N/O	N/O	-	few fractures	white/grey - matrix	
12	8.4-9.1	N/O	N/O	N/O	-	N/O	N/O	-	-	-	
12	9.1-9.9	N/O	N/O	N/O	-	N/O	N/O	-	few hor fractures	white/grey - matrix	
12	9.9-10.7	N/O	N/O	N/O	40 cm, 45	N/O	N/O	-	hor fractures	white/grey - matrix	
13	0-0.8	W (0-0.2 m)	10YR2/1d	-	-	C	W FM SB	F F I	F F I	carbonates	Fe, Mn deposits
		M (>0.2 m)	2.5Y5/4d	FFP(10YR5/6d)		Si	M MC SB		P F I	carbonates	silt mixed in with clay
13	0.8-1.5	V (clay) M (silt)	2.5Y4/2 2.5Y4/2	FFP(10YR5/6d)	-	SiC	SL - MA	-	P F I	carbonates	mottles; silt mixed in with clay
13	1.5-2.3	V (clay) M (silt)	2.5Y4/2 2.5Y4/2	CMP(10YR5/6d)	-	SiC	SL - MA	-	F F I	carbonates	hor fractures; Si mixed w/C (50cm)

Test Hole	Depth (m)	Effervescence* (10% HCl test)	Moist Color	Mottles^	Slickensides (location, angle)	Texture	Structure^^	Roots***	Porosity^^^	Salts	Notes
13	2.3-3.0	W (clay&silt) V (clay)	2.5Y6/4 2.5Y4/2	CMP(10YR5/6)	-	SiC	SL - MA	-	VF VF I	carbonates	horizontal fractures
13	3.0-3.8	V	2.5Y4/2(<30cm) 5Y3/2 (>30cm)	FFP(10YR5/6)	-	SiC	SL - MA	VF VF I (55cm)	VF VF I	-	
13	3.8-4.6	V	5Y3/1	-	-	SiC	SL - MA	-	-	few salts	horizontal fractures
13	4.6-5.3	V	5Y3/1	-	-	SiC	SL - MA	-	-	few salts	
13	5.3-6.1	V	5Y3/1	-	25 cm, 30	SiC	SL - MA	-	-	few salts	
13	6.1-6.9	V	5Y3/1	-	20 cm, 50	SiC	SL - MA	-	-	few salts	
13	6.9-7.6	V	5Y3/1	-	-	SiC	SL - MA	-	-	few salts	horizontal fractures
13	7.6-8.4	V	5Y3/1	-	-	SiC	SL - MA	-	-	few salts	
13	8.4-9.1	V	5Y3/1	-	15 cm, 20	SiC	SL - MA	-	-	few salts	horizontal fractures
13	9.1-9.9	V	5Y3/1	-	-	SiC	SL - MA	-	-	few salts	
13	9.9-10.7	V	5Y3/1	-	-	SiC	SL - MA	-	-	few salts	horizontal fractures
14	0-0.8	carb @ 0.4 m	N/O	N/O	-	N/O	N/O	F F I (<40cm)	P F I		
14	0.8-1.5	N/O	N/O	N/O	-	N/O	N/O	-	F F Ifractures	-	
14	1.5-2.3	N/O	N/O	N/O	-	N/O	N/O	-	fractures	-	mottles
14	2.3-3.0	N/O	N/O	N/O	45 cm, 30	N/O	N/O	-	fractures	-	mottles
14	3.0-3.8	N/O	N/O	N/O	-	N/O	N/O	-	fractures	-	mottles
14	3.8-4.6	N/O	N/O	N/O	30 cm, 55 45 cm, 35	N/O	N/O	-	few hor fractures	v.few white/grey	
14	4.6-5.3	N/O	N/O	N/O	20 cm, 20	N/O	N/O	-	few hor fractures	few white/grey/orange	
14	5.3-6.1	N/O	N/O	N/O	15 cm, 45 40 cm, 40	N/O	N/O	-	few hor fractures	few white/grey/orange	

Test Hole	Depth (m)	Effervescence* (10% HCl test)	Moist Color	Mottles^	Slickensides (location, angle)	Texture	Structure^^	Roots***	Porosity^^^	Salts	Notes
14	6.1-6.9	N/O	N/O	N/O	-	N/O	N/O	-	few hor fractures	few white/grey/orange	
14	6.9-7.6	N/O	N/O	N/O	25 cm, 30	N/O	N/O	-	few hor fractures	few white/grey/orange	
					30 cm, 35						
14	7.6-8.4	N/O	N/O	N/O	40 cm, 35	N/O	N/O	-	few hor fractures	few white/grey/orange	
14	8.4-9.1	N/O	N/O	N/O	20 cm, 35	N/O	N/O	-	few hor fractures	few white/grey/orange	
14	9.1-9.9	N/O	N/O	N/O	-	N/O	N/O	-	few hor fractures	few white/grey/orange	
14	9.9-10.7	N/O	N/O	N/O	50 cm, 20	N/O	N/O	-	few hor fractures	few white/grey/orange	
15	0-0.8	N/O	N/O	N/O	-	N/O	N/O	F F I	F F I	carbonates	
15	0.8-1.5	N/O	N/O	N/O	-	N/O	N/O	-	ext. fractures	-	mottles
15	1.5-2.3	N/O	N/O	N/O	-	N/O	N/O	-	F F I fractures	-	mottles
15	2.3-3.0	N/O	N/O	N/O	-	N/O	N/O	-	F F Ifew fractures	-	mottles
15	3.0-3.8	N/O	N/O	N/O	35 cm, 60	N/O	N/O	root channel	vert&hor fractures	white salts-matrix	mottles
15	3.8-4.6	N/O	N/O	N/O	50 cm, 40	N/O	N/O	(35-55cm)	vert&hor fractures	large salt deposits	
					40 cm, 50						
15	4.6-5.3	N/O	N/O	N/O	-	N/O	N/O	-	vert&hor fractures	few white/grey	
15	5.3-6.1	N/O	N/O	N/O	-	N/O	N/O	-	few hor fractures	few white/grey	gypsum crystals (35cm)
15	6.1-6.9	N/O	N/O	N/O	-	N/O	N/O	-	few hor fractures	few salts-matrix	
15	6.9-7.6	N/O	N/O	N/O	-	N/O	N/O	-	few hor fractures	few salts-matrix	
15	7.6-8.4	N/O	N/O	N/O	20 cm, 30	N/O	N/O	-	few hor fractures	large salt deposits	
15	8.4-9.1	N/O	N/O	N/O	-	N/O	N/O	-	few hor fractures	large salt deposits	
15	9.1-9.9	N/O	N/O	N/O	40 cm, 55	N/O	N/O	-	few hor fractures	few white/grey	
15	9.9-10.7	N/O	N/O	N/O	15 cm, 30	N/O	N/O	-	few hor fractures	few white/grey	
					20 cm, 50						

Test Hole	Depth (m)	Effervescence* (10% HCl test)	Moist Color	Mottles^	Slickensides (location, angle)	Texture	Structure^^	Roots***	Porosity^^^	Salts	Notes
16	0-0.8	V (0-0.3 m)	10YR2/1	-	-	C	VW FM SB	A F/M I	F F/VF I	-	
		W (>0.3 m)	10YR3.5/2			SiC	VW FF SB	P F I	F F/VF I	-	
16	0.8-1.5	W (0.8-1.1 m)	10YR3/2	-	-	C	VW FM SB	F F I	P F/VF I	-	
		M (>1.1 m)	5Y4/2	CFP-10YR4.5/6		SiC	VW FM SB	F F I	P F/VF I	-	mottles at 35cm
16	1.5-2.3	W (1.5-1.9 m)	5Y4/2	MMP-10YR5.5/6	35 cm, 50	SiC	VW FF SB	F F I	P F/VF I	-	orange, brown and black deposits
		V (>1.9 m)	5Y4/2	CMD-2.5Y4/4	42 cm, 50 52 cm, 45		SL - MA		F VF I		
16	2.3-3.0	V	2.5Y4/2	CMP-10YR4/6	-	C	SL - MA	-	F VF I	-	root ch's to 10 ft w/precipitates
16	3.0-3.8	V	2.5Y4/2	FMF-2.5Y4/4	-	C	SL - MA	-	F F/VF I	white salts-rc/matrix	root ch's to 12.5ft w/salts,mottles
16	3.8-4.6	V	2.5Y4/2	CMD-10YR3/6	25 cm, 40	C	SL - MA	-	F F/VF I	white salts-matrix	
16	4.6-5.3	V	5Y3/2	FFD-2.5Y4/4	35 cm, 35	C	SL - MA	VF VF E	VF F/VF I	white/grey - matrix	orange root ~7cm long @ 55cm
16	5.3-6.1	V	2.5Y3/2	FFD-2.5Y4/4	25 cm, 45	C	SL - MA	-	VF VF I	salts in matrix	
16	6.1-6.9	V	5Y3/1	FMP-10YR4/6	-	C	SL - MA	-	VF VF I	various salts-matrix	black stains (Mn) @ 5cm
16	6.9-7.6	V	5Y3/1	-	-	C	SL - MA	-	VF VF I	various salts-matrix	
16	7.6-8.4	W	5Y3/1	-	35 cm, 40	C	SL - MA	-	VF VF I	salts in matrix	
			Si - 5Y5/2d			Si	SL - MA				
16	8.4-9.1	V	5Y3/1	FMP-2.5Y5/6	-	C	SL - MA	-	VF VF I	salts in matrix	
16	9.1-9.9	V	5Y3/1	FMP-10YR3/3	20 cm, 50	C	SL - MA	-	-	few salts in matrix	
		M (Si lenses)	10YR7/2d			Si	SL - MA				
16	9.9-10.7	V	5Y3/1	FMP-10YR4/6	-	C	SL - MA	-	-	few salts in matrix	

Test Hole	Depth (m)	Effervescence* (10% HCl test)	Moist Color	Mottles^	Slickensides (location, angle)	Texture	Structure^^	Roots***	Porosity^^^	Salts	Notes
M '93	0-0.2	W	10YR2/1	-	@20 cm, 50	N/O	N/O	A F/M I	P F/VF	-	
					@23 cm, 30	N/O	N/O				
M '93	0.2-0.4	W	10YR3/1	N/O	-	N/O	N/O	F F I	P F/VF	-	
M '93	0.4-0.6	M	10YR4/2	N/O	-	N/O	N/O	-	F F/VF	-	
M '93	0.6-0.8	W	10YR4/4	N/O	-	N/O	N/O	-	F F/VF	-	silty
M '93	0.8-1.0	W	10YR4/3	N/O	@80cm, 40	N/O	N/O	-	P F/VF	-	
M '93	1.0-1.3	M	10YR4/3	N/O	@110 cm, 40	N/O	N/O	VF VF I	P F/M	-	mottles
					@130 cm, 35						
M '93	1.3-1.8	M	10YR4/4	N/O	-	N/O	N/O	-	F F/VF	-	mottles
M '93	1.8-2.3	W	10YR4/4	N/O	@215 cm, 35	N/O	N/O	-	VF VF	-	mottles
M '93	2.3-2.8	V	10YR4/4	N/O	-	N/O	N/O	-	VF VF	-	mottles
M '93	2.8-3.3	V	10YR4/4	N/O	-	N/O	N/O	-	VF VF	-	mottles
M '93	3.3-3.9	V	10YR4/4	N/O	-	N/O	N/O	-	VF VF	-	mottles, Fe staining, brown/grey clay @ 365 cm
M '93	3.9-4.4	V	10YR4/4	N/O	-	N/O	N/O	-	-	-	mottles, grey clay
M '93	4.4-4.6	V	10YR4/4	N/O	-	N/O	N/O	root material?	-	-	mottles
M '93	4.6-4.8	V	10YR4/4	N/O	@480 cm, 45	N/O	N/O	-	-	-	mottles
M '93	4.8-5.5	V	10YR4/4	N/O	@495 cm, 60	N/O	N/O	-	VF VF	-	mottles less frequent
M '93	5.5-6.2	V	10YR4/4	N/O	-	N/O	N/O	-	-	-	mottles
M '93	6.2-6.8	V	10YR4/4	N/O	-	N/O	N/O	-	-	-	mottles
M '93	6.8-7.2	W/M	10YR4/4	N/O	-	N/O	N/O	-	VF VF	-	mottles, Si lens w/M effer.
M '93	7.2-7.8	V	10YR4/4	N/O	-	N/O	N/O	-	-	-	mottles
M '93	7.8-8.4	V	10YR4/4	N/O	-	N/O	N/O	-	-	-	mottles

Test Hole	Depth (m)	Effervescence* (10% HCl test)	Moist Color	Mottles^	Slickensides (location, angle)	Texture	Structure^^	Roots***	Porosity^^^	Salts	Notes
M '93	8.4-8.9	V	10YR4/4	N/O	-	N/O	N/O	-	-	-	mottles
M '93	8.9-9.5	V	10YR4/4	N/O	-	N/O	N/O	-	-	-	mottles
M '93	9.5-10.1	M	10YR4/4	N/O	-	N/O	N/O	-	-	-	mottles
M '93	10.1-10.7	V	10YR4/4	N/O	-	N/O	N/O	-	-	-	few mottles
M '93	10.7-11.3	V	10YR4/4	N/O	-	N/O	N/O	-	-	-	few mottles
M '93	11.3-11.9	V	10YR4/4	N/O	-	N/O	N/O	-	-	-	few mottles
M '93	11.9-12.4	V	10YR4/4	N/O	-	N/O	N/O	-	-	-	few mottles
M '93	12.4-13.0	V	10YR4/4	N/O	-	N/O	N/O	-	-	-	few mottles
W '93	0-0.2	M/S	10YR2/1	N/O	@12 cm, 45 @17 cm, 25	N/O	N/O	A M I	F F/VF	some white salts	
W '93	0.2-0.9	W	10YR3/2	N/O	@27 cm, 40 @43 cm, 25	N/O	N/O	P F/M I	P F/M	-	
W '93	0.9-1.5	W	10YR3/2	N/O	-	N/O	N/O	-	VF VF	salts	Fe staining @ 145 cm
W '93	1.5-2.3	M	10YR3/2	N/O	-	N/O	N/O	-	VF VF	salts	Fe staining, carb. lenses, mottles
W '93	2.3-3.1	W	10YR3/2	N/O	-	N/O	N/O	-	VF VF	salts	Fe staining, mottles
W '93	3.1-3.7	W	10YR3/2	N/O	-	N/O	N/O	-	F VF	salts	Fe staining, mottles
W '93	3.7-4.5	M	10YR5/2	N/O	-	N/O	N/O	-	VF VF	salts	mottles, till @ 410 cm
W '93	4.5-5.3	M	10YR5/2	N/O	-	N/O	N/O	-	-	salts	mottles
W '93	5.3-6.1	M	10YR5/2	N/O	-	N/O	N/O	-	-	salts	mottles, till sandier @ 540 cm
W '93	6.1-6.7	M/S	10YR5/3	N/O	-	N/O	N/O	-	-	salts	mottles, bedrock @ 650 cm

Test Hole	Depth (m)	Effervescence* (10% HCl test)	Moist Color	Mottles^	Slickensides (location, angle)	Texture	Structure^^	Roots***	Porosity^^^	Salts	Notes

N/O = NOT OBSERVED **- = ABSENT**

***Effervescence:**

V = very weak
W = weak
M = moderate
S = strong

^Mottles:

Abundance	Size	Contrast
F = few	F = fine	D = distinct
C = common	M = medium	P = prominent

****Texture**

Si = silt
C = clay
SiC = silty clay

^^Structure

Grade	Class	Kind
SL = structureless	FF = very fine to fine	MA = massive
VW = very weak	FM = fine to medium	SB = subangular blocky
W = weak	M = medium	
M = moderate	MC = medium to coarse	
	C = coarse	

*****Roots**

Number	Size	Distribution
VF = very few	VF = very fine	I = inped
F = few	F = fine	E = exped
P = plentiful	M = medium	B = both

^^^Porosity

Number	Size	Distribution
VF = very few	VF = very fine	I = inped
F = few	F = fine	
P = plentiful		hor = horizontal
A = abundant		vert = vertical
		ext = extensive

Refer to **<u>Manual for Describing Soils in the Field for Manitoba Soils</u>** by Canada-Manitoba Soil Survey.

Appendix B - Examination of 1.2 m long Cores from The Point

Core #	Plot #	Treatment #	Treatment Name	Texture**	Structure^	Carbonates*	Roots***	Porosity^^^	Slickensides	Salts
1	42	12	Alfalfa	SiC	massive	> 50 cm	P F E follow cracks found entire length	F F I infilled crack 0.5 cm wide to 50 cm depth P F I (>50 cm)	-	-
2	56	15	Alfalfa	C (0-50 cm) SiC (>50 cm)	MS F SB	V (localized)	P F I	P F I	-	-
3	57	12	Alfalfa	C (0-50 cm) SiC (>50 cm)	VW F SB	>80 cm	P F I	F F I (0-50 cm) infilled crack 0.5 cm wide to 20 cm depth P F I (>20 cm)	-	-
4	44	5	Fallow	SiC	SL - MA	V (<80 cm) S (>80 cm)	-	F VF I	-	-
5	53	5	Fallow	C (0-50 cm) SiC (> 50 cm)	SL - MA	>50 cm (localized)	F F I (old root channels)	F VF I	-	-
6	41	9	Alf.-Wheat	C(0-50 cm) SiC (>50 cm)	SL - MA hor. fractures	>60 cm	P F I to 90 cm	increased cracking below 50 cm	-	-
7	43	10	Alf.-Wheat	SiC	SL - MA	MS (>40 cm)	F F I to 40 cm	infilled crack 1 cm wide to 50 cm	-	-

Core #	Plot #	Treatment #	Treatment Name	Texture**	Structure^	Carbonates*	Roots***	Porosity^^^	Slickensides	Salts
8	50	10	Alf.-Wheat	C (0-50 cm) SiC (>50 cm)	SL - MA	MS (>50 cm)	P F I to 20 cm F F I to 55 cm infilled crack 2-3 mm wide at 60 cm	F F I to 20 cm F VF I to 60 cm F F I >60 cm	-	-
9	51	9	Alf.-Wheat	C (0-65 cm) SiC (>65 cm)	SL - MA	MS (> 65 cm)	P F I to 50 cm root ch's to 60 cm (2-5 mm wide)	F VF I to 50 cm F F I (>50 cm) increased cracking below 65 cm	-	-
10	38	1	Wheat	SiC	VW F SB	localized 50-65 cm MS (>65 cm)	P F I to 25 cm F F I to 50 cm	star-shaped infilled root ch. to 40 cm F F I to 50 cm P F I to 75cm increased cracking >75 cm	-	-
11	45	3	Wheat	C (0-40 cm) SiC (>40 cm)	SL - MA	MS (>45 cm)	P F I to 15 cm infilled crack 0.5 cm wide to 40 cm	F F I to 20 cm F VF I to 65 cm F F I, increased cracking >65 cm	-	-

Core #	Plot #	Treatment #	Treatment Name	Texture**	Structure^	Carbonates*	Roots***	Porosity^^^	Slickensides	Salts
12	47	1	Wheat	C (0-40 cm) SiC (>40 cm)	SL - MA	MS (>60 cm)	P F I to 40 cm	infilled crack 1 cm wide at 25 mm P F I at 10 cm (cracks) F F E at 25 cm P F I to 65 cm F F I, cracks >65 cm	-	-

N/O = NOT OBSERVED **- = ABSENT**

***Effervescence:**

V = very weak
W = weak
M = moderate
S = strong

^Mottles:

Abundance	Size	Contrast
F = few	F = fine	D = distinct
C = common	M = medium	P = prominent

****Texture**

Si = silt
C = clay
SiC = silty clay

^^Structure

Grade	Class	Kind
SL = structureless	FF = very fine to fine	MA = massive
VW = very weak	FM = fine to medium	SB = subangular blocky
W = weak	M = medium	
M = moderate	MC = medium to coarse	
	C = coarse	

*****Roots**

Number	Size	Distribution
VF = very few	VF = very fine	I = inped
F = few	F = fine	E = exped
P = plentiful	M = medium	B = both

^^^Porosity

Number	Size	Distribution
VF = very few	VF = very fine	I = inped
F = few	F = fine	
P = plentiful		hor = horizontal
A = abundant		vert = vertical
		ext = extensive

Refer to **Manual for Describing Soils in the Field for Manitoba Soils** by Canada-Manitoba Soil Survey.

Appendix C - Thin Section Analysis* With Light Microscope

C. A. Fox, R. K. Guertin, T. B. Goh and C. G. Cavers

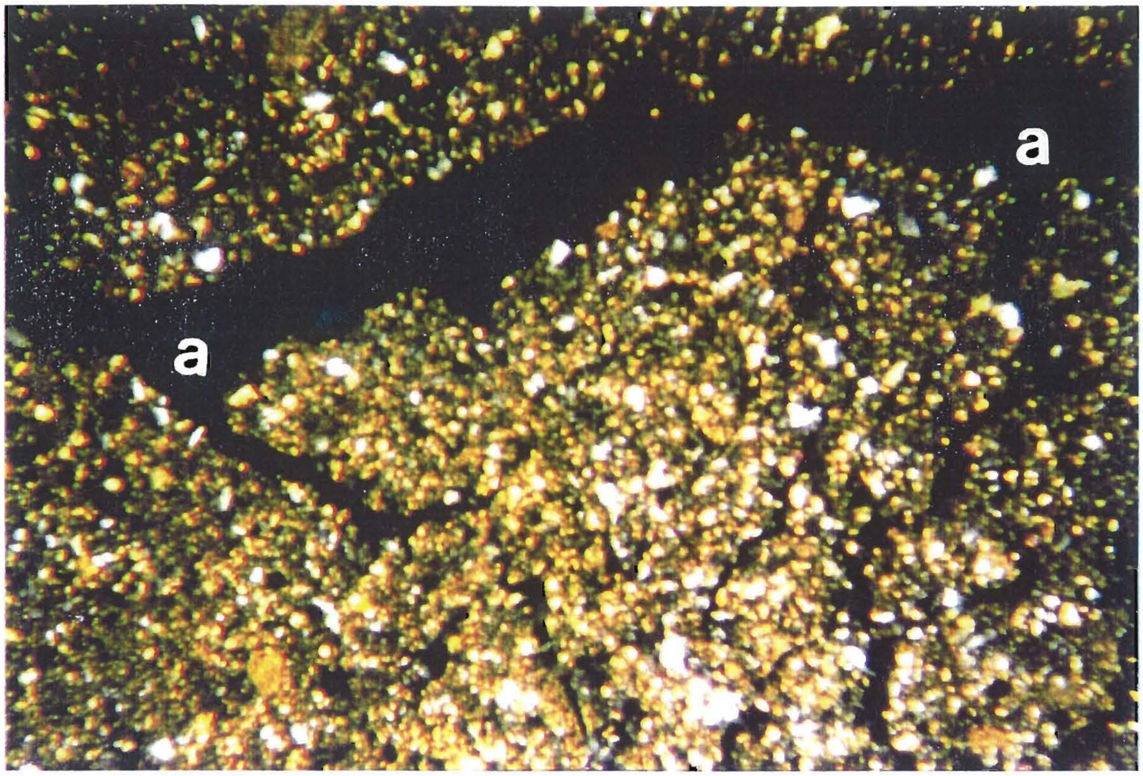

Scale: 5 cm = 0.1 mm

Sample 9350 @ 0.23 m depth under XPL.
Montcalm '93 - slickenside @ 0.23 m, 30°/

Vertical interconnected vughs and channels (may be some craze planes); irregular Fe nodules; irregular vughs connected by channels (**a**); extremely calcareous, moderately weathered, calcite < 60 μm; porphyroskelic fabric - compact silty clay, some sand grains (quartz), no evidence of clay skins; no evidence of slickenside features (too silty for clay re-orientation, also calcareous nature may be a factor).

*Thin sections were prepared from contiguous core samples by Mr. R. K. Guertin of Agriculture and Agri-Food Canada at the Central Experimental Farm in Ottawa, ON. Much of the interpretation of the micromorphology was performed by Dr. C. A. Fox of Agriculture and Agri-Food Canada, London, ON.

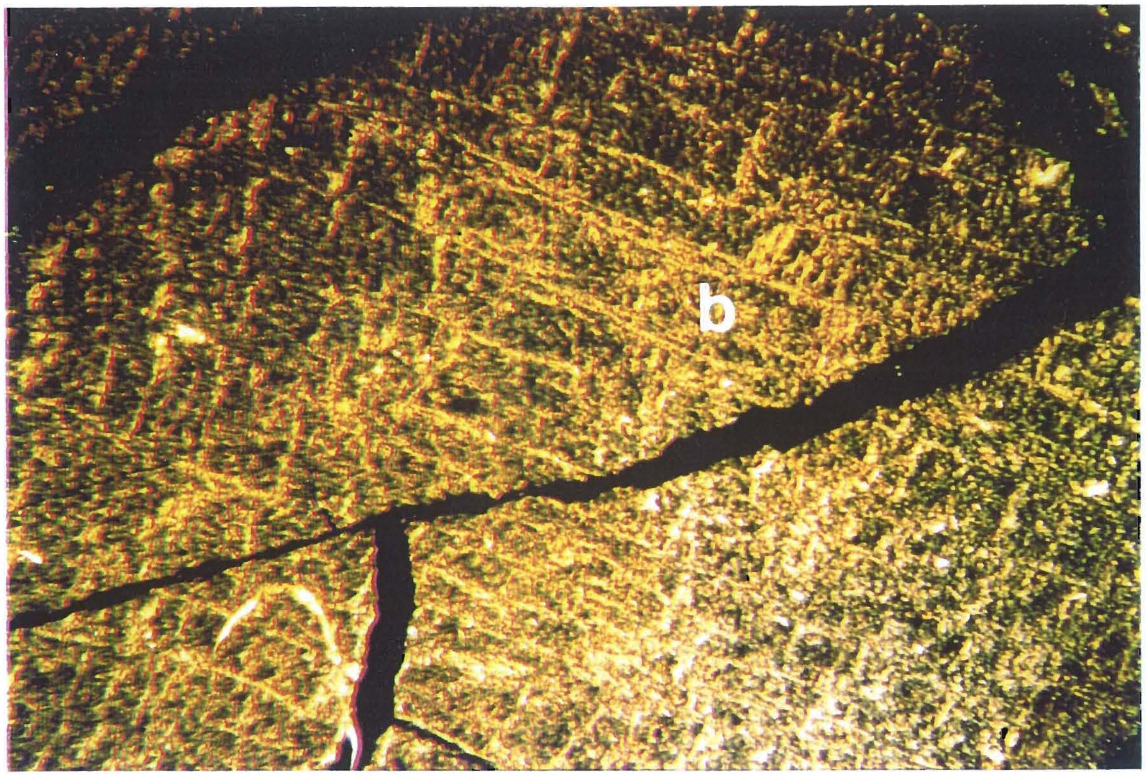

Scale: 5 cm = 0.1 mm

Sample 9352 @ 4.9 m depth under XPL.
Montcalm '91 - slickenside with 65°∠

Possible stress features due to swelling and shrinking, composed primarily of calcareous material; preferred orientation along planes; extremely fine clay dominates, highly calcareous, rare calcareous nodules - fill some pores; unique orientation of clays (**b**) may be related to original sediments, or structure formation of relic soil, ie. structural peds (portion of slide shows infilling with more silty material, also calcareous, in this area with possible stress features); highly weathered mica fragments, very rare; intersection of oriented plasma and clay band - stress cutan; fabric clino-bimasepic, strongly expressed.

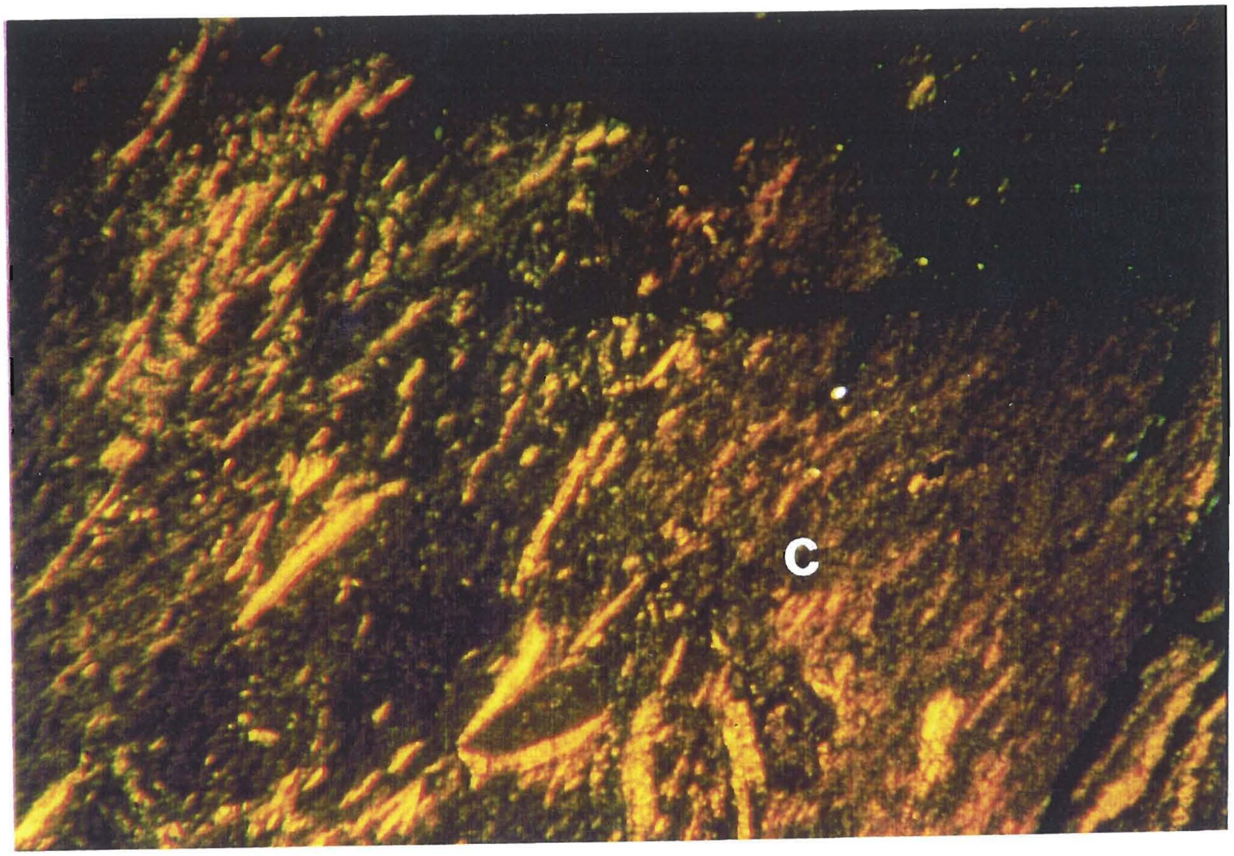

Scale: 6 cm = 0.1 mm

Sample 9354 @ 4.8 - 5.5 m depth under XPL.
Montcalm '93 - slickensides with 45°∠, 60°∠

Highly calcareous sediment, probably had particles of mica that are now weathered; micas weather to clay to produce speckling; distortion and appearance of movement may have been from pressures on the original sediments as in some areas these large pockets of micas are parallel to each other; direction of orientation approximately 65° from horizontal - therefore assuming sediments laid horizontally, pressures have oriented material at some time in past to approximately 65°; bands/flecks of clay (**c**); very straight birefringent band due to swelling; no slickensides - features derived from extreme weathering of mica flakes.

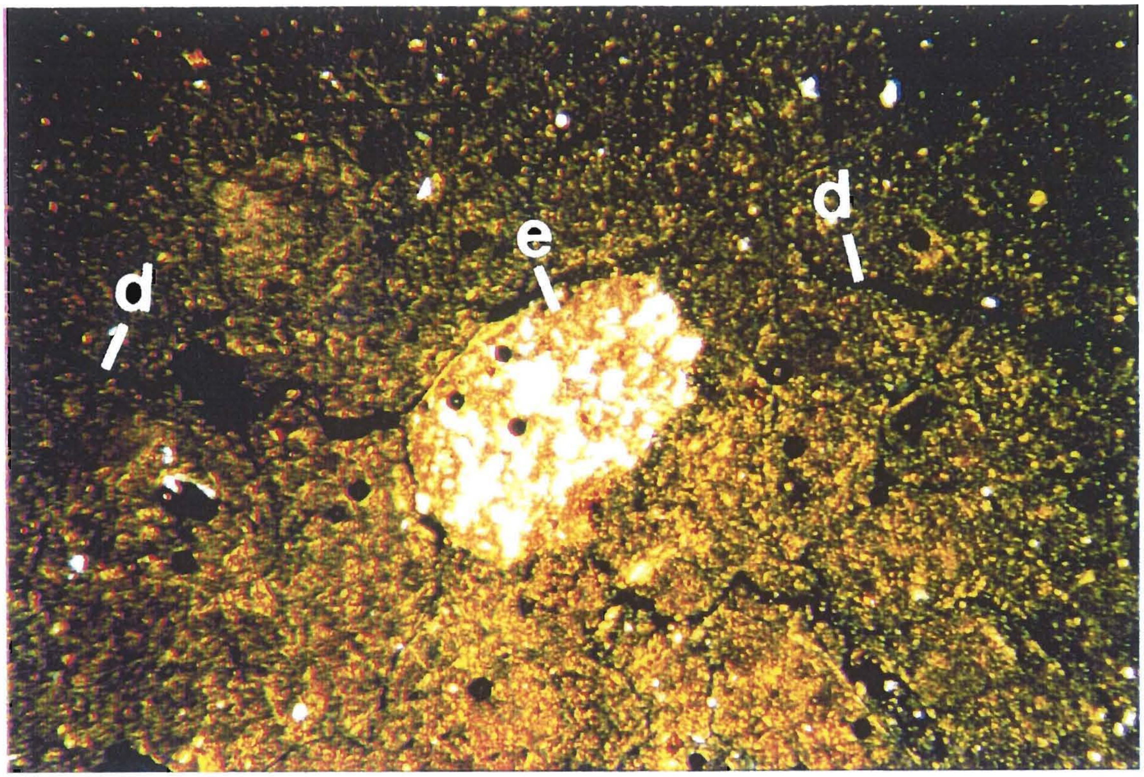

Scale: 5 cm = 0.1 mm

Sample 9357 @ 0.2 - 0.9 m depth under XPL.
Warren '93 - 2 slickensides, 40°$\angle$, 25°$\angle$

Horizontal channels (**d**); some voids the result of biologic - earthworm activity; no birefringence - higher silt content; for most part no orientation; remnants of orientation of clays in granular units, this orientation from original sediment material; lithorelic present (rare) (**e**); very weathered mica (rare); very few grains - diffuse Fe stains; rare nodules; highly calcareous; granular structure weak; granoidic-porphyroskelic voids around granular units due to shrinkage.

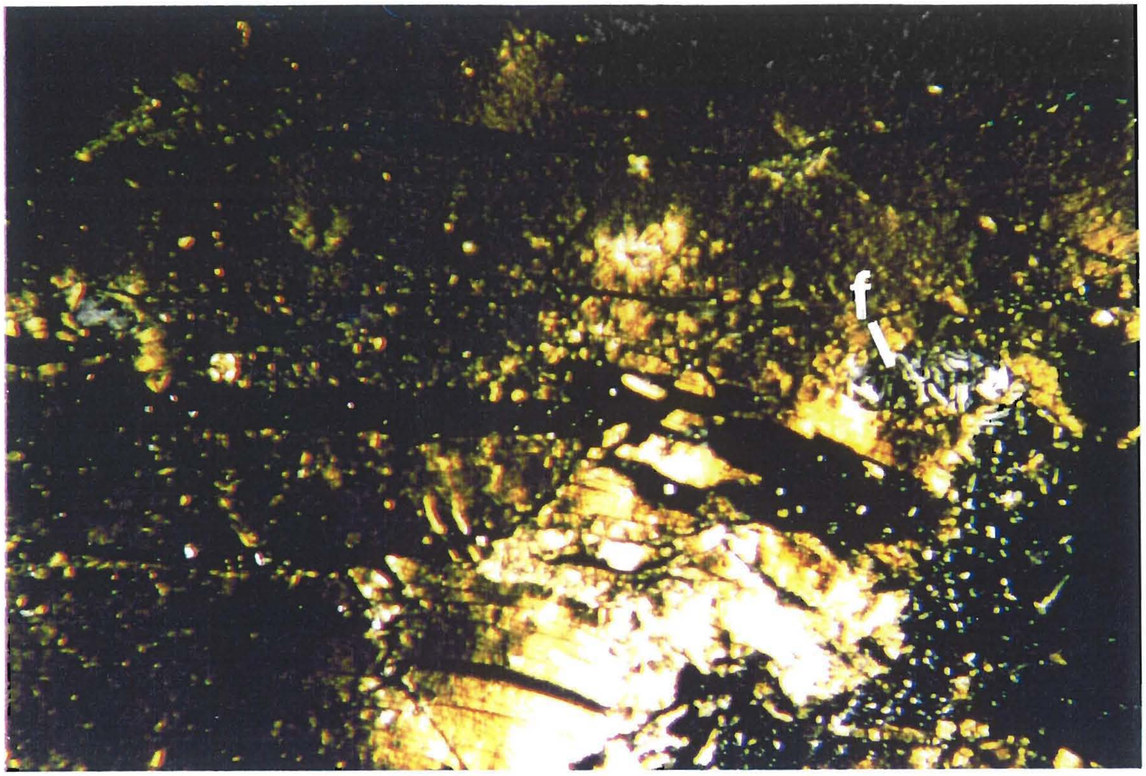

Scale: 5 cm = 0.1 mm

Sample 9358 @ 0.9 - 1.5 m depth under XPL.
Warren '93 - matrix, salts, carbonates

Very fine clays layered with fine calcareous silt - possible varved clay; high shrinkage - result of sample drying; rare occurrences of gypsum crystals in pores (f); calcareous nodules rare; shattering (may be related to sampling technique).

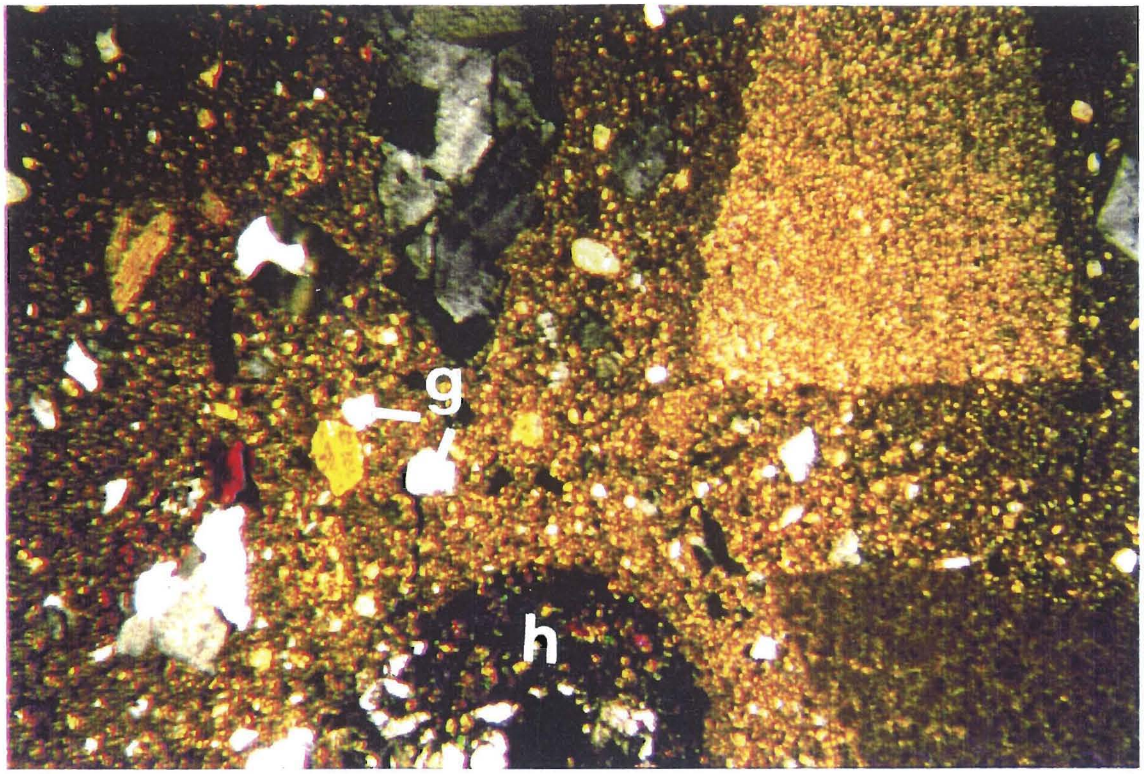

Scale: 5 cm = 0.1 mm

Sample 9360 @ 5.4 - 5.5 m depth under XPL.
Warren '93 - till/sandy till contact

Porphyric fabric; very rare feldspar, frequent quartz grains (**g**) common within fabric made up of calcareous clay and/or silt - very similar to sample 9359; lithorelic dominantly calcareous limestones, granitic (igneous) - similar to 9359; more clay than in 9359 because this region had more clay laid down in sediments; may have been washed in when sediments laid down (located at bottom of 9360 - layered suggests water laid, possibly varved); this region of clay associated with concretion, Mn deposit (**h**) - therefore it suggests a wet environment; some evidence for distortion - more likely from sediments pressures than vertisolic processes; material too coarse for vertisolic development.

Appendix D - Image Analysis of Thin Sections

Scale: 1 cm = 1.3 mm

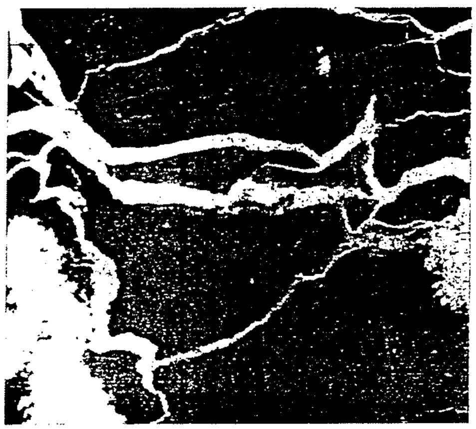

Sample 9351 @ 3.8 m depth
Montcalm site
23.7% void area

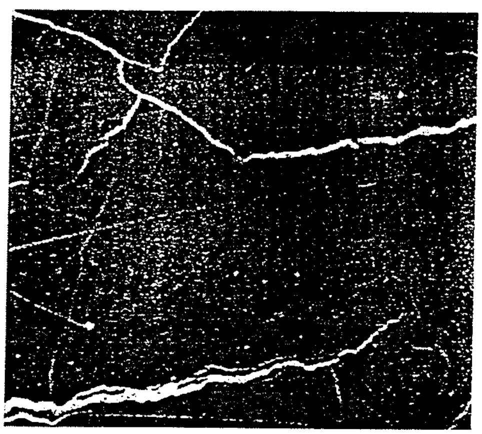

Sample 9352 @ 4.9 m depth
Montcalm site
3.3% void area

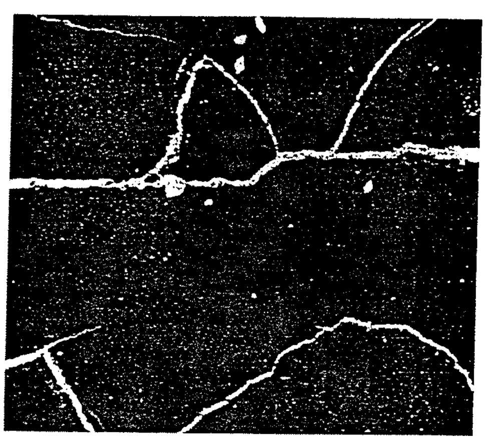

Sample 9353 @ 6.4 m depth
Montcalm site
4.5% void area

Sample 9354 @ 5.2 m depth
Montcalm site
18.1% void area

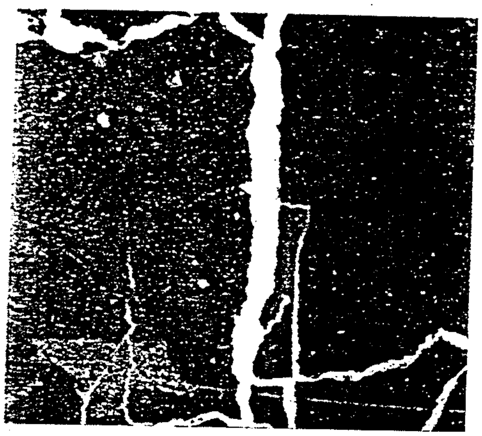

Sample 9355 @ 13.1 m depth
Montcalm site
10.8% void area

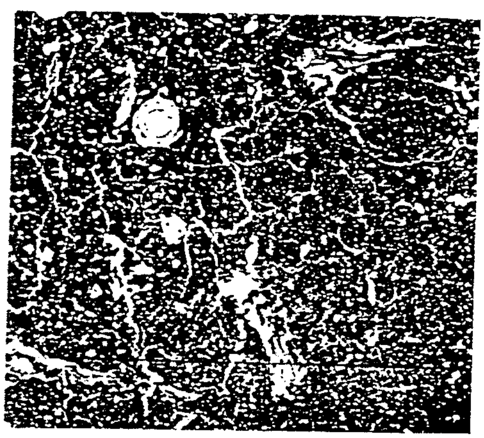

Sample 9356b @ 0.1 m depth
Warren site
15.9% void area

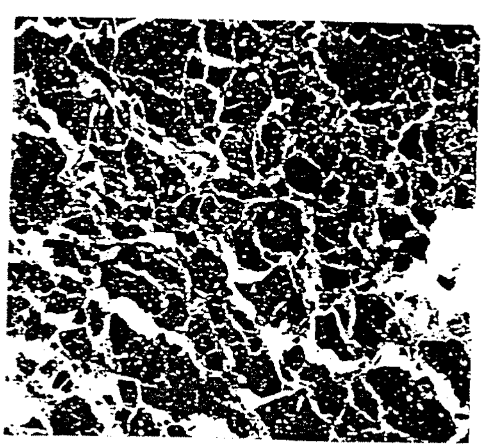

Sample 9357 @ 0.6 m depth
Warren site
16.4% void area

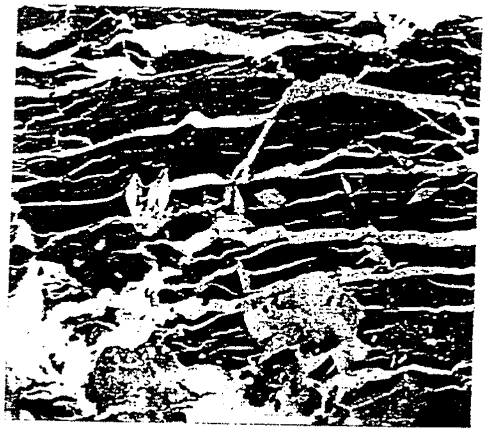

Sample 9358a @ 1.2 m depth
Warren site
22.3% void area

Sample 9358b @ 1.2 m depth
Warren site
11.1% void area

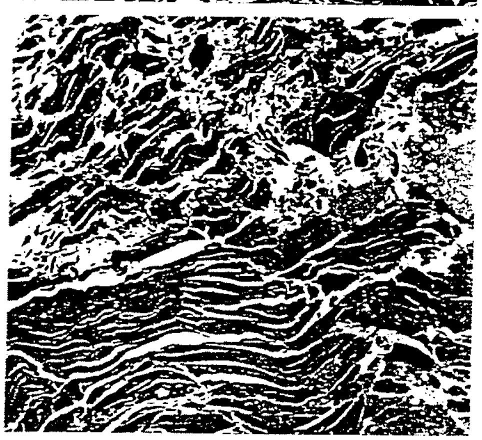

Sample 9358c @ 1.2 m depth
Warren site
13.0% void area

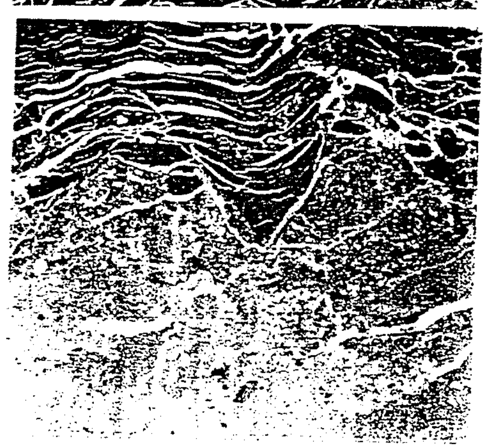

Sample 9358d @ 1.2 m depth
Warren site
8.7% void area

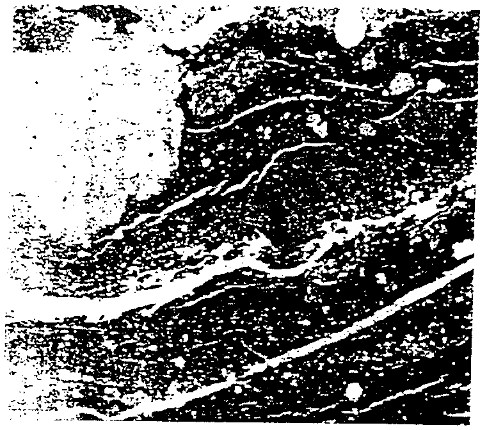

Sample 9359a @ 4.1 m depth
Warren site
11.2% void area

Sample 9359b @ 4.1 m depth
Warren site
13.8% void area

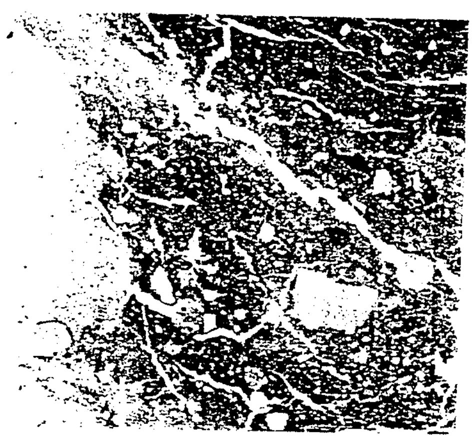

Sample 9359c @ 4.1 m depth
Warren site
10.2% void area

Sample 9359d @ 4.1 m depth
Warren site
27.9% void area

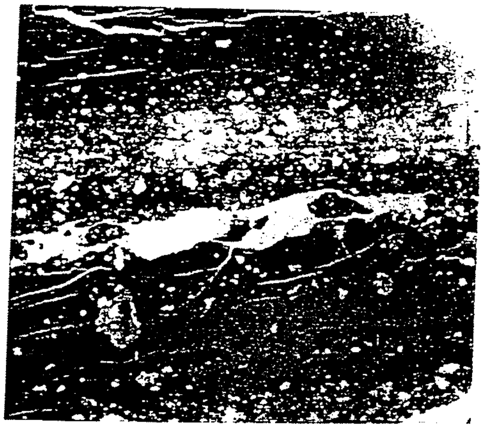

Sample 9360a @ 5.5 m depth
Warren site
9.3% void area

Sample 9360b @ 5.5 m depth
Warren site
13.8% void area

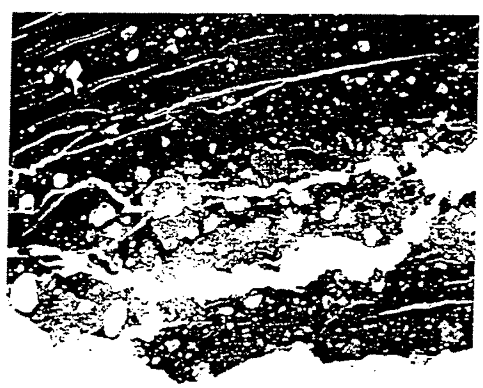

Sample 9360c @ 5.5 m depth
Warren site
28.4% void area

Sample 9360d @ 5.5 m depth
Warren site
0.6% void area

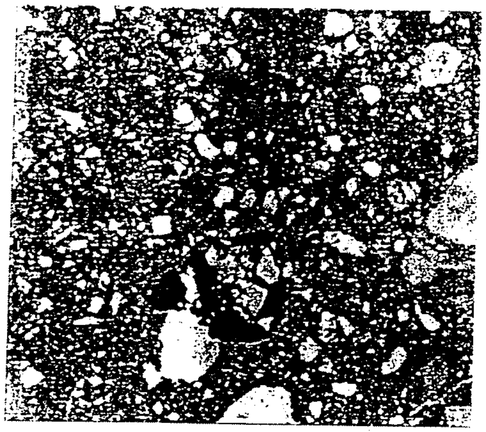

Sample 9360e @ 5.5 m depth
Warren site
8.8% void area

Appendix E - Field Measurements of Saturated Hydraulic Conductivity

Date	Plot #	Treatment #	Treatment	Depth (cm)	Reservoir Factor	Rate (cm/h)	K (cm/h)	K (m/s)	Avg. K (m/s)
6/2/93	43	10	Alfalfa	25	2.501	0.06	0.1501	4.2E-07	
8/30/94	56	15	Alfalfa	25	2.501	0.12	0.3001	8.3E-07	
6/1/93	50	10	Alfalfa	25	2.501	0.20	0.5002	1.4E-06	
6/1/93	43	10	Alfalfa	25	2.501	0.52	1.3005	3.6E-06	
7/14/93	50	10	Alfalfa	25	2.501	0.76	1.9008	5.3E-06	
7/14/93	50	10	Alfalfa	25	2.501	1.04	2.6010	7.2E-06	3.1E-06
7/14/93	50	10	Alfalfa	50	0.1536	1.32	0.2028	5.6E-07	
7/14/93	50	10	Alfalfa	50	2.501	0.05	0.1251	3.5E-07	
8/4/94	42	12	Alfalfa	50	2.501	0.12	0.3001	8.3E-07	
8/4/94	57	12	Alfalfa	50	2.501	0.19	0.4752	1.3E-06	
7/14/93	50	10	Alfalfa	50	2.501	0.24	0.6002	1.7E-06	9.5E-07
8/30/94	56	15	Alfalfa	75	2.501	0.08	0.2001	5.6E-07	
8/31/94	42	12	Alfalfa	75	2.501	0.08	0.2001	5.6E-07	
8/26/94	56	15	Alfalfa	75	2.501	0.10	0.2501	6.9E-07	
8/30/94	56	15	Alfalfa	75	2.501	0.12	0.3001	8.3E-07	
8/31/94	42	12	Alfalfa	75	2.501	0.22	0.5502	1.5E-06	8.3E-07
6/2/93	44	5	Summerfallow	25	0.1536	0.05	0.0077	2.1E-08	
6/2/93	44	5	Summerfallow	25	0.1536	0.05	0.0077	2.1E-08	
6/10/93	53	5	Summerfallow	25	0.1536	0.06	0.0092	2.6E-08	
6/2/93	44	5	Summerfallow	25	0.1536	0.06	0.0092	2.6E-08	
6/10/93	53	5	Summerfallow	25	0.1536	0.07	0.0108	3.0E-08	
6/1/93	53	5	Summerfallow	25	0.1536	0.16	0.0246	6.8E-08	3.2E-08
6/10/93	53	5	Summerfallow	50	0.1536	0.08	0.0123	3.4E-08	
8/4/94	44	5	Summerfallow	50	2.501	0.04	0.1000	2.8E-07	
8/4/94	53	5	Summerfallow	50	2.501	0.04	0.1000	2.8E-07	
8/4/94	53	5	Summerfallow	50	2.501	0.05	0.1251	3.5E-07	
8/4/94	44	5	Summerfallow	50	2.501	0.06	0.1501	4.2E-07	2.7E-07
9/8/94	44	5	Summerfallow	75	0.1536	0.04	0.0061	1.7E-08	
9/8/94	44	5	Summerfallow	75	0.1536	0.06	0.0092	2.6E-08	
8/26/94	53	5	Summerfallow	75	0.1536	0.08	0.0123	3.4E-08	
8/26/94	53	5	Summerfallow	75	0.1536	0.13	0.0200	5.5E-08	

Date	Plot #	Treatment #	Treatment	Depth (cm)	Reservoir Factor	Rate (cm/h)	K (cm/h)	K (m/s)	Avg. K (m/s)
8/26/94	53	5	Summerfallow	75	0.1536	0.19	0.0292	8.1E-08	4.3E-08
8/5/94	38	1	Wheat	25	0.1536	0.02	0.0031	8.5E-09	
9/9/94	45	3	Wheat	25	0.1536	0.05	0.0077	2.1E-08	
8/23/94	49	3	Wheat	25	0.1536	0.09	0.0138	3.8E-08	
6/2/93	38	1	Wheat	25	0.1536	0.16	0.0246	6.8E-08	
6/1/93	38	1	Wheat	25	0.1536	0.20	0.0307	8.5E-08	
6/1/93	47	1	Wheat	25	0.1536	0.21	0.0323	9.0E-08	5.2E-08
9/9/94	45	3	Wheat	50	0.1536	0.05	0.0077	2.1E-08	
6/10/93	38	1	Wheat	50	0.1536	0.05	0.0077	2.1E-08	
8/5/94	38	1	Wheat	50	0.1536	0.05	0.0077	2.1E-08	
9/9/94	45	3	Wheat	50	0.1536	0.07	0.0108	3.0E-08	
8/23/94	49	3	Wheat	50	0.1536	0.29	0.0445	1.2E-07	4.4E-08
9/8/94	45	3	Wheat	75	0.1536	0.04	0.0061	1.7E-08	
9/9/94	45	3	Wheat	75	0.1536	0.12	0.0184	5.1E-08	
9/9/94	38	1	Wheat	75	0.1536	0.14	0.0215	6.0E-08	
8/5/94	38	1	Wheat	75	0.1536	0.31	0.0476	1.3E-07	
8/23/94	49	3	Wheat	75	0.1536	0.83	0.1275	3.5E-07	1.2E-07
8/23/94	51	9	Wheat on Alfalfa	25	0.1536	0.01	0.0015	4.3E-09	
9/27/94	43	10	Wheat on Alfalfa	25	0.1536	0.09	0.0138	3.8E-08	
9/27/94	51	9	Wheat on Alfalfa	25	0.1536	0.12	0.0184	5.1E-08	
8/31/94	41	9	Wheat on Alfalfa	25	0.1536	0.14	0.0215	6.0E-08	
9/28/94	43	10	Wheat on Alfalfa	25	0.1536	0.23	0.0353	9.8E-08	
8/5/94	41	9	Wheat on Alfalfa	25	0.1536	0.26	0.0399	1.1E-07	6.0E-08
9/27/94	43	10	Wheat on Alfalfa	50	0.1536	0.11	0.0169	4.7E-08	
9/27/94	51	9	Wheat on Alfalfa	50	0.1536	0.13	0.0200	5.5E-08	
8/31/94	41	9	Wheat on Alfalfa	50	0.1536	0.16	0.0246	6.8E-08	
8/5/94	41	9	Wheat on Alfalfa	50	2.501	0.15	0.3752	1.0E-06	
8/23/94	51	9	Wheat on Alfalfa	50	2.501	0.57	1.4256	4.0E-06	1.0E-06
9/8/94	43	10	Wheat on Alfalfa	75	0.1536	0.04	0.0061	1.7E-08	
9/8/94	43	10	Wheat on Alfalfa	75	0.1536	0.06	0.0092	2.6E-08	
8/23/94	51	9	Wheat on Alfalfa	75	0.1536	1.18	0.1812	5.0E-07	
8/31/94	41	9	Wheat on Alfalfa	75	0.1536	1.24	0.1905	5.3E-07	
8/5/94	41	9	Wheat on Alfalfa	75	2.501	0.14	0.3501	9.7E-07	4.1E-07

Appendix F - Laboratory Measurements of Saturated Hydraulic Flux

Average Saturated Hydraulic Flux (m/s)

Sample:	1 Montcalm 13.1 m			2 Montcalm 1.7 m			3 Warren 0.6 m			4 Warren 3.9 m		
Hydraulic Gradient	# samples	mean	standard deviation	# samples	mean	standard deviation	# samples	mean	standard deviation	# samples	mean	standard deviation
0.2	-	-	-	-	-	-	6	3.6E-08	1.8E-08	12	3.5E-11	4.3E-11
0.3	-	-	-	-	-	-	6	6.7E-08	3.6E-09	12	8.4E-11	6.3E-11
0.4	-	-	-	6	1.5E-11	1.2E-11	6	1.3E-07	1.8E-08	12	1.1E-10	8.3E-11
0.6	11	2.4E-11	1.9E-11	12	5.0E-11	4.2E-11	6	2.2E-07	3.0E-08	12	1.3E-10	3.9E-11
0.8	11	1.4E-11	9.0E-12	12	1.4E-10	8.9E-11	6	3.0E-07	4.7E-08	12	1.3E-10	7.4E-11
1.0	12	3.1E-11	2.7E-11	18	2.6E-10	1.5E-10	6	4.1E-07	3.9E-08	12	1.8E-10	6.9E-11
1.2	12	3.9E-11	2.1E-11	18	4.2E-10	1.4E-10	6	5.8E-07	5.7E-08	12	2.6E-10	7.0E-11
1.5	12	5.3E-11	3.0E-11	18	5.7E-10	1.5E-10	6	6.9E-07	2.5E-08	6	3.7E-10	8.6E-11
2.0	12	7.8E-11	4.2E-11	18	8.5E-10	2.5E-10	6	1.0E-06	4.0E-16	12	3.9E-10	7.8E-11
3.0	-	-	-	6	1.2E-09	1.4E-10	6	1.6E-06	0	24	5.8E-10	1.6E-10
5.0	-	-	-	12	2.9E-09	7.3E-11	6	2.8E-06	7.9E-16	12	1.2E-09	3.0E-10
5.5	12	3.3E-10	9.0E-11	-	-	-	-	-	-	-	-	-
8.0	12	5.6E-10	3.8E-11	12	5.2E-09	3.0E-10	-	-	-	12	1.9E-09	1.3E-10
12.0	12	8.6E-10	1.4E-10	12	8.3E-09	6.0E-10	-	-	-	12	3.1E-09	8.8E-10
16.0	6	1.2E-09	1.2E-10	12	1.2E-08	4.8E-10	-	-	-	12	4.1E-09	8.1E-10
20.0	-	-	-	6	1.5E-08	7.7E-10	-	-	-	6	5.1E-09	1.0E-09

Raw data follows summary table.

Montcalm '91
TH 1
13.1 m

Continuous core sample from below the water table (Montcalm)
Feb 2 - Mar 2, 1994

Sample length =	44	mm	4.4
Sample diameter =	56.96	mm	5.696
Sample CSA =	25.4818	cm^2	
Capillary tube diameter =	0.8	mm	0.08
Capillary CSA =	0.00503	cm^2	
Area Ratio =	5069.44		

	In				Out				
Head (cm)	Gradient	l (mm)	time(s)	Flux(m/s)	l (mm)	time(s)	Flux(m/s)	In+out/2	avg-out
	0.6	6.98	14611	9.4E-11	2.58	14608	3.5E-11	6.45E-11	
	0.6	15.62	10069	3.1E-10	0.74	10071	1.4E-11	1.6E-10	
	0.6	6.83	6045	2.2E-10	0.92	6030	3.0E-11	1.26E-10	
	0.6	55.24	35558	3.1E-10	5.14	35569	2.9E-11	1.67E-10	
	0.6	19.51	17251	2.2E-10	1.09	17256	1.2E-11	1.18E-10	
	0.6	17.19	15416	2.2E-10	0.96	15432	1.2E-11	1.16E-10	2.2111E-11
	0.8	18.24	14403	2.5E-10	0.67	14415	9.2E-12	1.29E-10	
	0.8	23.91	16086	2.9E-10	2.00	16064	2.5E-11	1.59E-10	
	0.8	46.89	29065	3.2E-10	2.23	29047	1.5E-11	1.67E-10	
	0.8	14.22	12639	2.2E-10	1.46	12609	2.3E-11	1.22E-10	
	0.8	124.89	77080	3.2E-10	0.31	76969	7.9E-13	1.6E-10	1.4501E-11
	1.0	6.94	7893	1.7E-10	1.82	7877	4.6E-11	1.1E-10	
	1.0	6.11	8992	1.3E-10	1.31	9014	2.9E-11	8.14E-11	
	1.0	22.68	11530	3.9E-10	0.74	11515	1.3E-11	2E-10	
	1.0	18.35	10576	3.4E-10	0.36	10584	6.7E-12	1.74E-10	
	1.0	48.60	31103	3.1E-10	1.07	31107	6.8E-12	1.58E-10	
	1.0	15.63	9887	3.1E-10	0.16	9870	3.2E-12	1.58E-10	1.7269E-11
	1.2	6.49	6723	1.9E-10	1.29	6722	3.8E-11	1.14E-10	
	1.2	24.86	15148	3.2E-10	1.91	15155	2.5E-11	1.74E-10	
	1.2	14.80	9610	3.0E-10	1.55	9612	3.2E-11	1.68E-10	
	1.2	20.56	14969	2.7E-10	1.45	14944	1.9E-11	1.45E-10	
	1.2	48.15	32201	2.9E-10	1.84	32207	1.1E-11	1.53E-10	
	1.2	9.92	9312	2.1E-10	1.08	9299	2.3E-11	1.17E-10	2.4641E-11

1.5	11.12	9944	2.2E-10	3.92	9951	7.8E-11	1.49E-10	
1.5	12.63	7284	3.4E-10	1.59	7266	4.3E-11	1.93E-10	
1.5	18.46	9954	3.7E-10	0.34	9957	6.7E-12	1.86E-10	
1.5	18.17	11818	3.0E-10	4.57	11784	7.7E-11	1.9E-10	
1.5	61.94	36846	3.3E-10	3.14	36045	1.7E-11	1.74E-10	
1.5	17.35	10665	3.2E-10	4.46	10665	8.2E-11	2.02E-10	5.0631E-11
2.0	15.35	7264	4.2E-10	3.11	7236	8.5E-11	2.51E-10	
2.0	14.15	9094	3.1E-10	5.74	9071	1.2E-10	2.16E-10	
2.0	16.97	9040	3.7E-10	2.06	9034	4.5E-11	2.08E-10	
2.0	24.70	15246	3.2E-10	7.37	15214	9.6E-11	2.08E-10	
2.0	13.16	5749	4.5E-10	0.29	5770	9.9E-12	2.31E-10	
2.0	63.18	31475	4.0E-10	9.05	31415	5.7E-11	2.26E-10	6.9481E-11
5.5	59.74	10152	1.2E-09	18.33	10161	3.6E-10	7.58E-10	
5.5	34.23	5657	1.2E-09	10.00	5654	3.5E-10	7.71E-10	
5.5	92.63	15668	1.2E-09	28.69	15679	3.6E-10	7.64E-10	
5.5	44.65	7879	1.1E-09	13.89	7879	3.5E-10	7.33E-10	
5.5	143.65	29143	9.7E-10	50.41	29135	3.4E-10	6.57E-10	
5.5	45.02	10532	8.4E-10	17.82	10547	3.3E-10	5.88E-10	3.4801E-10
8.0	21.96	2762	1.6E-09	9.00	2762	6.4E-10	1.11E-09	
8.0	15.86	2309	1.4E-09	6.56	2309	5.6E-10	9.58E-10	
8.0	12.11	1975	1.2E-09	6.16	1956	6.2E-10	9.15E-10	
8.0	8.09	1371	1.2E-09	3.74	1357	5.4E-10	8.54E-10	
8.0	4.37	1323	6.5E-10	3.61	1300	5.5E-10	6E-10	
8.0	17.33	2405	1.4E-09	6.59	2402	5.4E-10	9.81E-10	5.7618E-10
12.0	13.28	1164	2.3E-09	5.41	1158	9.2E-10	1.59E-09	
12.0	3.35	364	1.8E-09	1.77	364	9.6E-10	1.39E-09	
12.0	3.53	395	1.8E-09	2.05	401	1.0E-09	1.39E-09	
12.0	3.26	328	2.0E-09	1.51	335	8.9E-10	1.42E-09	
12.0	3.65	370	1.9E-09	1.53	373	8.1E-10	1.38E-09	
12.0	7.48	776	1.9E-09	3.50	800	8.6E-10	1.38E-09	9.0842E-10
16.0	22.36	1540	2.9E-09	9.57	1540	1.2E-09	2.04E-09	
16.0	4.20	331	2.5E-09	1.72	302	1.1E-09	1.81E-09	
16.0	5.71	419	2.7E-09	2.85	419	1.3E-09	2.01E-09	
16.0	6.92	521	2.6E-09	3.18	519	1.2E-09	1.91E-09	
16.0	7.46	560	2.6E-09	3.02	573	1.0E-09	1.83E-09	
16.0	6.08	468	2.6E-09	2.46	465	1.0E-09	1.8E-09	1.1638E-09
12.0	90.10	8560	2.1E-09	34.92	8577	8.0E-10	1.44E-09	
12.0	5.41	458	2.3E-09	2.65	463	1.1E-09	1.73E-09	

12.0	3.78	319	2.3E-09	1.15	318	7.1E-10	1.53E-09	
12.0	9.89	464	4.2E-09	1.71	479	7.0E-10	2.45E-09	
12.0	9.35	620	3.0E-09	2.08	625	6.6E-10	1.82E-09	
12.0	9.20	784	2.3E-09	3.43	804	8.4E-10	1.58E-09	8.0796E-10
8.0	252.20	39517	1.3E-09	103.00	39532	5.1E-10	8.86E-10	
8.0	62.10	9947	1.2E-09	27.99	9961	5.5E-10	8.93E-10	
8.0	20.76	3642	1.1E-09	10.77	3622	5.9E-10	8.55E-10	
8.0	57.71	9048	1.3E-09	24.19	9051	5.3E-10	8.93E-10	
8.0	46.29	6803	1.3E-09	18.50	6818	5.4E-10	9.39E-10	
8.0	47.24	7067	1.3E-09	19.43	7088	5.4E-10	9.3E-10	5.43E-10
5.5	37.32	6529	1.1E-09	10.81	6512	3.3E-10	7.28E-10	
5.5	57.24	10224	1.1E-09	19.14	10223	3.7E-10	7.37E-10	
5.5	29.28	7310	7.9E-10	7.99	7321	2.2E-10	5.03E-10	
5.5	85.20	23976	7.0E-10	21.98	23974	1.8E-10	4.41E-10	
5.5	34.62	10767	6.3E-10	11.71	10772	2.1E-10	4.24E-10	
5.5	55.60	13930	7.9E-10	36.88	13947	5.2E-10	6.54E-10	3.0483E-10
2.0	71.17	21321	6.6E-10	7.25	21328	6.7E-11	3.63E-10	
2.0	159.91	37980	8.3E-10	15.14	37990	7.9E-11	4.55E-10	
2.0	45.82	10589	8.5E-10	5.38	10591	1.0E-10	4.77E-10	
2.0	18.23	3447	1.0E-09	0.28	3421	1.6E-11	5.3E-10	
2.0	32.43	7522	8.5E-10	4.21	7528	1.1E-10	4.8E-10	
2.0	42.14	15236	5.5E-10	11.69	15237	1.5E-10	3.48E-10	8.7279E-11
1.5	112.33	44728	5.0E-10	16.99	44729	7.5E-11	2.85E-10	
1.5	20.58	7144	5.7E-10	0.63	7147	1.7E-11	2.93E-10	
1.5	13.09	4208	6.1E-10	0.60	4210	2.8E-11	3.21E-10	
1.5	20.22	6804	5.9E-10	1.87	6803	5.4E-11	3.2E-10	
1.5	5.88	2654	4.4E-10	1.31	2651	9.7E-11	2.67E-10	
1.5	8.13	3882	4.1E-10	1.12	3880	5.7E-11	2.35E-10	5.4845E-11
1.2	139.62	55146	5.0E-10	3.93	55188	1.4E-11	2.57E-10	
1.2	11.97	4020	5.9E-10	1.11	4037	5.4E-11	3.21E-10	
1.2	10.09	5316	3.7E-10	1.44	5323	5.3E-11	2.14E-10	
1.2	8.73	5405	3.2E-10	1.96	5409	7.1E-11	1.95E-10	
1.2	13.38	7765	3.4E-10	2.71	7768	6.9E-11	2.04E-10	
1.2	30.80	19766	3.1E-10	5.25	19767	5.2E-11	1.8E-10	5.2389E-11
1.0	87.56	37212	4.6E-10	1.55	37236	8.2E-12	2.36E-10	
1.0	5.81	5629	2.0E-10	1.22	5625	4.3E-11	1.23E-10	
1.0	5.89	6056	1.9E-10	2.70	6070	8.8E-11	1.4E-10	
1.0	25.32	12888	3.9E-10	3.31	12897	5.1E-11	2.19E-10	

1.0	15.47	9368	3.3E-10	2.94	9364	6.2E-11	1.94E-10	
1.0	8.93	5333	3.3E-10	0.43	5337	1.6E-11	1.73E-10	4.4532E-11
0.8	92.82	36644	5.0E-10	0.71	36647	3.8E-12	2.52E-10	
0.8	22.34	8345	5.3E-10	0.43	8361	1.0E-11	2.69E-10	
0.8	11.87	5175	4.5E-10	0.45	5174	1.7E-11	2.35E-10	
0.8	18.06	7873	4.5E-10	0.31	7875	7.8E-12	2.3E-10	
0.8	18.42	9030	4.0E-10	0.26	9035	5.7E-12	2.04E-10	
0.8	6.69	2945	4.5E-10	0.41	2927	2.8E-11	2.38E-10	1.2033E-11
0.6	16.02	6294	5.0E-10	0.40	6269	1.3E-11	2.57E-10	
0.6	205.28	31961	1.3E-09	2.34	31697	1.5E-11	6.41E-10	
0.6	8.02	3685	4.3E-10	1.36	3684	7.3E-11	2.51E-10	
0.6	10.28	3846	5.3E-10	0.06	3848	3.1E-12	2.65E-10	
0.6	28.38	23455	2.4E-10	3.22	23426	2.7E-11	1.33E-10	2.6032E-11

Montcalm '91 | Continuous core sample from above the water table (Montcalm)

TH 8 | Apr 25 - Oct 25, 1994

1.5 - 2.3 m

Sample length =	42	mm	4.2	cm
Sample diameter =	56.96	mm	5.696	cm
Sample CSA =	25.4818	cm^2		
Capillary tube diameter =	0.8	mm	0.08	cm
Capillary CSA =	0.00503	cm^2		
Area Ratio =	5069.44			

	In				Out				
Head (cm)	Gradient	l (mm)	time(s)	Flux(m/s)	l (mm)	time(s)	Flux(m/s)	In+out/2	avg-out
	0.6	225.52	45198	9.8E-10	2.61	45113	1.1E-11	4.98E-10	
	0.6	19.10	13004	2.9E-10	1.39	12938	2.1E-11	1.55E-10	
	0.6	41.53	33595	2.4E-10	0.21	33582	1.2E-12	1.23E-10	
	0.6	7.33	16094	9.0E-11	4.91	16090	6.0E-11	7.5E-11	
	0.6	179.50	40085	8.8E-10	0.20	40004	9.9E-13	4.42E-10	
	0.6	8.92	4155	4.2E-10	0.09	4133	4.3E-12	2.14E-10	1.6553E-11
	0.8	16.53	13087	2.5E-10	4.79	13086	7.2E-11	1.61E-10	
	0.8	200.24	56932	6.9E-10	9.23	56924	3.2E-11	3.63E-10	
	0.8	159.22	73246	4.3E-10	8.99	73246	2.4E-11	2.27E-10	
	0.8	10.98	10573	2.0E-10	2.94	10570	5.5E-11	1.3E-10	
	0.8	6.56	4582	2.8E-10	3.42	4584	1.5E-10	2.15E-10	
	0.8	5.83	5701	2.0E-10	3.91	5706	1.4E-10	1.68E-10	7.7602E-11
	1.0	191.81	63752	5.9E-10	29.53	63760	9.1E-11	3.42E-10	
	1.0	51.31	12164	8.3E-10	14.62	12172	2.4E-10	5.35E-10	
	1.0	32.12	12191	5.2E-10	9.45	12200	1.5E-10	3.36E-10	
	1.0	243.54	60683	7.9E-10	24.74	60701	8.0E-11	4.36E-10	
	1.0	7.19	2531	5.6E-10	3.27	2498	2.6E-10	4.09E-10	
	1.0	37.03	16139	4.5E-10	21.62	16157	2.6E-10	3.58E-10	1.8061E-10
	1.2	59.56	4204	2.8E-09	10.56	4201	5.0E-10	1.65E-09	
	1.2	36.56	4447	1.6E-09	8.52	4449	3.8E-10	1E-09	
	1.2	37.14	6856	1.1E-09	15.28	6855	4.4E-10	7.54E-10	
	1.2	46.93	3759	2.5E-09	8.87	3753	4.7E-10	1.46E-09	
	1.2	98.79	13650	1.4E-09	22.86	13670	3.3E-10	8.79E-10	
	1.2	39.00	7055	1.1E-09	14.03	7067	3.9E-10	7.41E-10	4.1684E-10

1.5	12.19	909	2.6E-09	2.41	913	5.2E-10	1.58E-09	
1.5	58.89	3825	3.0E-09	9.07	3838	4.7E-10	1.75E-09	
1.5	131.58	11065	2.3E-09	29.98	11080	5.3E-10	1.44E-09	
1.5	7.99	983	1.6E-09	4.00	983	8.0E-10	1.2E-09	
1.5	90.70	9223	1.9E-09	26.75	9225	5.7E-10	1.26E-09	
1.5	108.10	13233	1.6E-09	39.90	13239	5.9E-10	1.1E-09	5.8163E-10
2.0	172.75	11245	3.0E-09	55.58	11250	9.7E-10	2E-09	
2.0	97.79	9357	2.1E-09	49.48	9355	1.0E-09	1.55E-09	
2.0	42.86	5133	1.6E-09	25.54	5136	9.8E-10	1.31E-09	
2.0	84.58	5011	3.3E-09	28.59	5025	1.1E-09	2.23E-09	
2.0	74.59	4973	3.0E-09	23.93	4975	9.5E-10	1.95E-09	
2.0	53.00	5269	2.0E-09	29.53	5284	1.1E-09	1.54E-09	1.0287E-09
5.0	120.11	3793	6.2E-09	54.30	3810	2.8E-09	4.53E-09	
5.0	94.39	1891	9.8E-09	27.15	1892	2.8E-09	6.34E-09	
5.0	121.47	3425	7.0E-09	49.08	3432	2.8E-09	4.91E-09	
5.0	51.87	1835	5.6E-09	27.17	1839	2.9E-09	4.25E-09	
5.0	119.11	4835	4.9E-09	68.96	4837	2.8E-09	3.84E-09	
5.0	57.52	2700	4.2E-09	39.83	2705	2.9E-09	3.55E-09	2.849E-09
8.0	27.52	662	8.2E-09	19.36	662	5.8E-09	6.98E-09	
8.0	100.79	2507	7.9E-09	65.99	2515	5.2E-09	6.55E-09	
8.0	134.37	3868	6.9E-09	102.87	3898	5.2E-09	6.03E-09	
8.0	197.45	2132	1.8E-08	58.66	2144	5.4E-09	1.18E-08	
8.0	125.88	2391	1.0E-08	67.62	2391	5.6E-09	7.98E-09	
8.0	13.55	380	7.0E-09	10.84	385	5.6E-09	6.29E-09	5.4467E-09
12.0	15.69	307	1.0E-08	13.63	312	8.6E-09	9.35E-09	
12.0	15.16	317	9.4E-09	14.60	320	9.0E-09	9.22E-09	
12.0	13.41	281	9.4E-09	12.95	287	8.9E-09	9.16E-09	
12.0	15.76	329	9.4E-09	14.94	338	8.7E-09	9.08E-09	
12.0	15.23	318	9.4E-09	14.77	321	9.1E-09	9.26E-09	
12.0	15.06	323	9.2E-09	14.26	326	8.6E-09	8.91E-09	8.8237E-09
16.0	27.77	326	1.7E-08	20.88	326	1.3E-08	1.47E-08	
16.0	32.95	433	1.5E-08	25.67	434	1.2E-08	1.33E-08	
16.0	22.12	313	1.4E-08	18.38	314	1.2E-08	1.27E-08	
16.0	27.94	394	1.4E-08	22.78	397	1.1E-08	1.27E-08	
16.0	22.64	311	1.4E-08	17.39	311	1.1E-08	1.27E-08	
16.0	25.79	267	1.9E-08	14.78	268	1.1E-08	1.5E-08	1.1513E-08
20.0	33.06	416	1.6E-08	31.96	415	1.5E-08	1.54E-08	

20.0	20.10	267	1.5E-08	20.29	269	1.5E-08	1.49E-08	
20.0	38.48	506	1.5E-08	38.15	513	1.5E-08	1.48E-08	
20.0	23.44	312	1.5E-08	23.47	311	1.5E-08	1.49E-08	
20.0	16.48	215	1.5E-08	15.26	231	1.3E-08	1.41E-08	
20.0	63.67	834	1.5E-08	61.93	842	1.5E-08	1.48E-08	1.4528E-08
16.0	27.43	314	1.7E-08	18.91	317	1.2E-08	1.45E-08	
16.0	46.41	306	3.0E-08	16.93	305	1.1E-08	2.04E-08	
16.0	87.43	523	3.3E-08	29.72	524	1.1E-08	2.21E-08	
16.0	75.48	508	2.9E-08	29.62	512	1.1E-08	2.04E-08	
16.0	55.94	430	2.6E-08	24.73	435	1.1E-08	1.84E-08	
16.0	27.79	248	2.2E-08	14.18	252	1.1E-08	1.66E-08	1.1272E-08
12.0	22.67	502	8.9E-09	21.32	510	8.2E-09	8.58E-09	
12.0	12.73	299	8.4E-09	12.33	308	7.9E-09	8.15E-09	
12.0	13.15	307	8.4E-09	12.14	309	7.7E-09	8.1E-09	
12.0	17.43	409	8.4E-09	16.23	413	7.8E-09	8.08E-09	
12.0	10.34	239	8.5E-09	8.84	241	7.2E-09	7.88E-09	
12.0	25.75	562	9.0E-09	22.16	555	7.9E-09	8.46E-09	7.7928E-09
8.0	16.91	603	5.5E-09	15.66	607	5.1E-09	5.31E-09	
8.0	56.58	1864	6.0E-09	45.88	1866	4.9E-09	5.42E-09	
8.0	9.11	313	5.7E-09	7.96	313	5.0E-09	5.38E-09	
8.0	37.06	1281	5.7E-09	32.78	1284	5.0E-09	5.37E-09	
8.0	105.64	3706	5.6E-09	91.79	3711	4.9E-09	5.25E-09	
8.0	8.81	310	5.6E-09	7.74	310	4.9E-09	5.27E-09	4.966E-09
5.0	35.94	1380	5.1E-09	21.64	1388	3.1E-09	4.11E-09	
5.0	23.21	969	4.7E-09	14.34	968	2.9E-09	3.82E-09	
5.0	26.63	1228	4.3E-09	18.19	1234	2.9E-09	3.59E-09	
5.0	40.38	2036	3.9E-09	29.52	2042	2.9E-09	3.38E-09	
5.0	11.05	594	3.7E-09	8.73	597	2.9E-09	3.28E-09	
5.0	15.67	861	3.6E-09	12.70	870	2.9E-09	3.23E-09	2.9202E-09
2.0	42.26	3524	2.4E-09	18.58	3520	1.0E-09	1.7E-09	
2.0	57.02	6114	1.8E-09	31.43	6115	1.0E-09	1.43E-09	
2.0	38.06	4872	1.5E-09	26.55	4876	1.1E-09	1.31E-09	
2.0	54.11	6887	1.5E-09	36.33	6897	1.0E-09	1.29E-09	
2.0	27.76	3459	1.6E-09	18.15	3458	1.0E-09	1.31E-09	
2.0	50.33	6615	1.5E-09	34.91	6618	1.0E-09	1.27E-09	1.0407E-09
1.5	80.32	4630	3.4E-09	15.58	4630	6.6E-10	2.04E-09	
1.5	59.19	4672	2.5E-09	16.31	4672	6.9E-10	1.59E-09	
1.5	35.61	3878	1.8E-09	13.55	3881	6.9E-10	1.25E-09	

	1.5	35.15	4110	1.7E-09	14.38	4113	6.9E-10	1.19E-09	
	1.5	76.08	11451	1.3E-09	43.15	11452	7.4E-10	1.03E-09	
	1.5	25.72	5120	9.9E-10	19.94	5121	7.7E-10	8.8E-10	7.0702E-10
	1.2	56.89	3382	3.3E-09	8.91	3389	5.2E-10	1.92E-09	
	1.2	37.81	3279	2.3E-09	10.23	3287	6.1E-10	1.44E-09	
	1.2	49.08	6285	1.5E-09	17.48	6281	5.5E-10	1.04E-09	
	1.2	24.06	4115	1.2E-09	11.83	4119	5.7E-10	8.6E-10	
	1.2	18.81	3459	1.1E-09	9.71	3465	5.5E-10	8.13E-10	
	1.2	18.73	3601	1.0E-09	10.84	3605	5.9E-10	8.1E-10	5.6567E-10
	1.0	78.56	4936	3.1E-09	7.93	4938	3.2E-10	1.73E-09	
	1.0	52.19	3577	2.9E-09	6.98	3577	3.8E-10	1.63E-09	
	1.0	34.77	3666	1.9E-09	7.91	3670	4.3E-10	1.15E-09	
	1.0	29.65	5132	1.1E-09	12.03	5134	4.6E-10	8.01E-10	
	1.0	17.20	3912	8.7E-10	9.83	3917	5.0E-10	6.81E-10	
	1.0	21.71	5660	7.6E-10	14.50	5662	5.1E-10	6.31E-10	4.3155E-10
	0.8	79.12	5198	3.0E-09	3.57	5201	1.4E-10	1.57E-09	
	0.8	37.28	3429	2.1E-09	3.45	3431	2.0E-10	1.17E-09	
	0.8	19.05	6021	6.2E-10	4.67	6023	1.5E-10	3.89E-10	
	0.8	9.21	4116	4.4E-10	6.43	4121	3.1E-10	3.75E-10	
	0.8	19.57	7642	5.1E-10	7.75	7645	2.0E-10	3.53E-10	
	0.8	24.16	10294	4.6E-10	13.54	10297	2.6E-10	3.61E-10	2.0897E-10
	0.6	18.93	4266	8.8E-10	1.58	4246	7.3E-11	4.74E-10	
	0.6	21.52	5277	8.0E-10	1.86	5280	6.9E-11	4.37E-10	
	0.6	16.27	6671	4.8E-10	3.07	6673	9.1E-11	2.86E-10	
	0.6	35.20	23276	3.0E-10	6.06	23276	5.1E-11	1.75E-10	
	0.6	28.93	4942	1.2E-09	3.23	4942	1.3E-10	6.42E-10	
	0.6	17.00	4880	6.9E-10	2.03	4883	8.2E-11	3.85E-10	8.2656E-11
	0.4	96.75	8765	2.2E-09	1.61	8768	3.6E-11	1.11E-09	
	0.4	26.12	5652	9.1E-10	0.21	5652	7.3E-12	4.59E-10	
	0.4	18.04	4669	7.6E-10	0.07	4647	3.0E-12	3.83E-10	
	0.4	21.00	7400	5.6E-10	0.61	7382	1.6E-11	2.88E-10	
	0.4	69.60	7303	1.9E-09	0.83	7286	2.2E-11	9.51E-10	
	0.4	30.71	10498	5.8E-10	0.39	10311	7.5E-12	2.92E-10	1.5459E-11
T	0.2	2.19	6821	6.3E-11	2.66	6824	7.7E-11	7.01E-11	
T	0.2	3.89	4454	1.7E-10	0.58	4438	2.6E-11	9.9E-11	
T	0.2	2.73	8681	6.2E-11	2.36	8683	5.4E-11	5.78E-11	5.2096E-11
	0.2	20.49	5338	7.6E-10	0.08	5326	3.0E-12	3.8E-10	
	0.2	27.58	2961	1.8E-09	0.75	2943	5.0E-11	1.19E-10	4.1904E-11

T	0.3	17.28	18081	1.9E-10	2.08	18076	2.3E-11	1.12E-10	
T	0.3	67.10	64499	2.1E-10	2.29	64493	7.0E-12	1.17E-10	
T	0.3	19.23	18921	2.0E-10	3.62	18926	3.8E-11	6.52E-11	
T	0.3	18.72	16231	2.3E-10	0.18	16235	2.2E-12	1.05E-10	
T	0.3	2.67	5685	9.3E-11	3.99	5666	1.4E-10	6.95E-11	
T	0.3	12.18	11602	2.1E-10	3.57	11606	6.1E-11	1.38E-10	4.4868E-11
T	0.4	12.67	11635	2.1E-10	4.70	11645	8.0E-11	1.65E-10	
T	0.4	17.07	8871	3.8E-10	0.24	8872	5.3E-12	1.13E-10	
T	0.4	12.99	10225	2.5E-10	5.83	10226	1.1E-10	1.36E-10	
T	0.4	2.89	2576	2.2E-10	3.43	2562	2.6E-10	1.72E-10	
T	0.4	8.36	10310	1.6E-10	12.01	10310	2.3E-10	1.15E-10	
T	0.4	2.11	5167	8.1E-11	9.60	5167	3.7E-10	2.29E-10	1.763E-10
T	0.8	2.98	6407	9.2E-11	22.18	6410	6.8E-10	6.14E-10	
T	0.8	89.12	46536	3.8E-10	52.24	46566	2.2E-10	3.39E-10	
T	0.8	20.29	7325	5.5E-10	6.68	7321	1.8E-10	2.01E-10	
T	0.8	29.07	12546	4.6E-10	12.61	12550	2.0E-10	1.97E-10	
T	0.8	6.27	5596	2.2E-10	11.55	5604	4.1E-10	2.03E-10	
T	0.8	3.70	3713	2.0E-10	8.09	3709	4.3E-10	2.15E-10	3.5315E-10
T	1.0	16.29	5288	6.1E-10	1.62	5290	6.0E-11	3.02E-11	
T	1.0	20.39	8379	4.8E-10	9.45	8378	2.2E-10	1.11E-10	
T	1.0	15.74	6672	4.7E-10	9.85	6671	2.9E-10	1.46E-10	
T	1.0	16.29	5770	5.6E-10	4.67	5770	1.6E-10	7.98E-11	
T	1.0	13.30	3705	7.1E-10	1.02	3700	5.4E-11	2.72E-11	
T	1.0	26.16	10226	5.0E-10	15.60	10229	3.0E-10	1.5E-10	1.8151E-10
T	1.2	25.12	7574	6.5E-10	10.21	7573	2.7E-10	1.33E-10	
T	1.2	19.55	10000	3.9E-10	19.78	10002	3.9E-10	1.95E-10	
T	1.2	12.34	3233	7.5E-10	2.99	3234	1.8E-10	9.12E-11	
T	1.2	26.68	7212	7.3E-10	6.16	7212	1.7E-10	8.42E-11	
T	1.2	18.98	5736	6.5E-10	7.28	5740	2.5E-10	1.25E-10	
T	1.2	20.08	7075	5.6E-10	9.80	7075	2.7E-10	1.37E-10	2.5506E-10
T	1.5	12.36	3722	6.6E-10	8.65	3725	4.6E-10	2.29E-10	
T	1.5	44.39	12555	7.0E-10	32.32	12558	5.1E-10	2.54E-10	
T	1.5	14.35	4848	5.8E-10	11.87	4852	4.8E-10	2.41E-10	
T	1.5	15.38	4399	6.9E-10	9.21	4402	4.1E-10	2.06E-10	
T	1.5	28.64	9091	6.2E-10	22.82	9096	4.9E-10	2.47E-10	
T	1.5	40.63	8825	9.1E-10	9.08	8828	2.0E-10	1.01E-10	4.2647E-10
T	2.0	20.44	3142	1.3E-09	5.28	3135	3.3E-10	1.66E-10	

T	2.0	31.16	5334	1.2E-09	11.37	5338	4.2E-10	2.1E-10	
T	2.0	19.44	4962	7.7E-10	19.86	4965	7.9E-10	3.95E-10	
T	2.0	5.87	1466	7.9E-10	5.83	1461	7.9E-10	3.94E-10	
T	2.0	24.24	4211	1.1E-09	10.06	4213	4.7E-10	2.36E-10	
T	2.0	22.60	3672	1.2E-09	10.76	3677	5.8E-10	2.89E-10	5.6281E-10
T	3.0	22.22	3780	1.2E-09	26.29	3780	1.4E-09	6.86E-10	
T	3.0	25.19	4900	1.0E-09	34.69	4903	1.4E-09	6.98E-10	
T	3.0	37.79	5999	1.2E-09	33.06	6001	1.1E-09	5.43E-10	
T	3.0	27.35	4283	1.3E-09	23.10	4286	1.1E-09	5.32E-10	
T	3.0	32.91	5177	1.3E-09	31.35	5177	1.2E-09	5.97E-10	
T	3.0	33.58	5395	1.2E-09	33.43	5401	1.2E-09	6.1E-10	1.2222E-09

T = Used pressure transducer to measure imposed gradient

Warren '93

Continuous core sample from above the water table

Oct 26, 1994

0.2 - 0.9 m

Sample length =	41	mm	4.1	cm
Sample diameter =	56.96	mm	5.696	cm
Sample CSA =	25.48178474	cm^2		
Volume of water drop =	0.05	cm^3		

		Out			
Head (cm)	Gradient	vol (mL)	time(s)	Flux(m/s)	avg-out
0.82	0.2	0.05	284	6.9E-08	
0.82	0.2	0.05	644	3.0E-08	
0.82	0.2	0.05	1473	1.3E-08	3.7627E-08
1.23	0.3	0.05	277	7.1E-08	
1.23	0.3	0.05	278	7.1E-08	
1.23	0.3	0.05	285	6.9E-08	7.0E-08
1.64	0.4	0.05	162	1.2E-07	
1.64	0.4	0.05	121	1.6E-07	
1.64	0.4	0.05	165	1.2E-07	1.3407E-07
2.46	0.6	0.05	92	2.1E-07	
2.46	0.6	0.05	93	2.1E-07	
2.46	0.6	0.05	70	2.8E-07	2.3486E-07
3.28	0.8	0.05	70	2.8E-07	
3.28	0.8	0.05	50	3.9E-07	
3.28	0.8	0.05	67	2.9E-07	3.2187E-07
4.10	1.0	0.05	52	3.8E-07	
4.10	1.0	0.05	41	4.8E-07	
4.10	1.0	0.05	51	3.8E-07	4.1356E-07
4.92	1.2	0.05	32	6.1E-07	
4.92	1.2	0.05	29	6.8E-07	
4.92	1.2	0.05	36	5.5E-07	6.1162E-07

6.15	1.5	0.05	28	7.0E-07	
6.15	1.5	0.05	30	6.5E-07	
6.15	1.5	0.05	27	7.3E-07	6.9386E-07
8.20	2.0	0.05	19	1.0E-06	
8.20	2.0	0.05	19	1.0E-06	
8.20	2.0	0.05	19	1.0E-06	1.0E-06
12.30	3.0	0.05	12	1.6E-06	
12.30	3.0	0.05	12	1.6E-06	
12.30	3.0	0.05	12	1.6E-06	1.6E-06
20.50	5.0	0.05	7	2.8E-06	
20.50	5.0	0.05	7	2.8E-06	
20.50	5.0	0.05	7	2.8E-06	2.8E-06
20.50	5.0	0.05	7	2.8E-06	
20.50	5.0	0.05	7	2.8E-06	
20.50	5.0	0.05	7	2.8E-06	2.8E-06
12.30	3.0	0.05	12	1.6E-06	
12.30	3.0	0.05	12	1.6E-06	
12.30	3.0	0.05	12	1.6E-06	1.6E-06
8.20	2.0	0.05	19	1.0E-06	
8.20	2.0	0.05	19	1.0E-06	
8.20	2.0	0.05	19	1.0E-06	1.0E-06
6.15	1.5	0.05	28	7.0E-07	
6.15	1.5	0.05	29	6.8E-07	
6.15	1.5	0.05	29	6.8E-07	6.8E-07
4.92	1.2	0.05	36	5.5E-07	
4.92	1.2	0.05	36	5.5E-07	
4.92	1.2	0.05	37	5.3E-07	5.4E-07
4.10	1.0	0.05	47	4.2E-07	
4.10	1.0	0.05	48	4.1E-07	
4.10	1.0	0.05	52	3.8E-07	4.0E-07
3.28	0.8	0.05	68	2.9E-07	
3.28	0.8	0.05	71	2.8E-07	
3.28	0.8	0.05	74	2.7E-07	2.8E-07

2.46	0.6	0.05	93	2.1E-07	
2.46	0.6	0.05	95	2.1E-07	
2.46	0.6	0.05	98	2.0E-07	2.1E-07
1.64	0.4	0.05	165	1.2E-07	
1.64	0.4	0.05	168	1.2E-07	
1.64	0.4	0.05	173	1.1E-07	1.2E-07
1.23	0.3	0.05	304	6.5E-08	
1.23	0.3	0.05	314	6.2E-08	
1.23	0.3	0.05	306	6.4E-08	6.4E-08
0.82	0.2	0.05	538	3.6E-08	
0.82	0.2	0.05	575	3.4E-08	
0.82	0.2	0.05	607	3.2E-08	3.4E-08

Warren '93 Continuous core sample from below the water table (Warren)

Nov 3, 1994 - Jan 24, 1995

3.9 - 4.0 m

Sample length =	42	mm	4.2	cm
Sample diameter =	56.96	mm	5.696	cm
Sample CSA =	25.4818	cm^2		
Capillary tube diameter =	0.8	mm	0.08	cm
Capillary CSA =	0.00503	cm^2		
Area Ratio =	5069.44			

		In			Out				
Head (cm)	Gradient	l (mm)	time(s)	Flux(m/s)	l (mm)	time(s)	Flux(m/s)	In+out/2	avg-out
T	0.2	19.41	16198	2.4E-10	0.39	16182	4.8E-12	1.2E-10	
T	0.2	10.55	11474	1.8E-10	6.46	11474	1.1E-10	1.5E-10	
T	0.2	12.55	8449	2.9E-10	1.68	8492	3.9E-11	1.7E-10	
T	0.2	19.55	14381	2.7E-10	2.13	14383	2.9E-11	1.5E-10	
T	0.2	9.13	7805	2.3E-10	0.81	7811	2.0E-11	1.3E-10	
T	0.2	4.91	7921	1.2E-10	5.44	7921	1.4E-10	1.3E-10	5.7E-11
T	0.3	13.86	12976	2.1E-10	8.55	12979	1.3E-10	1.7E-10	
T	0.3	16.28	13839	2.3E-10	7.45	13845	1.1E-10	1.7E-10	
T	0.3	19.94	13857	2.8E-10	3.63	13869	5.2E-11	1.7E-10	
T	0.3	38.37	38865	1.9E-10	27.50	38866	1.4E-10	1.7E-10	
T	0.3	4.83	5902	1.6E-10	3.56	5904	1.2E-10	1.4E-10	
T	0.3	3.41	4641	1.4E-10	3.77	4643	1.6E-10	1.5E-10	1.2E-10
T	0.4	16.17	8843	3.6E-10	0.39	8890	8.7E-12	1.8E-10	
T	0.4	17.61	10281	3.4E-10	0.70	10287	1.3E-11	1.8E-10	
T	0.4	50.14	35827	2.8E-10	27.54	35829	1.5E-10	2.1E-10	
T	0.4	15.93	10603	3.0E-10	5.56	10604	1.0E-10	2.0E-10	
T	0.4	6.87	4121	3.3E-10	2.38	4127	1.1E-10	2.2E-10	
T	0.4	8.11	5697	2.8E-10	3.67	5701	1.3E-10	2.0E-10	8.6E-11
T	0.6	17.85	11501	3.1E-10	10.44	11499	1.8E-10	2.4E-10	
T	0.6	4.64	3624	2.5E-10	3.62	3626	2.0E-10	2.2E-10	
T	0.6	6.65	6650	2.0E-10	6.07	6647	1.8E-10	1.9E-10	
T	0.6	10.28	7611	2.7E-10	5.97	7612	1.5E-10	2.1E-10	
T	0.6	14.18	8773	3.2E-10	4.02	8777	9.0E-11	2.0E-10	
T	0.6	10.63	3777	5.6E-10	1.58	3774	8.3E-11	3.2E-10	1.5E-10

T	0.8	7.77	3346	4.6E-10	0.46	3346	2.7E-11	2.4E-10	
T	0.8	6.26	2441	5.1E-10	0.67	2451	5.4E-11	2.8E-10	
T	0.8	26.43	12667	4.1E-10	9.15	12672	1.4E-10	2.8E-10	
T	0.8	22.40	11262	3.9E-10	8.23	11266	1.4E-10	2.7E-10	
T	0.8	74.39	40847	3.6E-10	37.04	40854	1.8E-10	2.7E-10	
T	0.8	14.72	8998	3.2E-10	11.13	9006	2.4E-10	2.8E-10	1.3E-10
T	1.0	22.59	10606	4.2E-10	10.36	10605	1.9E-10	3.1E-10	
T	1.0	7.49	4163	3.5E-10	6.07	4170	2.9E-10	3.2E-10	
T	1.0	12.22	5948	4.1E-10	5.28	5949	1.8E-10	2.9E-10	
T	1.0	11.24	5607	4.0E-10	4.83	5610	1.7E-10	2.8E-10	
T	1.0	52.95	27264	3.8E-10	31.57	27265	2.3E-10	3.1E-10	
T	1.0	79.49	39514	4.0E-10	47.24	39548	2.4E-10	3.2E-10	2.1E-10
T	1.2	9.45	4966	3.8E-10	7.00	4969	2.8E-10	3.3E-10	
T	1.2	12.18	5030	4.8E-10	4.54	5032	1.8E-10	3.3E-10	
T	1.2	7.85	4474	3.5E-10	6.07	4475	2.7E-10	3.1E-10	
T	1.2	10.25	6351	3.2E-10	10.75	6352	3.3E-10	3.3E-10	
T	1.2	2.18	3828	1.1E-10	8.45	3830	4.4E-10	2.7E-10	
T	1.2	37.03	20200	3.6E-10	27.15	20205	2.7E-10	3.1E-10	2.9E-10
T	1.5	12.91	3987	6.4E-10	10.31	3986	5.1E-10	5.7E-10	
T	1.5	12.71	5965	4.2E-10	11.06	5964	3.7E-10	3.9E-10	
T	1.5	15.55	7339	4.2E-10	15.32	7340	4.1E-10	4.1E-10	
T	1.5	38.08	13066	5.7E-10	19.67	13076	3.0E-10	4.4E-10	
T	1.5	25.51	8736	5.8E-10	11.88	8735	2.7E-10	4.2E-10	
T	1.5	74.29	32591	4.5E-10	61.98	32594	3.8E-10	4.1E-10	3.7E-10
T	2.0	96.45	33524	5.7E-10	80.20	33528	4.7E-10	5.2E-10	
T	2.0	107.05	38884	5.4E-10	96.11	38889	4.9E-10	5.2E-10	
T	2.0	11.28	4049	5.5E-10	9.48	4050	4.6E-10	5.1E-10	
T	2.0	11.73	3264	7.1E-10	5.69	3264	3.4E-10	5.3E-10	
T	2.0	9.20	3622	5.0E-10	8.80	3625	4.8E-10	4.9E-10	
T	2.0	17.03	6449	5.2E-10	15.32	6451	4.7E-10	4.9E-10	4.5E-10
T	3.0	22.82	5269	8.5E-10	17.22	5259	6.5E-10	7.5E-10	
T	3.0	9.77	1411	1.4E-09	0.73	1398	1.0E-10	7.3E-10	
T	3.0	27.18	3649	1.5E-09	3.16	3650	1.7E-10	8.2E-10	
T	3.0	59.22	14178	8.2E-10	51.76	14176	7.2E-10	7.7E-10	
T	3.0	21.61	5324	8.0E-10	21.60	5323	8.0E-10	8.0E-10	
T	3.0	22.23	4369	1.0E-09	11.77	4375	5.3E-10	7.7E-10	5.0E-10
	3.3	29.36	4699	1.2E-09	13.61	4697	5.7E-10	9.0E-10	
	3.3	17.16	3813	8.9E-10	13.75	3820	7.1E-10	8.0E-10	

3.3	10.15	1969	1.0E-09	5.83	1973	5.8E-10	8.0E-10	
3.3	18.30	3131	1.2E-09	8.99	3134	5.7E-10	8.6E-10	
3.3	58.79	11432	1.0E-09	37.94	11430	6.5E-10	8.3E-10	
3.3	71.48	16257	8.7E-10	58.86	16260	7.1E-10	7.9E-10	6.3E-10
5.5	37.39	4058	1.8E-09	27.35	4052	1.3E-09	1.6E-09	
5.5	15.10	1834	1.6E-09	12.74	1836	1.4E-09	1.5E-09	
5.5	12.34	1236	2.0E-09	7.48	1237	1.2E-09	1.6E-09	
5.5	98.06	12800	1.5E-09	87.18	12804	1.3E-09	1.4E-09	
5.5	4.59	1894	4.8E-10	18.77	1936	1.9E-09	1.2E-09	
5.5	12.33	954	2.5E-09	3.23	953	6.7E-10	1.6E-09	1.3E-09
8.8	50.04	2257	4.4E-09	23.82	2263	2.1E-09	3.2E-09	
8.8	13.70	948	2.9E-09	8.99	953	1.9E-09	2.4E-09	
8.8	55.62	4543	2.4E-09	46.87	4543	2.0E-09	2.2E-09	
8.8	28.03	2245	2.5E-09	20.24	2245	1.8E-09	2.1E-09	
8.8	14.91	1376	2.1E-09	13.87	1378	2.0E-09	2.1E-09	
8.8	70.13	6304	2.2E-09	59.42	6310	1.9E-09	2.0E-09	1.9E-09
13.2	20.05	611	6.5E-09	15.32	617	4.9E-09	5.7E-09	
13.2	13.65	802	3.4E-09	11.72	811	2.9E-09	3.1E-09	
13.2	30.45	2027	3.0E-09	27.53	2030	2.7E-09	2.8E-09	
13.2	9.60	717	2.6E-09	10.57	718	2.9E-09	2.8E-09	
13.2	37.48	2624	2.8E-09	36.62	2626	2.8E-09	2.8E-09	
13.2	10.94	965	2.2E-09	14.76	969	3.0E-09	2.6E-09	3.2E-09
17.6	68.88	3611	3.8E-09	69.86	3613	3.8E-09	3.8E-09	
17.6	11.17	570	3.9E-09	11.01	576	3.8E-09	3.8E-09	
17.6	14.94	633	4.7E-09	11.10	634	3.5E-09	4.1E-09	
17.6	13.89	460	6.0E-09	12.87	456	5.6E-09	5.8E-09	
17.6	56.41	2905	3.8E-09	57.66	2916	3.9E-09	3.9E-09	
17.6	13.59	704	3.8E-09	13.03	708	3.6E-09	3.7E-09	4.0E-09
22.0	19.83	473	8.3E-09	17.06	481	7.0E-09	7.6E-09	
22.0	10.03	454	4.4E-09	11.85	458	5.1E-09	4.7E-09	
22.0	6.42	363	3.5E-09	10.01	363	5.4E-09	4.5E-09	
22.0	7.30	302	4.8E-09	6.81	302	4.4E-09	4.6E-09	
22.0	17.05	630	5.3E-09	13.42	635	4.2E-09	4.8E-09	
22.0	14.75	680	4.3E-09	16.26	682	4.7E-09	4.5E-09	5.1E-09
17.6	13.52	355	7.5E-09	10.60	355	5.9E-09	6.7E-09	
17.6	8.38	313	5.3E-09	5.93	310	3.8E-09	4.5E-09	
17.6	5.46	309	3.5E-09	6.02	311	3.8E-09	3.7E-09	
17.6	5.09	338	3.0E-09	7.38	341	4.3E-09	3.6E-09	

	17.6	7.11	353	4.0E-09	6.90	353	3.9E-09	3.9E-09	
	17.6	6.47	302	4.2E-09	5.01	304	3.3E-09	3.7E-09	4.1E-09
	13.2	73.08	4861	3.0E-09	71.21	4867	2.9E-09	2.9E-09	
	13.2	6.43	326	3.9E-09	3.29	325	2.0E-09	2.9E-09	
	13.2	8.99	480	3.7E-09	5.08	483	2.1E-09	2.9E-09	
	13.2	48.03	3285	2.9E-09	47.72	3288	2.9E-09	2.9E-09	
	13.2	2.46	330	1.5E-09	7.77	329	4.7E-09	3.1E-09	
	13.2	2.37	359	1.3E-09	5.79	358	3.2E-09	2.2E-09	2.9E-09
	8.8	18.60	1604	2.3E-09	16.67	1599	2.1E-09	2.2E-09	
	8.8	9.13	1072	1.7E-09	10.08	1075	1.8E-09	1.8E-09	
	8.8	27.70	3422	1.6E-09	31.19	3422	1.8E-09	1.7E-09	
	8.8	69.78	7842	1.8E-09	67.21	7847	1.7E-09	1.7E-09	
	8.8	18.84	2176	1.7E-09	18.71	2176	1.7E-09	1.7E-09	
	8.8	5.85	660	1.7E-09	6.16	665	1.8E-09	1.8E-09	1.8E-09
	5.5	21.64	3599	1.2E-09	22.09	3598	1.2E-09	1.2E-09	
	5.5	14.29	2735	1.0E-09	14.39	2736	1.0E-09	1.0E-09	
	5.5	14.94	2700	1.1E-09	13.45	2708	9.8E-10	1.0E-09	
	5.5	27.74	5060	1.1E-09	26.42	5055	1.0E-09	1.1E-09	
	5.5	3.57	793	8.9E-10	4.65	797	1.2E-09	1.0E-09	
	5.5	20.39	3734	1.1E-09	19.25	3734	1.0E-09	1.0E-09	1.1E-09
	3.3	12.07	4358	5.5E-10	14.67	4359	6.6E-10	6.1E-10	
	3.3	9.41	3247	5.7E-10	9.85	3246	6.0E-10	5.9E-10	
	3.3	5.53	1802	6.1E-10	5.14	1807	5.6E-10	5.8E-10	
	3.3	9.11	3217	5.6E-10	9.31	3222	5.7E-10	5.6E-10	
	3.3	13.47	4310	6.2E-10	12.23	4315	5.6E-10	5.9E-10	
	3.3	3.23	1000	6.4E-10	2.58	1008	5.0E-10	5.7E-10	5.8E-10
T	3.0	25.31	7613	6.6E-10	18.39	7610	4.8E-10	5.7E-10	
T	3.0	1.88	1051	3.5E-10	3.86	1047	7.3E-10	5.4E-10	
T	3.0	26.77	8199	6.4E-10	18.57	8204	4.5E-10	5.5E-10	
T	3.0	10.20	3985	5.0E-10	11.35	3988	5.6E-10	5.3E-10	
T	3.0	33.17	12126	5.4E-10	30.91	12134	5.0E-10	5.2E-10	
T	3.0	7.05	2563	5.4E-10	9.67	2560	7.5E-10	6.4E-10	5.8E-10
T	2.0	9.10	5169	3.5E-10	8.86	5174	3.4E-10	3.4E-10	
T	2.0	18.05	9071	3.9E-10	15.52	9077	3.4E-10	3.6E-10	
T	2.0	2.26	1206	3.7E-10	1.74	1206	2.8E-10	3.3E-10	
T	2.0	21.29	9850	4.3E-10	15.82	9845	3.2E-10	3.7E-10	
T	2.0	10.10	5404	3.7E-10	9.44	5404	3.4E-10	3.6E-10	
T	2.0	8.69	4088	4.2E-10	6.66	4092	3.2E-10	3.7E-10	3.2E-10

T	1.2	2.55	1834	2.7E-10	2.02	1837	2.2E-10	2.5E-10	
T	1.2	10.96	8423	2.6E-10	8.50	8426	2.0E-10	2.3E-10	
T	1.2	8.75	6957	2.5E-10	7.55	6962	2.1E-10	2.3E-10	
T	1.2	0.94	1226	1.5E-10	1.82	1227	2.9E-10	2.2E-10	
T	1.2	1.10	1147	1.9E-10	1.45	1148	2.5E-10	2.2E-10	
T	1.2	0.71	1554	9.0E-11	1.78	1554	2.3E-10	1.6E-10	2.3E-10
T	1.0	1.81	2850	1.3E-10	2.23	2849	1.5E-10	1.4E-10	
T	1.0	6.04	7816	1.5E-10	7.78	7817	2.0E-10	1.7E-10	
T	1.0	6.37	3328	3.8E-10	2.12	3328	1.3E-10	2.5E-10	
T	1.0	1.95	1336	2.9E-10	1.54	1338	2.3E-10	2.6E-10	
T	1.0	11.34	7598	2.9E-10	4.66	7596	1.2E-10	2.1E-10	
T	1.0	3.56	859	8.2E-10	0.09	860	2.1E-11	4.2E-10	1.4E-10
T	0.8	2.49	3268	1.5E-10	4.04	3267	2.4E-10	2.0E-10	
T	0.8	8.11	5778	2.8E-10	1.96	5781	6.7E-11	1.7E-10	
T	0.8	3.16	3192	2.0E-10	1.93	3199	1.2E-10	1.6E-10	
T	0.8	5.09	3736	2.7E-10	2.00	3738	1.1E-10	1.9E-10	
T	0.8	5.44	2961	3.6E-10	0.57	2964	3.8E-11	2.0E-10	
T	0.8	4.32	4682	1.8E-10	4.19	4685	1.8E-10	1.8E-10	1.2E-10
T	0.6	1.33	3405	7.7E-11	1.93	3409	1.1E-10	9.4E-11	
T	0.6	4.86	8845	1.1E-10	6.23	8848	1.4E-10	1.2E-10	
T	0.6	5.53	6777	1.6E-10	3.41	6780	9.9E-11	1.3E-10	
T	0.6	4.02	4581	1.7E-10	2.37	4581	1.0E-10	1.4E-10	
T	0.6	4.27	5647	1.5E-10	3.49	5647	1.2E-10	1.4E-10	
T	0.6	2.48	4170	1.2E-10	2.09	4172	9.9E-11	1.1E-10	1.1E-10
T	0.4	1.89	3569	1.0E-10	0.74	3568	4.1E-11	7.3E-11	
T	0.4	10.72	20870	1.0E-10	8.48	20876	8.0E-11	9.1E-11	
T	0.4	2.24	3707	1.2E-10	2.99	3659	1.6E-10	1.4E-10	
T	0.4	40.23	48416	1.6E-10	7.93	48426	3.2E-11	9.8E-11	
T	0.4	0.56	2104	5.3E-11	3.24	2118	3.0E-10	1.8E-10	
T	0.4	1.14	3271	6.9E-11	2.72	3277	1.6E-10	1.2E-10	1.3E-10
T	0.3	1.39	3732	7.3E-11	3.46	3671	1.9E-10	1.3E-10	
T	0.3	1.06	3347	6.2E-11	0.25	3332	1.5E-11	3.9E-11	
T	0.3	3.15	4594	1.4E-10	0.48	4594	2.1E-11	7.8E-11	
T	0.3	30.63	51030	1.2E-10	2.04	51040	7.9E-12	6.3E-11	
T	0.3	1.21	3690	6.5E-11	0.92	3692	4.9E-11	5.7E-11	
T	0.3	9.92	16447	1.2E-10	1.75	16447	2.1E-11	7.0E-11	5.0E-11
T	0.2	5.77	14020	8.1E-11	0.56	14020	7.9E-12	4.5E-11	

T	0.2	1.63	4937	6.5E-11	0.30	4937	1.2E-11	3.9E-11	
T	0.2	2.50	8278	6.0E-11	0.65	8280	1.5E-11	3.8E-11	
T	0.2	10.48	20720	1.0E-10	0.86	20722	8.2E-12	5.4E-11	
T	0.2	10.19	17324	1.2E-10	0.50	17351	5.7E-12	6.1E-11	
T	0.2	9.00	19460	9.1E-11	2.47	19460	2.5E-11	5.8E-11	1.2E-11

T = Used pressure transducer to measure imposed gradient